

The Effects of Copper Availability on Mitochondrial Function in *Saccharomyces cerevisiae*

by

Alicia Dubinski

A thesis

presented to the University of Waterloo

in fulfilment of the

thesis requirement for the degree of

Master of Science

in

Biology

Waterloo, ON, Canada, 2019

© Alicia Dubinski 2019

Authors Declaration

I hereby declare that I am the sole author of this thesis. This is a true copy of the thesis, including any required final revisions, as accepted by my examiners.

I understand that my thesis may be made electronically available to the public.

Statement of Contributions

All data in this thesis are original and are novel contributions to the field. I conceived, designed, and analyzed experiments presented in this thesis and interpreted the data together with Dr. Moira Glerum. I assembled all figures presented in this thesis.

I personally performed all presented experiments, except for: Tyler Soule performed one mitochondrial isolation for Cu deficient conditions, performed Oxyblots presented in Figure 3.11 and Figure 4.10, optimized and obtained raw data for the cell cycle experiments presented in Figure 5.2 and Figure 5.3, and carried out the Western blots in Figure 5.1. Renée Hilker performed viability analysis displayed in Figure 3.2 and Figure 4.5, and optimized qPCR primers for *SCO1*, *COX11*, *CTR1*, *CUP1*, *MAC1*, *CUP2*, *TDH2* and *CCS1*.

Abstract

Copper (Cu) is crucial for cell function and survival and plays important roles in enzyme-catalyzed metabolic processes, transport of cargo through cellular membranes, and protein breakdown. The mitochondria are home to two important Cu-containing enzymes: cytochrome *c* oxidase (COX) and superoxide dismutase 1 (Sod1). Delivery of Cu to COX, the terminal electron acceptor in the respiratory chain, is suggested to happen in a bucket brigade fashion *via* the proteins Cox17, Sco1, and Cox11. Sod1, the other major mitochondrial cuproprotein, is thought to obtain Cu from its chaperone, Ccs1. Because the mitochondria are a central player in Cu storage and regulation, our goal in this study is to analyze how changes in extracellular Cu concentration impact mitochondrial function in *Saccharomyces cerevisiae*.

Our results showed that Cox17, Sco1, and Cox11 responded differently to excess and limiting Cu, suggesting alternate functions for these proteins in mitochondria unrelated to COX assembly. During Cu deficient conditions we noticed an interesting redistribution of mitochondrial Cu: retention of Cu in mitochondrial Sod1 is accompanied by a complete loss of COX activity. This phenotype suggests a regulatory mechanism where Cu is preferentially donated to mitochondrial Sod1 instead of COX when Cu is limited. Interestingly, we also find that Cu redistribution in the mitochondria is affected when we change the primary carbon source from glucose to galactose. We propose that Cu distribution in mitochondria is controlled by an affinity gradient.

Analysis of cell cycle progression showed that in excess Cu, yeast displayed a cell cycle defect while Cu deficient conditions did not affect cell cycle progression. Strikingly, changing the primary carbon source to galactose led to a cell cycle defect in the presence of a Cu specific chelator. Overall, we suggest that the presence of mitochondrial Sod1 is essential for cell cycle progression.

The protein machinery responsible for Cu homeostasis has been well characterized, however the transport of Cu to cellular compartments and regulatory mechanisms involved in Cu import and export are not fully understood. We now demonstrate a novel phenotype that provides insight into regulation of Cu within the mitochondria. Additionally, we find that mitochondrial Cu distribution is affected by carbon source, and is associated with changes in cell cycle progression. These findings further our understanding of Cu homeostasis in yeast, and will likely have implications on Cu-related disorders, such as Menkes disease.

Acknowledgements

First and foremost, I would like to thank my incredible supervisor, Dr. D. Moira Glerum. Moira is hard working, knowledgeable, and passionate about her work and I am very grateful that I had the opportunity to be part of her lab for almost four years. Moira has inspired to pursue a career in research and has immensely helped me develop and mature scientifically and personally. She has been an amazing mentor and I will definitely miss working with her.

I would also like to thank NSERC, WIN, ASBMB, and the University of Waterloo for supporting me financially during the course of my degree.

To my committee members, Dr. Mungo Marsden and Dr. Andrew Doxey, thank you for asking difficult questions and encouraging me through both the ups and downs of this program. I am very appreciative of their support.

Thank you to Dr. Liz Meiering for her support on my work with Sod1 and for helping me develop my skills as a critical thinker. She constantly provided new insight to me when I presented my ideas and was also extremely supportive of my personal struggles.

To the other members of the Glerum lab: Tyler, Renée, Raffaele, and Seville. Thank you for bringing me food when I refused to eat lunch, and for listening to my ideas and providing critical insight. I will never forget the time we pulled the best April fool's prank on Moira.

Thank you to Nivetha, who sat with me almost every day to write our theses and pushed me to keep going when I told her I wanted to stop working.

Lastly, I would like to thank my family. My parents and my brother have been so loving and supportive throughout these years and I feel very fortunate to have such a close family. And thank you to Eric, the love of my life, who is one of the best listeners I know.

Table of Contents

Authors Declaration	ii
Statement of Contributions.....	iii
Abstract	iv
Acknowledgements	v
List of Figures	ix
List of Tables.....	xi
List of Abbreviations.....	xii
Chapter 1: Introduction	1
1.1 Copper (Cu) Homeostasis in Eukaryotes	1
1.1.1 Cellular Cu import	2
1.1.2 Cellular Cu export.....	3
1.1.3 Cu chaperones	4
1.1.4 Cu-responsive transcription factors	5
1.2 Cu Related Diseases	6
1.2.1 Historical context of Cu disorders	6
1.2.2 Implications of Cu defects in mitochondrial and neurodegenerative disorders.....	7
1.3 Cu and Mitochondrial Function	8
1.3.1 Cytochrome c Oxidase (COX) Function and Assembly.....	9
1.3.2 Delivery of Cu to Cox1 and Cox2	10
1.3.3 Superoxide Dismutase 1 (Sod1) Function and Assembly.....	12
1.3.4 Cu delivery to Sod1 in the absence of Ccs1	13
1.3.5 Cu delivery to Sod1 in the mitochondria and cytosol.....	14
1.4 Mitochondrial Cu Import	15
1.4.1 Cu import <i>via</i> a dually-localized Cu chaperone.....	15
1.4.2 Cu is stored in the mitochondrial matrix.....	17
1.4.3 Cu import <i>via</i> glutathione (GSH).....	18
1.5 Cu Homeostasis and Cell Cycle	20
1.5.1 Yeast cell cycle	20
1.5.2 Influence of Cu on cell cycle	22
1.5.3 Other pathways connected to Cu homeostasis.....	23
1.6 Goals of this study.....	25
Chapter 2: Materials and Methods	27
2.1 Yeast strains & Maintenance.....	27
2.1.1 Mating and Sporulation.....	28
2.2 Treatment with Cu availability reagents	28
2.3 Cell Viability	29

2.3.1 Spot Plate Assays	29
2.3.2 Trypan Blue Staining	29
2.4 Suppressor screen	29
2.5 Subcellular Fractionations	30
2.5.1 Whole Cell Lysate (WCL) preparation	30
2.6.2 Isolation of Mitochondria	30
2.7 RNA Isolations	31
2.8 Quantitative PCR (qPCR)	31
2.8.1 Nuclear DNA (nDNA) preparation and primer optimization	31
2.8.2 cDNA synthesis	33
2.8.3 RT-qPCR.....	33
2.8.4 Analysis & Statistics	33
2.9 Western Blotting	34
2.9.1 SDS-PAGE and Western blotting.....	34
2.9.2 Analysis.....	35
2.9.3 Oxyblot	35
2.10 Enzyme Activity Assays	36
2.10.1 COX activity	36
2.10.2 SOD activity.....	36
2.10.3 Aconitase activity.....	37
2.11 Cell Cycle.....	37
2.11.1 Sample preparation	37
2.11.2 Flow cytometry parameters.....	38
2.11.3 Analysis using FACSDiva software	38
Chapter 3: Impacts of Excess Cu	39
3.1 Optimization of Cu availability conditions in <i>S. cerevisiae</i>	39
3.1.1. Determining the appropriate concentrations of CuSO ₄ and BCS	39
3.1.2. Effect of Cu availability on cell viability.....	41
3.1.3 Response of <i>MAC1</i> and <i>CUP2</i> to extracellular Cu changes	42
3.2 Mitochondrial Cuproproteins in Cu Excess conditions.....	43
3.2.1 COX in the face of Cu excess	43
3.2.2 Sod1 in the face of Cu excess	48
3.2.3 Non-Cu related mitochondrial functions in the face in Cu excess.....	50
3.3 Summary of Results	54
Chapter 4: Analysis of Cu Deficient Conditions	55
4.1 Mitochondrial Proteins in Cu Deplete Conditions	55
4.1.1 COX in the face of Cu deficiency.....	55
4.1.2 Sod1 in the face of Cu deficiency	61
4.1.3 Non-Cu related mitochondrial functions in the face in Cu deficiency	63
4.2 Examining Cu Deficiency in Mitochondria with Galactose	67
4.2.2 Effect of carbon source on COX during Cu depletion.....	69

4.2.3 Effect of carbon source on mtSod1 during Cu depletion.....	71
4.2.4 Effect of carbon source on mitochondrial function during Cu deficiency.....	71
4.3 Summary of Results	73
Chapter 5: Cu Availability and Cell Cycle Progression	75
5.1 COX Assembly Mutants and Cell Cycle.....	75
5.2 Cu Availability and Cell Cycle Progression	77
5.3 Summary of Results	83
Chapter 6: Discussion	84
6.1 Existence of a Mitochondrial Matrix Cu Pool	84
6.2 Cox17: the outlier among COX assembly factors.....	86
6.3 Comparison of behavior of Sco1 and Cox11	90
6.4 Mitochondrial Cu Distribution with Limiting Cu	92
6.5 Divergent Cell Cycle Phenotypes with Cu Availability.....	96
6.6 Conclusions and Future directions	98
References	101
Appendix A: qPCR Data with Galactose as a Carbon Source	116

List of Figures

Chapter 1: Introduction

Figure 1.1 Pathways important in cellular Cu distribution.....	2
Figure 1.2 Proposed pathway for monomeric COX assembly in humans.....	10
Figure 1.3 Two unique pathways for Sod1 maturation	13
Figure 1.4 Depiction of Ccs1 and Sod1 import into mitochondria.....	15
Figure 1.5 Proposed model of Cu trafficking in mitochondria based on the CuL.....	17
Figure 1.6 Roles of GSH in the mitochondrial IMS	19
Figure 1.7 Monitoring progression of the yeast cell cycle by flow cytometry	22

Chapter 2: Materials and Methods

Figure 2.1 Sample qPCR curve.....	33
-----------------------------------	----

Chapter 3: Impacts of Excess Cu

Figure 3.1 RT-qPCR of <i>CTR1</i> and <i>CUP1</i> in Cu excess and Cu deplete conditions.....	40
Figure 3.2 Cell viability analysis with CuSO ₄ and BCS.....	41
Figure 3.3 RT-qPCR of <i>MAC1</i> and <i>CUP2</i> in Cu excess and Cu deplete conditions.....	43
Figure 3.4 RT-qPCR of <i>COX17</i> , <i>SCO1</i> , <i>COX11</i> and <i>COX4</i> in Cu excess conditions	44
Figure 3.5 Mitochondrial protein levels in Cu excess conditions.....	46
Figure 3.6 Cox17 protein levels in Cu excess conditions.....	47
Figure 3.7 COX activities in Cu excess conditions	48
Figure 3.8 RT-qPCR of <i>CCSI</i> and <i>SOD1</i> in Cu excess conditions.....	49
Figure 3.9 Sod1 protein and activity levels in Cu excess conditions	50
Figure 3.10 TCA cycle protein levels and Aco1 activity levels in Cu excess conditions	51
Figure 3.11 Oxidative damage in Cu excess conditions.....	52
Figure 3.12 Analysis of mitochondrial Lon protease in Cu excess conditions.....	53

Chapter 4: Analysis of Cu Deficient Conditions

Figure 4.1 RT-qPCR of <i>COX17</i> , <i>SCO1</i> , <i>COX11</i> and <i>COX4</i> in Cu depletion conditions.....	56
Figure 4.2 Mitochondrial protein levels in Cu depletion conditions	57
Figure 4.3 Cox17 protein levels in Cu deficiency	58
Figure 4.4 COX activities in Cu depletion conditions.....	59
Figure 4.5 Analysis of yeast on non-fermentable carbon source during Cu deficiency	60
Figure 4.6 Analysis of suppressors isolated from plates containing EG + 500 μ M BCS.....	61
Figure 4.7 RT-qPCR of <i>CCSI</i> and <i>SOD1</i> in Cu deplete conditions.....	62
Figure 4.8 Sod1 protein and activity levels in Cu deplete conditions	63

Figure 4.9 TCA cycle protein levels and Aco1 activity levels in Cu depletion conditions.....	64
Figure 4.10 Oxidative damage in Cu depletion conditions	65
Figure 4.11 Analysis of mitochondrial Lon protease in Cu depletion conditions	66
Figure 4.12 RT-qPCR of <i>CTR1</i> , <i>CUP1</i> , <i>MAC1</i> , and <i>CUP2</i> with galactose as a carbon source.....	68
Figure 4.13 Mitochondrial protein levels and COX activities with glucose (Glc) and galactose (Gal) in Cu deficient conditions	70
Figure 4.14 Sod1 protein and activity levels in glucose (Glc) and galactose (Gal)	71
Figure 4.15 TCA cycle analysis in glucose (Glc) and galactose (Gal).....	73

Chapter 5: Cu Availability and Cell Cycle

Figure 6.1 Model for Cells in Cu deficiency	93
---	----

List of Tables

Chapter 1: Introduction

Table 1.1 Known cuproproteins and their functions.....	5
--	---

Chapter 2: Materials and Methods

Table 2.1 Yeast Strains used in this study	27
Table 2.2 Media used in this study	27
Table 2.3 Primers used in this study	32
Table 2.4 List of antibodies used in this study	35

List of Abbreviations

Ace1	Activator of Cup1 expression
AD	Alzheimer disease
Aif1	Apoptosis inducing factor 1
ALS	Amyotrophic lateral sclerosis
ANOVA	Analysis of variance
APP	Amyloid precursor protein
ATP	Adenosine triphosphate
ATP7	ATPase copper transporting 7
Atx1/Atox1	Antioxidant protein 1
AOX	Alternative oxidase
BCS	Bathocuproine disulphate
Ccc2	Cross-complements Ca ²⁺ phenotype 2 protein
Ccs1	Copper Chaperone for Sod1
CDK	Cyclin dependent kinase
cDNA	Complementary DNA
COX	Cytochrome <i>c</i> oxidase
Cox	Cytochrome <i>c</i> oxidase protein
Ctr	Copper transporter
Cu	Copper
CuL	Copper ligand
CuRE	Copper responsive element
CuSO ₄	Copper sulphate
Cyc1	Cytochrome <i>c</i>
dH ₂ O	Deionized water
DMT	Divalent metal transporter
dNTP	Nucleoside triphosphate
DNA	Deoxyribonucleic acid
EG	Ethanol glycerol medium
Erv1	Essential for respiration and viability protein 1
Fe	Iron
Fet	Ferrous transporter
FeS	Iron-sulfur cluster
FES	Free energy surface
FRE	Ferric reductases
Grx	Glutaredoxin

GSH	Glutathione
hSod1	Human superoxide dismutase
HU	Hydroxyurea
IECs	Intestinal epithelial cells
IMM	Inner mitochondrial membrane
IMS	Inter membrane space
KAc	Potassium acetate medium
KD	Knockdown
KO	Knockout
LHON	Leber hereditary optic neuropathy
Mac1	Metal binding activator 1
MAT	Mating type
Mcm	Mini chromosome maintenance
MD	Menadione
Mia40	Mitochondrial IMS import and assembly
MICOS	Mitochondrial contact site and cristae organizing system
Mir1	Mitochondrial import receptor 1 protein
MMS	Methyl methanesulfonate
Mn	Manganese
mtDNA	Mitochondrial DNA
Mtf1	Metal regulatory transcription factor 1
MRE	Metal responsive element
Mrs	Mitochondrial RNA splicing factor
MTS	Mitochondrial targeting signal
mtSod1	Mitochondrial Sod1
MW	Molecular weight
OMM	Outer mitochondrial membrane
ND4	NADH dehydrogenase subunit 4
nDNA	Nuclear DNA
PCR	Polymerase chain reaction
Pic2	Phosphate carrier 2
PMS	Post-mitochondrial supernatant
PMSF	Phenylmethanesulphonyl fluoride
Por1	Porin
PQ	Paraquat
Pt	Platinum
qPCR	Quantitative polymerase chain reaction
Rad53	Radiation sensitive protein 53

RNA	Ribonucleic acid
RNR	Ribonucleotide reductase
ROS	Reactive oxygen species
RT	Room temperature
Sco	Synthesis of cytochrome <i>c</i> oxidase
Siz1	SAP and MIZ finger domain protein 1
Sod1	Superoxide dismutase 1
STEAP	Six transmembrane epithelial antigen of prostate
SUMO	Small ubiquitin like modifier
TMPD	<i>N, N, N', N'</i> -tetramethyl- <i>p</i> -phenylenediamine dihydrochloride
TOM	Translocase of the outer membrane
TRAF	TNF-receptor associated factor 4
WD	Wilson disease
WO	Yeast nitrogen-base medium without amino acids
WCL	Whole cell lysate
wtSod1	Wild type Sod1
XIAP	X-linked inhibitor of apoptosis
Yck	Yeast casein kinase
YPD	Yeast peptone dextrose medium
YPGal	Yeast peptone galactose medium
Ysl	Yellow-Stripe 1-Like
Zn	Zinc

Chapter 1: Introduction

1.1 Copper (Cu) Homeostasis in Eukaryotes

Copper (Cu) is crucial for cell function and survival, and plays important roles in enzyme-catalyzed metabolic processes, transport of cargo through cellular membranes, and protein breakdown. Over the past few decades, the proteins and pathways known to regulate Cu homeostasis in yeast and mammalian cells have been studied in detail. However, many questions related to Cu trafficking in and out of organelles and regulation of cross-talk between Cu-dependent pathways remain unanswered. In a healthy cell, intracellular concentrations of Cu are approximately 10^{-18} M (Rae *et al*, 1999). It is suggested that intracellular Cu does not exist as a free radical – instead, it is bound to a cuproprotein (Cu-containing protein) or a signaling molecule, such as glutathione (GSH) (Maryon *et al*, 2013). Cellular Cu homeostasis is critical since both Cu deficiency and excess are toxic to cells and cause a variety of disease phenotypes (discussed in section 1.2). Reduced concentrations of Cu result in poor functionality of Cu-dependent proteins and higher than normal Cu levels lead to the Fenton reaction, which produces the toxic hydroxyl radical.

Many known cuproproteins were initially discovered in the model organism *Saccharomyces cerevisiae*. The majority of Cu metabolic and regulatory pathways are conserved between *S. cerevisiae* and higher eukaryotes (Figure 1.1) (Nevitt *et al*, 2012) and studies in yeast continue to shed further light on our understanding of Cu metabolism and disease in humans.

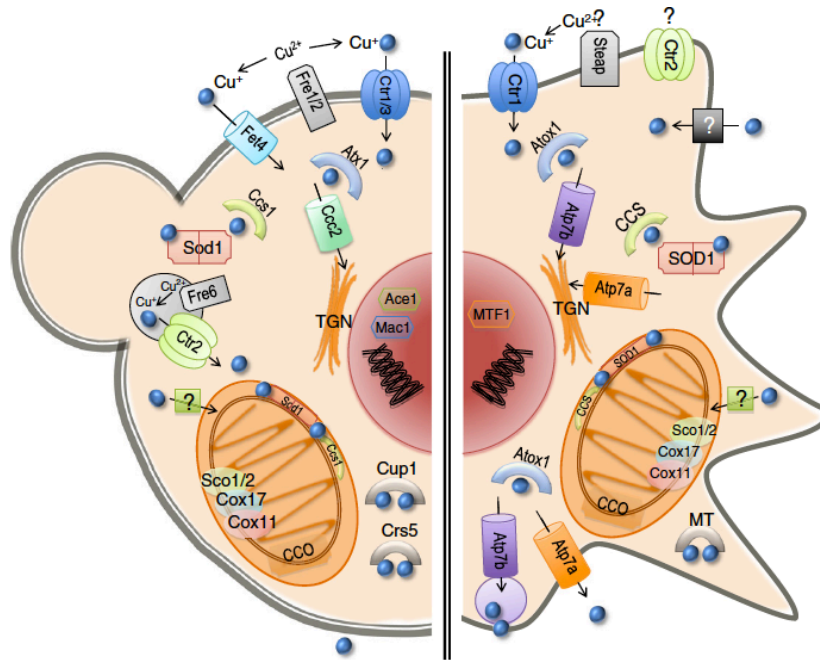


Figure 1.1 Pathways important in cellular Cu distribution

Comparison of pathways involved in Cu homeostasis in yeast (left) and mammalian cells (right). Many pathways are conserved from yeast to mammalian systems (Nevitt *et al*, 2012).

1.1.1 Cellular Cu import

Before Cu enters the cell it must be in a Cu^+ (cuprous) state, which is accomplished by cell surface reductases. In mammalian systems, the Six Transmembrane Epithelial Antigen of Prostate (STEAP) family proteins are known for their roles in extracellular Cu and iron (Fe) reduction (Ohgami *et al*, 2006). Steap2 was discovered first and this was followed by discovery of homologs Steap3 and Steap4 (Ohgami *et al*, 2006). Interestingly, some Steap family proteins have been shown to be overexpressed in human cancers and are thought to be a viable therapeutic (Gomes *et al*, 2012).

In yeast, the Ferric REDuctases 1 and 2 (Fre1/2), which were originally discovered to reduce extracellular Fe (Dancis *et al*, 1992), were also shown to be able to reduce extracellular Cu (Hassett & Kosman, 1995) (Georgatsou *et al*, 1997). It was also reported that Fre1 is transcriptionally upregulated during Cu-deficient conditions in yeast (Gross *et al*, 2000).

Cu enters the cell using Cu-specific transporters on the plasma membrane, the Copper TRANSPORTER (Ctr) proteins. Ctr1 was the first Cu specific importer discovered in *S. cerevisiae* (Dancis *et al*, 1994) and a mammalian ortholog, which serves a similar function, was identified soon thereafter (Zhou & Gitschier, 1997). Four Cu^+ atoms bind to each monomer

of Ctr1 on the extracellular amino terminus of the protein, then are carried across the lipid bilayer and handed off to Cu chaperones at the Ctr1 carboxy terminus in the cytosol (Öhrvik & Thiele, 2014). Other membrane proteins have also been shown to translocate Cu into the cell in yeast; similarly to Ctr1, Ctr3 is also a high-affinity transporter on the plasma membrane (Nevitt *et al*, 2012). On the other hand, Ctr2 is associated with low-affinity Cu transport and resides on the vacuolar membrane (Kampfenkel *et al*, 1995). Additionally, FERrous Transporter 4 (Fet4), originally identified as a Fe transporter, can transport Cu across the plasma membrane (Nevitt *et al*, 2012).

1.1.2 Cellular Cu export

Cu export is very important in human cells, based on Cu circulation around the body, and is carried out by two isoforms of the ATPase copper transporting 7 (Atp7) protein: Atp7 alpha (Atp7a) and Atp7 beta (Atp7b). Dietary Cu is absorbed into the bloodstream via the intestine, where Cu is imported into intestinal epithelial cells (IECs) and exported through the basement membrane into the blood stream. Atp7a, a protein that lies on the Golgi membrane, performs this process by transportation to the basement membrane through vesicular trafficking mechanisms (Ohja & Prasad, 2016). Additionally, Atp7a is responsible for bringing Cu across the blood-brain barrier (Ohja & Prasad, 2016). In contrast, Atp7b is primarily expressed in the liver and functions to excrete excess Cu from the body through the bile duct. In cells where both isoforms are present, their trafficking properties differ, highlighting their distinct roles in a single cell (Linz & Lutsenko, 2007).

In yeast, the Cross-Complements Ca^{2+} phenotype 2 protein (Ccc2) is orthologous to human Atp7a and Atp7b. In fact, a yeast Ccc2 knockout (KO) is complemented by both Atp7a and Atp7b, demonstrating overlap in their functionalities (Hung *et al*, 1997) (Payne & Gitlin, 1998). Both Cu and Fe can also recover the sick phenotype present in the Ccc2 KO, and this observation led to the discovery of the role of Ccc2 in delivery of Cu to Fet3, a cell surface Fe transporter (Yuan *et al*, 1995).

1.1.3 Cu chaperones

Because Cu is thought not to exist freely in the cell, it travels to its subcellular destinations while bound to Cu chaperones. Currently, three Cu chaperone proteins are accepted to play major roles in delivery of Cu to its subcellular destinations. In yeast, two of these Cu chaperones have been found to interact directly with Ctr1: AnTioXidant protein 1 (Atx1) and Copper Chaperone for Sod1 (Ccs1) (Nevitt *et al*, 2012). Cytochrome Oxidase protein 17 (Cox17) is the other accepted Cu-chaperone that is responsible for delivery of Cu to cytochrome *c* oxidase (COX), the final electron acceptor in the electron transport chain, but it has not been shown to interact with Ctr1.

Atx1, which was initially shown to suppress the oxidative damage phenotype seen in yeast lacking a functional SuperOxide Dismutase 1 gene (*SOD1*), was later found to deliver Cu to Ccc2 (Lin *et al*, 1997), a trans-Golgi resident protein involved in cellular Cu efflux. In humans, Atox1 is the ortholog of Atx1 and delivers Cu to both Atp7a and Atp7b. Ccs1, which is found in both yeast and humans, is now the accepted Cu chaperone for Sod1 (Fetherolf *et al*, 2017). Sod1 has an important role in antioxidant defense and is dually localized to the mitochondria and cytosol (see section 1.3). Ccs1 knockouts in yeast have defects in lysine metabolism, and therefore Sod1 and Ccs1 knockouts in yeast are unable to grow without supplemented lysine (Culotta *et al*, 1997).

Many other potential Cu-chaperones have been discovered but do not have a defined delivery pathway or final destination. There are also many cuproproteins that do not have a strictly defined Cu-chaperone (Table 1.1), suggesting that there are likely undiscovered Cu-chaperones or defined Cu-chaperones that are multifunctional. Further research is needed in order to understand regulation of the distribution of Cu around the cell.

Table 1.1 Known cuproproteins and their functions

Many of these proteins do not have a defined Cu-chaperone (modified from Turski & Thiele, 2009)

Protein	Function
Cu, Zn Superoxide Dismutase	Superoxide disproportionation; signaling
Cytochrome <i>c</i> Oxidase	Mitochondrial oxidative phosphorylation; ATP production
Tyrosinase/Laccase	Melanin synthesis; virulence and pathogenicity in fungi; innate immunity
Peptidylglycine alpha-amidating monooxygenase	Peptide amidation/maturation
Dopamine beta-hydroxylase	Noradrenaline synthesis
Ceruloplasmin	Ferroxidase: Fe loading onto transferrin
Hephaestin	Ferroxidase for ferroprotein-mediated iron efflux
Lysyl Oxidase	Covalent cross-linking of collagens and elastin
Lysyl Oxidase-like proteins	Oxidation of snail transcription factors resulting in E-cadherin silencing and promoting EMT
Coagulation Factors V and VIII	Blot clotting
Nitrous Oxide Reductase	Catalyzes reduction of N ₂ O to N ₂ in denitrification pathway of bacteria
Ethylene Receptor	Ethylene signal transduction
XIAP	Inhibitor of apoptosis
Ace1	<i>S. cerevisiae</i> transcription factor active under conditions of high intracellular copper
Copper Amine Oxidase	Deamination of primary amines to aldehyde

1.1.4 Cu-responsive transcription factors

Since both Cu excess and Cu deficiency lead to cellular toxicity, the cell quickly responds to these circumstances by initiating transcription of proteins that will help mitigate the resulting cellular stress. Metal binding activator 1 (Mac1) is a transcription factor in yeast that responds to low concentrations of Cu by binding to a Cu responsive element (CuRE) on nuclear DNA to promote transcription of Ctr1 and Ctr3 (Nevitt *et al*, 2012). In contrast, Activator of Cup1 expression (Ace1), another Cu-responsive transcription factor in yeast, is activated by high concentrations of Cu and promotes transcription of metallothioneins and other genes that have roles in antioxidant defense (Nevitt *et al*, 2012).

For their activity, Mac1 and Ace1, which are localized to the nucleus, are required to bind Cu. Mac1 always has Cu bound and is activated when Cu levels are below a given threshold: above the threshold, the enzyme is inactive (Keller *et al*, 2005). Ace1 behaves reciprocally and is activated when Cu levels are high. Metalation of Mac1 and Ace1 and their regulation have been shown to be independent of each other (Keller *et al*, 2005). Even though both of these nuclear proteins require Cu for function, no pathway for Cu import into the

nucleus has been established and no Cu chaperone for these transcription factors has yet been identified. Transcription initiation in response to changing Cu levels in humans is poorly understood. A nucleocytoplasmic protein, metal regulatory transcription factor 1 (Mtf1), is known to induce transcription of metallothioneins in response to heavy metals and does so by binding to a metal responsive element (MRE) on DNA (Saydam *et al*, 2003).

1.2 Cu Related Diseases

1.2.1 Historical context of Cu disorders

Historically, Cu disorders are classified by an imbalance in cellular Cu concentration. Wilson disease (WD) was described by Kinneer Wilson in 1912 and is classified as an autosomal recessive disorder (Rodriguez-Castro *et al*, 2015). WD is caused by a class of mutations in *Atp7b*, the protein responsible for excretion of Cu through the bile duct. Minimal function of *Atp7b* in the liver causes toxic amounts of Cu to build up in both the liver and other organs in the body, leading to the disease phenotype.

Onset of WD happens in early childhood or teenage years and usually presents as a liver problem, which is sometimes accompanied by neurological or psychiatric problems. The treatment of WD is aimed at chelating Cu so it is no longer toxic, either by induction of metallothioneins or with Cu chelating chemicals that aim to prevent Cu absorption into the bloodstream (Rodriguez-Castro *et al*, 2015). In severe cases of WD, liver transplantation may be required.

In contrast to WD, Menkes disease is classified by having a global Cu deficiency in the body and is an X-linked recessive disorder caused by mutations in *Atp7a*. Because *Atp7a* functions to bring Cu from the digestive tract into the bloodstream, mutations lead to poor absorption of Cu and result in dysfunction of important cuproproteins (Ohja & Prasad, 2016).

Menkes disease patients have a life expectancy ranging from 3 months - 3 years; disease symptoms usually present between 6 - 8 weeks of life with seizures and neurological regression, caused by a Cu deficiency in the brain. Another common symptom of patients is kinky hair, which is due to a deficiency in the cuproprotein lysyl oxidase. The most effective treatment for these patients is Cu-histidine, which works to get more Cu into the bloodstream, but is not always successful as the lifespan of these patients is extremely short (Ohja & Prasad, 2016).

1.2.2 Implications of Cu defects in mitochondrial and neurodegenerative disorders

More recently, it has been appreciated that imbalance in cellular Cu availability is present in a broader scope of diseases. Mutations in Suppressor of Cytochrome Oxidase deficiency 1 and 2 (Sco1/2), two inner mitochondrial membrane (IMM) cuproproteins that are important for respiratory chain function, have been shown to cause mitochondrial defects, and are also correlated with cellular Cu deficiency (Baker *et al*, 2017b). Because of their role in respiration, patients with mutations in Sco1 and Sco2 have severe problems with ATP production. While many pedigrees have been mapped to the E140K mutation in Sco2, Sco1 mutations are more rare and are found throughout the protein sequence (Baker *et al*, 2017a). Interestingly, no mutations in other mitochondrial cuproproteins, such as Cox11 and Cox17, have been implicated in mitochondrial diseases.

Although Sco1 and Sco2 have similar functions, mutations in these proteins lead to different clinical phenotypes. Mutations in Sco1 result in hepatopathy, while mutations in Sco2 lead to cardiomyopathy, and both types of mutations are associated with encephalopathy (Leary *et al*, 2007). Mitochondrial disease patients are given a mixture of non-toxic dietary supplements including coenzyme Q, lipoic acid, and creatine that ameliorates symptoms, but there is no definitive evidence of their effectiveness as a treatment (Rak *et al*, 2016). Recently, gene therapy has been more promising for treatment of mitochondrial defects. Symptoms of Leber Hereditary Optic Neuropathy (LHON), another type of mitochondrial disorder, were reversed in a mouse model by allotropically expressing NADH dehydrogenase subunit 4 (*ND4*) (Cwerman-Thibault *et al*, 2015). Other treatments for mitochondrial disease have been aimed at minimizing oxidative stress, but these are less promising as there is no clear evidence that a mitochondrial deficiency is associated with increased levels of oxidative stress (Rak *et al*, 2016).

Cu homeostasis is also implicated in neurodegenerative disease. Alzheimer's disease (AD) patients have severe memory problems and struggle to complete familiar tasks, which is thought to be partially caused by the presence of amyloid beta ($\text{a}\beta$) plaques in the brain, leading to destruction of nerve connections. Amyloid precursor protein (APP), which is cleaved to form the $\text{a}\beta$ plaques seen in AD, is important for transport of Cu into the brain (Macreadie, 2008). Studies have also shown that changing Cu concentration correlates with regulation of $\text{a}\beta$ folding and regulation (Singh *et al*, 2013) (Lang *et al*, 2013). Although many

Alzheimer's drugs have been targeted towards the $\text{A}\beta$ plaques, none of them have proven to be successful in reversal of symptoms. Drug development work for AD is moving towards targeting pathways adversely affected in AD brains, such as Cu transport and regulation.

Similar to AD, amyotrophic lateral sclerosis (ALS) is a fatal neurodegenerative disease that affects motor neurons in the brain stem, spinal cord, and cortex (Valentine *et al*, 2005), and cells display Cu trafficking defects. While 10% of patients have mutations linked to ALS, the other 90% of cases are sporadic. Both familial ALS (FALS) and sporadic ALS (SALS) cases have been linked to dysfunction of Sod1, a cuproprotein that plays an important role in oxidative stress (Rosen *et al*, 1993) (Graffmo *et al*, 2013). More than 150 mutations in the *SOD1* gene have been identified in FALS patients, which all lead to presentation of similar clinical phenotypes. These Sod1 mutations are characterized as gain-of-function because Sod1 KO mouse models did not develop ALS (Reaume *et al*, 1996) and the observation that wild-type Sod1 (wtSod1) on its own can lead to ALS symptoms (Martins & English, 2014) (Graffmo *et al*, 2013). Only one drug, a glutamate antagonist, has been approved for ALS treatment and works to extend median survival of ALS patients (Georgouloupoulou *et al*, 2013).

1.3 Cu and Mitochondrial Function

The mitochondria are home to two important Cu-containing enzymes: COX and Sod1. Therefore, mitochondrial function is greatly influenced by both intracellular and extracellular Cu levels. Besides cuproproteins, it is thought that the remaining 70-80% of mitochondrial Cu is attached to a non-proteinacious structure, termed the Cu ligand (CuL), which exists in the mitochondrial matrix (Cobine *et al*, 2004). The CuL pool in the matrix was shown to be the source of Cu for both COX and mitochondrial Sod1 (mtSod1) (Cobine *et al*, 2006). More recently, work has focused on the impact of mitochondrial cuproproteins on broader cellular Cu homeostasis. Overall, it seems that mitochondrial Cu is a central signaling point, yet the mechanisms surrounding this hypothesis have yet to be studied in detail.

1.3.1 Cytochrome c Oxidase (COX) function and assembly

Located on the IMM, COX is the terminal electron acceptor in the electron transport chain and harbours three Cu atoms. COX has two main functions: to reduce molecular oxygen and to pump protons into the inter-membrane space (IMS). Oxygen becomes reduced as electrons are passed one-by-one from cytochrome *c* (Cyc1) and proton translocation contributes to the mitochondrial electrochemical gradient. The catalytic core of COX is extremely hydrophobic and is made of three mitochondrial-encoded subunits (Cox1, Cox2, Cox3) that are surrounded by other subunits to form an 11-subunit (yeast) or 13-subunit (mammalian) holoenzyme (Timon-Gomez *et al*, 2018). The catalytic core incorporates two Cu centres during the assembly process. The Cu_A site, located in the Cox2 subunit, contains two Cu atoms and is important for accepting electrons from Cyc1. On the other hand, the Cu_B site is incorporated into Cox1 and has a single Cu atom that helps catalyze proton movement through the enzyme (Blomberg & Siegbahn, 2014).

COX assembly is a complex process, with subunits encoded on both genomes and the need to coordinate the incorporation of multiple prosthetic groups. More than 40 proteins, referred to as assembly factors, are required for generation of the holoenzyme. A big question in studying COX assembly has been whether subunits are added in a linear or modular fashion. The linear model proposes that subunits are added one-by-one, while the modular approach suggests that individual parts are made first and then put together at the end. In humans, the most likely scenario according to a recent review is a combination of these two theories. Three core entities are assembled individually, each of them containing one of the mitochondrial DNA (mtDNA) encoded proteins, and then these are added in a linear fashion to create a fully functional COX (Figure 1.2). There is evidence that COX exists as part of a respiratory supercomplex and that if a COX monomer were to be incorporated into that supercomplex the assembly pathway would change (Timon-Gomez *et al*, 2018).

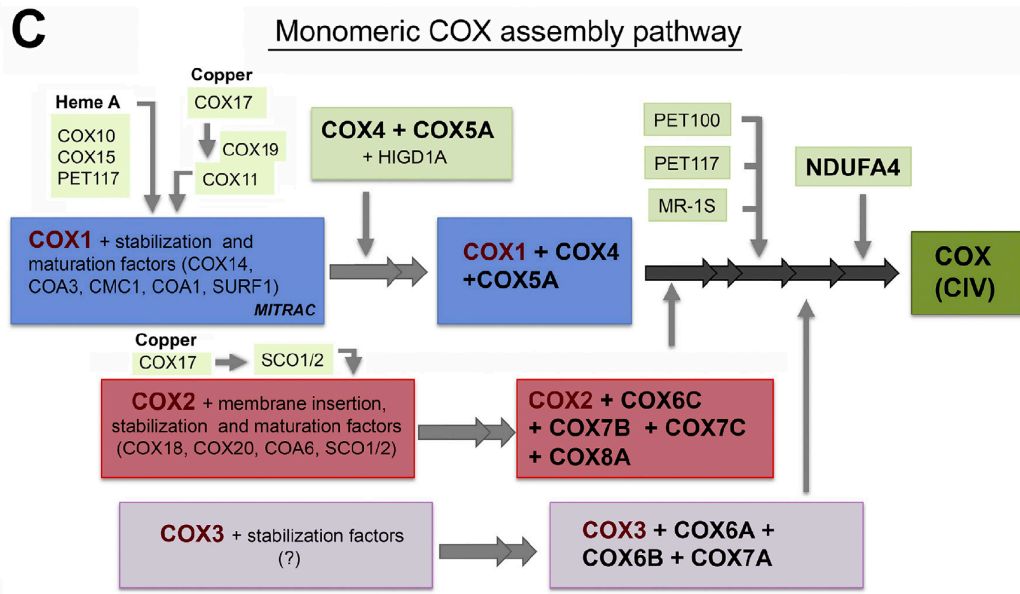


Figure 1.2 Proposed pathway for monomeric COX assembly in humans

Three core entities centered on Cox1, Cox2, and Cox3 are assembled individually and added in a modular fashion to form a fully functional COX monomer (Timon-Gomez *et al*, 2018)

1.3.2 Delivery of Cu to Cox1 and Cox2

As stated above, COX contains a Cu_A site in Cox2 that requires two Cu atoms for function, and a Cu_B site in Cox1 that requires one Cu atom for function. The work to understand the mechanism of Cu delivery to COX was originally carried out in yeast. Cox17 was the first protein defined to have a role in Cu delivery to COX due to the finding that a Cox17 KO in yeast has a COX defect, which can be rescued with excess Cu (Glerum *et al*, 1996a). Cox17 is a small, cysteine-rich protein that is dually localized: 40% exists in the cytoplasm and the remaining 60% is found in the IMS of mitochondria (Beers *et al*, 1997). Overexpression of either of the homologous transmembrane proteins Sco1 or Sco2 can recover the COX deficiency in the yeast Cox17 KO (Glerum *et al*, 1996b), demonstrating that these proteins also play roles in Cu delivery to COX. Additionally, Sco1 and Sco2 are able to exchange Cu (Banci *et al*, 2008) but have non-overlapping functions in COX assembly (Glerum *et al*, 1996b). Thorough characterization of Sco1 led to the hypothesis that Sco1 delivers Cu specifically to the Cu_A site in Cox2 (Beers *et al*, 2002). The observations that Sco1 physically interacts with Cox2 (Lode *et al*, 2000) and that Sco1 can bind both Cu^+ and Cu^{2+} (Timon-Gomez *et al*, 2018) both provide strong evidence to support this hypothesis.

Another transmembrane protein, Cox11, was identified to deliver Cu to the Cu_B site in Cox1 based on studying the bacterium *Rhodobacter sphaeroides* (Hiser *et al*, 2000). In a

R. sphaeroides Cox11 KO, assembly of COX is incomplete because of the lack of Cu_B, indicating that Cox11 is likely responsible for incorporation of this metal centre (Hiser *et al*, 2000). Together, Cox17, Sco1, and Cox11 were predicted to transfer Cu in a bucket brigade fashion: Cox17 donates Cu to Sco1 and Cox11, which then integrate it into the respective sites of COX. This model was justified *in vitro* when purified Cox17 was able to transfer Cu to Sco1 and Cox11 (Horng *et al*, 2004). The model was also shown to work in the cytoplasm of yeast when Sco1 and Cox11 had their mitochondrial targeting signals (MTSs) and transmembrane domains removed; they could not obtain Cu unless they were co-expressed with Cox17 (Horng *et al*, 2004).

The discovery of other COX assembly factors that were suggested to have a role in Cu delivery to COX resulted in adjustments to the initial model. Because Cox17 point mutants showed a specific loss of Cox2, it was proposed that in the IMS, Cox17 delivered Cu to only Sco1 (Punter & Glerum, 2003). More recently, it has been speculated that Cox16 may also be involved in delivery of Cu to Cox2 because of its physical interaction with both Sco1 and Cox2 (Aich *et al*, 2018). Similar to Cox17, Cox19 and Cox23 also bind Cu and deletion of their genes results in an isolated COX deficiency (Nobrega *et al*, 2002) (Barros *et al*, 2004). One proposal is that Cox19 and Cox23 play roles upstream of Cox17 in delivery of Cu to COX (Horn & Barrientos, 2008). However, other evidence suggests that Cox19 is only involved in delivery to the Cu_B site because of its redox-based interaction with Cox11 (Bode *et al*, 2015). Alternatively, Cox19 and Cox23 could work together to deliver to the Cu_B site since a mutation in Cox1 rescued the COX deficiency of a Cox23 KO in yeast (Dela Cruz *et al*, 2016).

Two other proteins, Pet191 and Cmc1, have been thought to have roles in Cu delivery to COX due to their ability to bind Cu, their localization to the IMM, and the fact that KO strains display a loss in respiratory function. Pet191 is unique because, unlike other mitochondrial cuproproteins, it does not use the Mitochondrial IMS import and Assembly 40 (Mia40) pathway for mitochondrial import (Khalimonchuk *et al*, 2008). Cmc1 is suggested to be involved in regulation of distribution of Cu between COX and Sod1 (Horn *et al*, 2008). There are no clear hypotheses of how they function in conjunction with Sco1, Cox11, Cox17, Cox19, and Cox23.

1.3.3 Superoxide dismutase 1 (Sod1) function and assembly

Sod1 is a 32 kDa homodimeric protein that plays a central role in the management of oxidative stress and is dually localized: approximately 10% of Sod1 exists in the IMS of mitochondria, with the other 90% existing in the cytosol. The main function of Sod1 is to break down superoxide into oxygen and hydrogen peroxide, which reduces cellular oxidative stress (Valentine *et al*, 2005). Breakdown of superoxide by Sod1 has been shown to take place in the nucleus, cytosol, mitochondria, and peroxisomes of eukaryotic cells (Wood & Thiele, 2009) (Tsang *et al*, 2014) (Reddi & Culotta, 2013) (Islinger *et al*, 2009), suggesting that Sod1 may also exist in other cellular compartments. Cu lies at the dimer interface of Sod1 and is crucial for the catalytic mechanism of dismutating superoxide (Tainer *et al*, 1983), participating *via* a two-step process. In the first step, Cu takes an electron from a molecule of superoxide and it becomes oxidized to form molecular oxygen. In the second step, Cu donates that electron back to another molecule of superoxide to reduce it to hydrogen peroxide (Tainer *et al*, 1983). Sod1 dimers also contain two zinc (Zn) atoms, which were initially thought to be a structural component of this protein, but more recent work suggests that Zn is required for Sod1 catalytic activity (Nedd *et al*, 2014). It is thought that the function of mtSod1 is to remove superoxide released by the respiratory chain, although this has never been directly demonstrated. Moreover, this is at odds with the fact that Sod2, the Mn-Sod located in the mitochondrial matrix, is already well known for this role. Thus, the function of mtSod1 continues to be a mystery.

Folding of Sod1 into the fully metallated homodimer is a complex process due to the numerous conformations that immature forms of the protein can exhibit, and it is hypothesized that overpopulation of these immature forms leads to formation of the toxic aggregates that are observed in ALS (Karch *et al*, 2009). The fully mature Sod1 homodimer (Cu,Zn-Sod1^{S-S}) is extremely stable (Stathopulous *et al*, 2006) and is formed by non-metallated (apoSod1^{2SH}) molecules maturing through many events that gradually increase stability (Furukawa *et al*, 2004). A recent report suggests that throughout the maturation steps of Cu,Zn-Sod1^{S-S}, the free-energy surfaces (FESs) become smoother, suggesting the protein is less likely to aggregate as it matures (Figure 1.3) (Culik *et al*, 2018). Whether the apoSod1^{2SH} first binds Zn or makes the intramolecular disulfide bond greatly influences the affinity of Ccs1, the Cu chaperone for Sod1, for the dimer. If Zn binds first, the monomers

will form a preorganized dimer interface that has a high affinity for Ccs1 binding and Cu delivery. However, if the disulfide forms first, the binding with Ccs1 is much weaker. Therefore, the protein will preferentially populate the E,Zn-Sod1^{2SH} state (addition of Zn before formation of disulfide) instead of the apoSod1^{S-S} state (formation of the disulfide before addition of Zn) to enhance binding with the Cu chaperone (Culik *et al*, 2018). In addition to helping with the insertion of Cu, there is also evidence that Ccs1 mediates intermolecular disulfide bond formation (Fetherolf *et al*, 2017), however the mechanism for this process remains unknown.

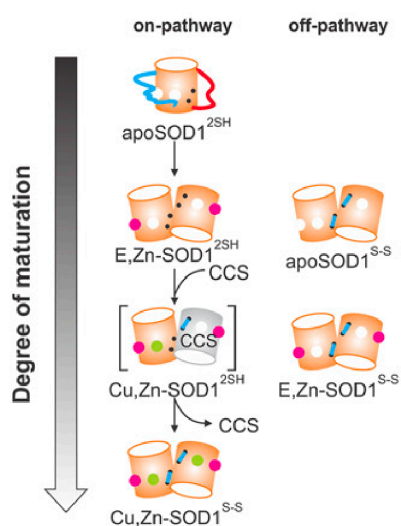


Figure 1.3 Two unique pathways for Sod1 maturation

In the on-pathway, Zn is added to before formation of the disulfide, while the opposite occurs in the off-pathway (Culik *et al*, 2018)

1.3.4 Cu delivery to Sod1 in the absence of Ccs1

Although the apoSod1^{S-S} state has a lower affinity for the Ccs1 chaperone, it can still be populated by Cu because Sod1 is able to gain the metal independent of Ccs1 (Carroll *et al*, 2004) (Sea *et al*, 2013). A Ccs1-independent pathway was originally discovered for human Sod1 (hSod1) and is suggested to happen in a GSH-mediated fashion (Carroll *et al*, 2004). Interestingly, *C. elegans* has no Ccs1 homolog and must therefore activate Sod1 independently of Ccs1 (Jensen & Culotta, 2005). *S. cerevisiae* Sod1 also exhibits a Cu acquisition pathway independent of Ccs1, but the mechanism for this remains unclear (Sea *et al*, 2013). Currently, there are no known species in which the activation of Sod1 is completely dependent on Ccs1.

It is easy to hypothesize that delivery of Cu to Sod1 in the absence of Ccs1 can happen via other copper chaperones in the cell, such as Atx1 or Cox17. However, this possibility is not likely the case as neither Atx1 nor Cox17 overexpression can rescue the Ccs1 knockout phenotype (Carroll *et al*, 2004). In addition, other COX assembly proteins that localize in the mitochondria have not been shown to donate Cu to Sod1 (Kawamata & Manfredi, 2008). Two alternate Cu donors that may be involved are GSH, which is suggested to be involved in Ccs1-independent activation of hSod1 (Carroll *et al*, 2004) or the anionic Cu ligand in the mitochondrial matrix that is suggested to contain up to 85% of mitochondrial Cu (Cobine *et al*, 2004). This ligand also exists in the cytosol in a mostly non-metallated form, but the small proportion that is metallated has potential to donate a copper atom to Sod1 (Sea *et al*, 2013). Overall, the Ccs1-independent pathway for Sod1 intermolecular disulfide bond acquisition is poorly understood and requires further investigation.

1.3.5 Cu delivery to Sod1 in the mitochondria and cytosol

The nature of mitochondrial import dictates that proteins entering the mitochondria must be unfolded. Therefore, both Ccs1 and Sod1 must enter the mitochondria without Cu, since Cu binding requires a protein in its secondary structure. Ccs1 enters mitochondria through the translocase of the outer membrane (TOM) and then uses the Mia40/Erv1 import relay, where it gains its disulfide bond (Kawamata & Manfredi, 2010). If Sod1 also used the Mia40/Erv1 import machinery, then Sod1 would form the disulfide bond before gaining the metals, which provides a less effective binding surface for Ccs1 (Culik *et al*, 2018). Alternatively, if Sod1 were to enter mitochondria using TOM and not interact with the Mia40/Erv1 system, Ccs1 could mediate both the formation of the disulfide and addition of Cu (Figure 1.4). Intracellular partitioning of Ccs1 determines Sod1 distribution between the mitochondria and cytosol (Kawamata & Manfredi, 2010), suggesting some Sod1 molecules interact with Mia40 and others do not. This is in conjunction with the observation that in a Ccs1 KO, Sod1 only enters mitochondria via the Mia40/Erv1 import relay (Varabyova *et al*, 2013). The questions still remain: in the absence of Ccs1, how does mtSod1 get Cu? And in the presence of Ccs1, how does mitochondrial Ccs1 get its Cu?

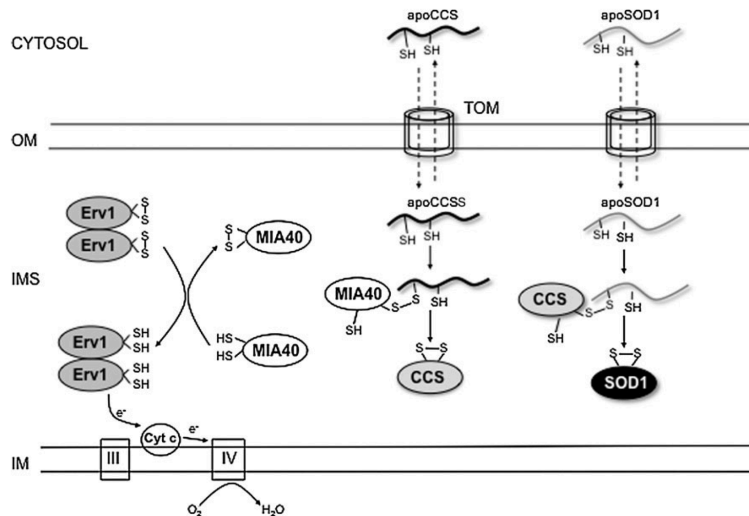


Figure 1.4 Depiction of Ccs1 and Sod1 import into mitochondria

In this illustration, Ccs1 mediates formation of the Sod1 disulfide bond, since Sod1 does not interact with the Mia40/Erv1 import relay (Kawamata & Manfredi, 2010)

1.4 Mitochondrial Cu Import

The pathways for Cu delivery to COX and Sod1 have been studied in detail, but the starting point for these mechanisms is in the IMS and how Cu is delivered to the IMS is still a mystery. With Ctr1 located on the plasma membrane and no free Cu in the cell, there is clearly a need for Cu chaperones for delivery of the metal to mitochondria.

1.4.1 Cu import *via* a dually-localized Cu chaperone

Cox17 was first discovered to exist in the cytosol (Glerum *et al*, 1996a) and was proposed to act as a Cu shuttle between the cytosol and IMS (Beers *et al*, 1997). Theoretically, Cox19 and Cox23 can also carry out this role since they are both homologous to Cox17. The proposed model is that one of Cox17, Cox19, or Cox23 picks up Cu in the cytosol, crosses the outer mitochondrial membrane (OMM), and then delivers Cu to COX *via* Sco1 and Cox11. This also suggests that one of these COX assembly factors is the starting point of Cu delivery to Sod1 in the IMS, and can deliver Cu to newly folded Ccs1 once it crosses the OMM.

Once piece of evidence that supports this theory is the fact that Cox17 is thought to be involved in cisplatin delivery to mitochondria (Zhao *et al*, 2014). Cisplatin is a platinum (Pt) drug that is used to treat cancer, and is known to cause DNA damage in cancer cells. Specifically, the cisplatin mode of action involves its delivery to mitochondria and mutation

of mtDNA to induce apoptosis (Wisnovsky *et al*, 2013). Overexpression of Cox17 with cisplatin led to increased apoptosis in cells, suggesting that Cox17 was mediating cisplatin delivery to mitochondria. On the other hand, knockdown (KD) of Cox17 led to cisplatin being less effective at promoting apoptosis (Zhao *et al*, 2014). These results are also in conjunction with results from the Glerum lab suggesting that Cox17 exhibits pro-apoptotic properties in yeast (Dubinski, unpublished). Additionally, cisplatin is found to bind Cox17 at the same site in which it binds Cu (Zhao *et al*, 2014). Taken together, these results support the pathway that Cox17 shuttles Cu into the mitochondria.

If Cox17 did deliver Cu to the mitochondria, then its affinity for Cu should be higher in the cytosol than in the IMS. Cox17 carries approximately 0.2 – 0.3 mol of Cu per mol of protein, but how this differs between the cytosol and IMS is unknown (Beers *et al*, 1997). Unfortunately, purification of Cox17 is difficult because tagging the protein interferes with both its location and its function.

In 2004, Maxfield *et al* performed an experiment in which they tethered Cox17 to the IMM by fusing the protein to the transmembrane domain of Sco2. Therefore, all Cox17 in cells was trapped in the mitochondria. Overexpression of the Sco2/Cox17 fusion protein in a Cox17 KO in yeast resulted in complete rescue of COX function, suggesting that Cox17 is not needed for delivery of Cu from the cytosol into the mitochondria (Maxfield *et al*, 2004). However, these experiments did not consider that either Cox19 or Cox23 could also be compensating for loss of Cox17 function.

The biggest flaw in the hypothesis that Cox17 shuttles Cu into mitochondria is that folded proteins cannot cross the OMM. Cox17, Cox19, and Cox23 are 8 kDa, 11 kDa, and 17 kDa respectively. In order for them to carry Cu, they must be in a folded state, but there is no entry point to the mitochondria that is able to transport folded proteins from the OMM into the IMS. Porin 1 (Por1), a β -barrel protein residing in the OMM, is able to transport ions and small metabolites. Unless another channel that could transport proteins across the outer membrane is discovered, it seems very unlikely that one of these small cuproproteins can mediate Cu entry into mitochondria.

1.4.2 Cu is stored in the mitochondrial matrix

The discovery of CuL, which resides mainly in the mitochondrial matrix, led to another proposed model by which Cu enters the mitochondria. CuL is thought to contain up to 85% of mitochondrial Cu (Cobine *et al*, 2004) and has been shown to be the source of Cu for both mtSod1 and COX (Cobine *et al*, 2006). In 2013, Phosphate Carrier 2 (Pic2) was suggested to be one of the proteins responsible for transport into the mitochondrial matrix from the IMS (Vest *et al*, 2013). A few years later, Mitochondrial RNA splicing factor 3 (Mrs3), which is also a Fe transporter, was shown to work together with Pic2 to transport Cu into the matrix (Vest *et al*, 2016). In yeast, a double KO of Pic2 and Mrs3 leads to almost complete loss of COX activity, suggesting that these proteins have overlapping roles in Cu transport (Vest *et al*, 2016). In humans, SLC25A3 was shown to be orthologous to Pic2, and have a redundant role in transporting Cu from the IMS into the matrix (Boulet *et al*, 2017). Therefore, this model of mitochondrial Cu import proposes that Cu entering the mitochondria first travels to the mitochondrial matrix with help from Pic2 and Mrs3, and is then pumped back into the IMS where it is delivered to Ccs1 and Cox17 for incorporation into mtSod1 and COX (Figure 1.5). No method of import from the cytosol into the IMS or from the matrix back into the IMS has been proposed to date.

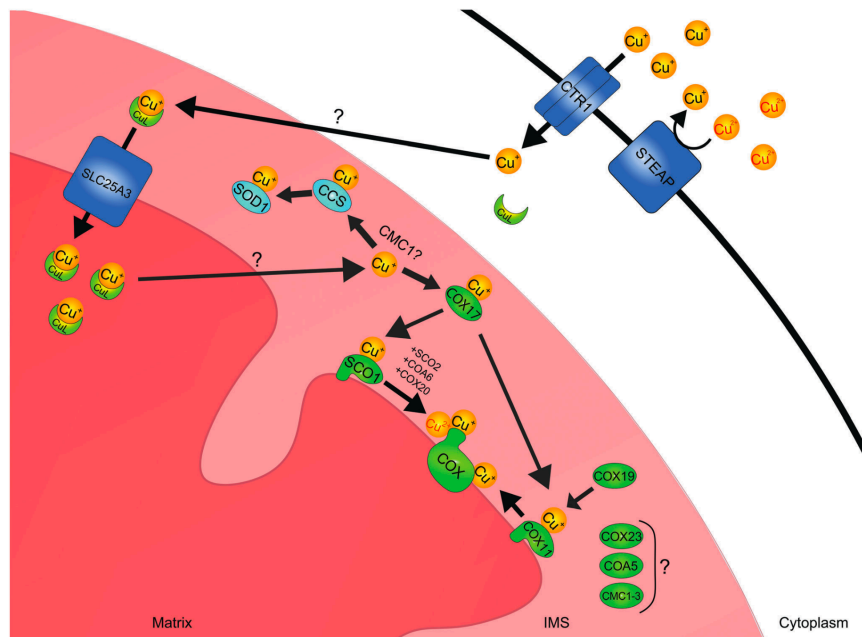


Figure 1.5 Proposed model of Cu trafficking in mitochondria based on the CuL

Cu is transported from the cytosol into the matrix with help from the SLC25A3 transporter in mammalian systems. In yeast, Pic2 is analogous to SLC25A3 (Baker *et al*, 2017a).

Since the important mitochondrial cuproproteins are located in the IMS and no known cuproproteins are known to exist in the matrix, it is difficult to imagine the matrix as a storage space for mitochondrial Cu. The big difference between the matrix and the IMS is that the mitochondrial matrix has a higher pH, which could be a reason that Cu would be stored in the matrix. If this were the case, there would also need to be a mechanism to prevent Cox17 and Ccs1 from binding to Cu that is destined for the mitochondrial matrix as it travels through the IMS.

The work surrounding this model of Cu import began with the finding of CuL (Cobine *et al*, 2004). Although an isolation protocol of CuL from cells is defined (Cobine *et al*, 2006), the structure of this non-proteinacious ligand remains unknown. Because CuL exists in both the cytosol and mitochondria, it seems likely that Cu will travel through both membranes when attached to the CuL.

Pic2 was initially defined to be a phosphate carrier that transports inorganic phosphate (Pi) into the matrix to be used by ATP synthase (Hamel *et al*, 2004). In fact, the discovery of the function of Pic2 was based on its redundancy with the Mitochondrial Import Receptor 1 protein (Mir1), which was the first known IMM mitochondrial Pi transporter. However, the work defining Pic2 as having a secondary function in Cu transport does not investigate whether Mir1 exhibits a similar function (Vest *et al*, 2013), even though Mir1 is the main Pi carrier in the IMM (Hamel *et al*, 2004). In the same article, the authors defined a Pic2 KO to have a minor respiratory defect. Since Pic2 is a phosphate transporter, the respiratory defect may be a consequence of a dysfunctional ATP synthase and not necessarily a Cu transport problem. Additionally, the Pic2/Mrs3 double KO still displays some COX activity, indicative of other Cu transport pathways (Vest *et al*, 2016).

1.4.3 Cu import *via* glutathione (GSH)

To enter the mitochondria, Cu must cross the OMM and this could happen *via* a small molecule such as glutathione (GSH). GSH is a three amino acid peptide (Glu-Cys-Gly) and is able to bind Cu through the thiol group on its cysteine residue. GSH cannot be synthesized or degraded in the mitochondria, since the mitochondrial proteome does not consist of any of the enzymes in these pathways (Calabrese *et al*, 2017). The most likely method of GSH entry into mitochondria is through Por1 and Por2, since the net negative charge on GSH restricts

passage through lipid bilayers (Calabrese *et al*, 2017). In the IMS, GSH is known to break down hydrogen peroxide to water by a reaction in which GSH becomes oxidized to GSSG, a structure in which the thiol groups on two molecules of GSH form a disulfide bond. GSH also modulates the Mia40/Erv1 pathway through an interaction with glutaredoxin 2 (Grx2) (Kojer *et al*, 2012) (Figure 1.6). Another important factor is that the GSH to GSSG ratio in the cytosol and the IMS is similar, meaning most GSH exists in a reduced state - the state that is more likely to bind Cu. The proposed mechanism for this Cu import pathway is as follows: (1) GSH is synthesized in the cytosol and obtains Cu from Ctr1 (2) Por1 and Por2 mediate GSH-Cu import into mitochondria (3) GSH-Cu located in the IMS transfers Cu to Cox17 and Ccs1 as they are imported and folded through the Mia40/Erv1 relay.

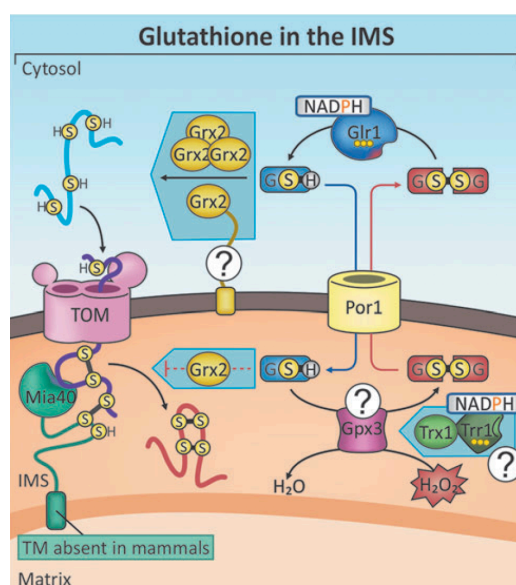


Figure 1.6 Roles of GSH in the mitochondrial IMS

GSH travels into mitochondria using OMM resident Por1 and is involved with various pathways in the IMS (Calabrese *et al*, 2017).

It has been shown previously that GSH has a large role in Cu entry into the cell through Ctr1 (Maryon *et al*, 2013). Specifically, GSH is thought to be an intermediary step between Ctr1 and the Cu chaperones Ccs1 and Atox1, strongly suggesting that a GSH-Cu complex forms in the cytosol and theoretically could travel into mitochondria. Because GSH is thought to enter mitochondria through Por1 and Por2 and a GSH-Cu complex could be the source of Cu for mtSod1 and COX, a Por1/Por2 double KO should negatively impact both mtSod1 and COX activity. In fact, during the first characterization of Por2 the authors reported that a Por1/Por2 double KO does not grow on glycerol, a non-fermentable carbon

source, suggesting the strain may have a COX defect (Blachly-Dyson *et al*, 1997). Additionally, our lab has demonstrated that a COX defect is not necessarily associated with increased oxidative stress (Dubinski *et al*, 2018), and the Por1 KO in yeast is associated with decreased oxidative stress (Magri *et al*, 2016). One explanation for the decreased oxidative stress in the Por1 KO could be the loss of COX activity, which is caused by limited Cu transport into the mitochondria.

If the GSH-Cu complex does enter mitochondria, it must lose Cu to other cuproproteins. Using *in vitro* affinity measures, it was demonstrated that both Cox17 and Ccs1 have much higher affinities for Cu than GSH (Banci *et al*, 2010), meaning Cu transfer from GSH to these cuproproteins is feasible. Another report demonstrated delivery of Pt from GSH to Cox17 (Zhao *et al*, 2015), further supporting that Cu transfer between these proteins is possible. However, the mechanism for transfer of Cu from GSH to Cox17 and Ccs1 must be preferred in the IMS and not the cytosol. This model proposes a feasible pathway for Cu import but there is no direct experimental evidence demonstrating its functionality *in vivo*.

1.5 Cu Homeostasis and Cell Cycle

1.5.1 Yeast cell cycle

Actively dividing cells undergo the cell cycle, which consists of two important stages: DNA replication and cell division. To prepare for these, cells have growth and development phases, the Gap1 (G1) and Gap2 (G2) phases (Barnum & O'Connell, 2014). Before replication, cells obtain mass and integrate growth signals in the G1 phase, while in the G2 phase cells organize a newly replicated genome and prepare for chromosome segregation. The cyclin dependent kinases (CDKs) are an important protein family that play a central role in cell cycle control and are regulated by phosphorylation. On average, it has been recorded that a *S. cerevisiae* cell takes 125 ± 9 minutes to complete one cell cycle (Shaw *et al*, 1998).

Progression of the cell cycle is monitored by a series of checkpoints, which are activated and interrupt normal progression if cells are unfit. Many of the proteins known to be involved in checkpoint activation were originally identified in yeast. One of the central players in the S-phase checkpoint pathway in yeast is RADiation sensitive protein 53 (Rad53), which has functions in both ceasing DNA replication and influencing levels of dNTP pools (Jossen & Bermejo, 2013). Rad53 is an effector kinase, which begins a

phosphorylation cascade that ends with prevention of the Mini Chromosome Maintenance 2-7 helicase complex (Mcm 2-7) from unwinding DNA at origins of replication. Rad53 also activates ribonucleotide reductase (RNR) after it phosphorylates Crt1, a repressor of the RNR complex. Therefore, activation of Rad53 results in halting DNA replication and increasing cellular concentrations of dNTPs (Jossen & Bermejo, 2013). In mammalian systems, faulty checkpoint pathways can lead to uncontrolled cell growth. p53, which is known for its high mutation rates in cancer, plays an important role in checkpoint control; it is a transcription factor that activates transcription of the CDK inhibitor p21, which arrests cell cycle progression until DNA damage is repaired (Kastan *et al*, 1992). This explains why mutations in p53 promote replication and division in damaged cells and lead to tumor growth.

Flow cytometry is commonly used to measure cell cycle progression. In this approach, cells are arrested in the G1 phase and then released so they all enter the cell cycle in a synchronous fashion. Cells are then collected at specific time points and stained with a DNA-specific dye, so fluorescence intensity can be measured per cell using a flow cytometer (Monje-Casas & Walker, 2017). The intensity for cells that have been synchronized to G1 phase is considered to be 1N copies of DNA, and cells displaying double the intensity (2N) are assumed to be finished replication and preparing for mitosis (Haase & Reed, 2002). By reading samples over time, these two peaks will shift and cell cycle progression can be monitored (Figure 1.7).

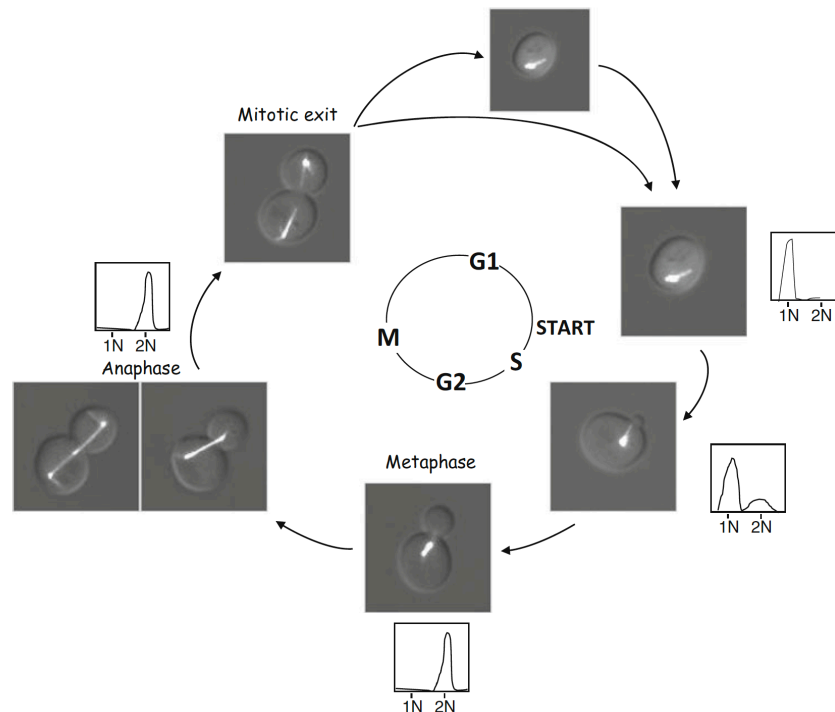


Figure 1.7 Monitoring progression of the yeast cell cycle by flow cytometry

S. cerevisiae cells expressing GFP-Tub1 as a mitotic spindle marker and the flow cytometry profiles expected at each phase of the cell cycle (Monje-Casas & Walker, 2017).

1.5.2 Influence of Cu on cell cycle

If free Cu exists in the cell, the Fenton reaction will lead to formation of reactive oxygen species (ROS), which will cause DNA damage. DNA damage is one of the major reasons cells will halt reproduction. A recent report shows that loss of function of the cuproproteins Sod1, COX, hemocyanin, and plastocyanin all affect the cell response to DNA damage, and thereby displaying a biological connection between Cu and cell cycle (Zhang *et al*, 2016).

Rad53 (yeast) and p53 (mammalian cells) are two important proteins that play central roles in DNA damage checkpoints in these eukaryotic organisms, and have previously been connected to Cu homeostasis. In yeast, Rad53 is thought to regulate Cu responsive genes while other cell cycle proteins such as Mec1, Dun1, and Crt1 are not (Dong *et al*, 2013). The authors describe a novel regulatory relationship between Cu and DNA-damage that also involves Sod1 activity. In the presence of DNA damaging agents methyl methanesulfonate (MMS) and hydroxyurea (HU), Cu import genes are induced and metallothioneins are repressed, suggesting a need for Cu in the presence of DNA damage. Under these conditions,

Rad53 senses DNA damage and responds by interacting with active Sod1 to upregulate *CTR1* and other import genes (Dong *et al*, 2013). This paper proposes a connection between Cu homeostasis and cell cycle regulation.

Similar to yeast Rad53, mammalian p53 is an important protein for regulation of cell cycle and when activated, can either activate DNA repair proteins or initiate the apoptotic cascade. A relationship was found between p53 and Sco2, a mitochondrial cuproprotein required for COX assembly (Turski *et al*, 2009). There is a canonical p53 binding site on the Sco2 promoter, suggesting that Sco2 is produced under stress conditions in healthy cells. This fits with the finding that Sco2 is downregulated in some cancers, because p53 is normally dysregulated in cancerous cells (Turski *et al*, 2009).

Other work has found direct links between cuproproteins and cell cycle progression. Atx1 is responsible for Cu transport to the Golgi apparatus in yeast. Interestingly, many cell cycle genes were differentially regulated in a transcriptomic analysis of Atx1 KO cells, suggesting that Atx1 has a potential role in cell cycle control (Cankorur-Cetinkaya *et al*, 2016). Our lab has also found that losing COX assembly factors related to Cu delivery correlates with a cell cycle defect, suggesting a relationship between Cu deficiency and cell cycle (Camasta, unpublished).

1.5.3 Other pathways connected to Cu homeostasis

Fe Transport: Interplay between Cu and Fe was first suspected in the 1800s through study of hypochromic anemia in Italy and France. Hypochromic anemia patients have lower hemoglobin levels, which correspond to a Fe deficiency. However, women working in Cu factories did not contract the disease, suggesting that high Cu could compensate for having a Fe deficiency (Gulec & Collins, 2014). Mechanistically, Cu is required for hemoglobin synthesis in erythrocytes but the process of where this happens and the regulation remain unknown (Gulec & Collins, 2014).

One example of a well-characterized protein that links Fe and Cu metabolism is ceruloplasmin, which binds many Cu atoms and is a ferroxidase in serum that helps with mobilization of Fe from storage tissues (Sharp, 2004). Low ceruloplasmin activity leads to anemia that is recovered by dietary Cu, but not Fe. Hephaestin, a homolog of ceruloplasmin, is intracellular and plays a role in Fe efflux from enterocytes and loads Fe onto transferrin,

the major Fe transport protein in the body (Sharp, 2004). In humans, dietary Cu and Fe are absorbed into the bloodstream through intestinal epithelial cells (IECs) in the duodenum. Atp7a, which is involved with transcytosis of Cu, is strongly induced during Fe deficiency (Gulec & Collins, 2014). Divalent metal transporter 1 (DMT1), initially classified for uptake of Fe, is also able to take up Cu (Illing *et al*, 2012). Many questions about DMT1 still remain: How does Cu uptake influence the interaction between DMT1 and Fe; does Cu uptake only happen during Fe deficiency; and is Cu transport through DMT1 physiologically relevant?

In yeast, Mrs3, a Fe transporter on the IMM, has been described to transport Cu to the matrix (Vest *et al*, 2016). Interestingly, Mrs4, another Fe transporter, does not have the same phenotype, meaning that not all Fe transporters can also transport Cu, outside a select few. Many other Fe and Cu interactions have been described in yeast and humans but these are outside the scope of this overview.

SUMOylation: Small ubiquitin-like modifiers (SUMO) are a family of proteins that act in post-translational modification and covalent linkage to other proteins in order to modify their functions. The pathways involved in SUMOylation of proteins are similar to those of ubiquitination; however, SUMOylated proteins are not always targets for degradation (Lumpkin *et al*, 2017).

Addition of the SUMO modification to target proteins requires the E3 ligase class of enzymes. One of these enzymes, SAP and mIZ finger domain protein 1 (Siz1), is thought to connect Cu homeostasis to SUMOylation (Chen *et al*, 2011). In *Arabidopsis thaliana*, Siz1 KO plants are hypersensitive to excess Cu and display decreased amounts of SUMOylated proteins compared to a healthy plant. This led to the finding that the Yellow-Stripe 1-Like (YSL) genes *YSL1* and *YSL3* genes are involved in Cu-induced SUMOylation, and the Siz1 KO displays lower levels of SUMO because it is unable to downregulate these genes (Chen *et al*, 2011).

At a protein level, some cuproproteins are also SUMOylated and have alternate functions. The Cu chaperone Atox1 is translocated to the nucleus when it is SUMOylated and is thought to act as a transcription factor (Itoh *et al*, 2008). SUMOylation of Atox1 is also necessary for its interaction with TNF-receptor associated factor 4 (TRAF4), which relies on Cu (Das *et al*, 2016 conference proceeding). Sod1 is also thought to be SUMOylated on

Lys75 and this modification is thought to play a role in stability and aggregation in ALS (Fei *et al*, 2006).

A recent study of SUMOylation in the yeast mitochondrial proteome revealed that many COX subunits and assembly factors, which rely on Cu for function, are SUMOylated (Paasch *et al*, 2018). Additionally, the authors found that Mia40, a protein responsible for import of several cuproproteins, is also SUMOylated. Because depleting proteasomal function led to an increase in SUMOylated mitochondrial proteins, the authors predicted that the SUMO modification on this subset of mitochondrial proteins is likely a marker of non-functional proteins and may result in their degradation (Paasch *et al*, 2018).

Apoptosis: Cu binding directly influences activity of X-linked inhibitor of apoptosis (XIAP), an anti-apoptotic protein (Mufti *et al*, 2007). Specifically, activated XIAP binds to and inhibits pro-apoptotic caspases; Cu binding inactivates the protein (Mufti *et al*, 2007). Since XIAP helps to promote apoptosis in conditions of excess Cu and exhibits different affinities for Cu^+ and Cu^{2+} (Liang *et al*, 2014), it has been proposed to act as a Cu sensor. In conjunction with this, XIAP helps regulate ubiquitination and degradation of Copper Metabolism Domain Containing protein 1 (COMMD1), known to increase Cu efflux from the cell (Mufti *et al*, 2007).

It has also been proposed that XIAP gains its Cu from Ccs1, and interaction that was found by looking at the E3 ubiquitin ligase activity of XIAP (Brady *et al*, 2010). Interestingly, when XIAP ubiquitinates Ccs1, the Cu chaperone for Sod1, Cu delivery from Ccs1 to Sod1 becomes more efficient (Brady *et al*, 2010). Although XIAP is a direct connection between Cu and apoptosis in humans, there is no XIAP ortholog in yeast (Carmona-Gutierrez *et al*, 2012).

1.6 Goals of this Study

Even though mitochondria are well known for their role in energy production, it is now appreciated that they also are a central point for many other pathways. For example, they are an important part of a signaling cascade in apoptosis when cytochrome *c* is released into the cytosol and are responsible for synthesis of Fe-S clusters, which are an important structural motif in a large subset of proteins (Alberts *et al*, 2015).

Mitochondrial cuproproteins have also been thoroughly studied and have recently been found to have ancillary roles in other cellular pathways. In 2005, when the crystal structure of Sco1 revealed a thioredoxin-like fold, hypotheses pointed to a potential secondary role of Sco1 and Cox11 in redox metabolism (Williams *et al*, 2005). There is no defined function for the 40% of Cox17 that resides in the cytosol, since it is unlikely a Cu shuttle between the cytosol and mitochondria. Finally, although Sod1 is known to break down superoxide, it is known that only 2% of Sod1 molecules in the cell are carrying out this role (Corson *et al*, 1998), posing the question for how the other 98% of Sod1 molecules are functioning.

In the past years, our lab has described a cell cycle defect in yeast strains missing Cox17, Sco1, or Cox11, and we think this problem is related to a Cu imbalance. Therefore, we undertook this study to more closely investigate how Cu availability impacts mitochondrial function. We **hypothesize** that mitochondrial cuproprotein pools are affected by changes in Cu availability and this leads to cell cycle defects. To approach this, we studied how mitochondrial cuproproteins respond to differences in levels of extracellular Cu and examined if and how a generalized Cu problem impacts cell cycle progression. We find that mitochondrial cuproprotein pools are majorly impacted by changes in Cu availability but this does not always correlate with a cell cycle defect.

Chapter 2: Materials and Methods

2.1 Yeast Strains & Maintenance

Table 2.1 Yeast Strains used in this study.

Strain	Genotype	Source
W303	MAT a, <i>ade2-1, his3-1,15, leu2-3,112, trp1-1, ura3-1</i>	Glerum lab
W303 Δ cox17	MAT a, <i>ade2-1, his3-1,15, leu2-3,112, trp1-1, ura3-1, COX17::TRP1</i>	Glerum lab
W303 Δ sco1	MAT a, <i>ade2-1, his3-1,15, leu2-3,112, trp1-1, ura3-1 SCO1::URA3</i>	Glerum lab
W303 Δ cox11	MAT a, <i>ade2-1, his3-1,15, leu2-3,112, trp1-1, ura3-1 COX11::HIS3</i>	Glerum lab
W303 Δ cox4	MAT a, <i>ade2-1, his3-1,15, leu2-3,112, trp1-1, ura3-1 COX4::URA3</i>	Glerum lab
W303 Δ cox15	MAT a, <i>ade2-1, his3-1,15, leu2-3,112, trp1-1, ura3-1 COX15::HIS3</i>	Glerum lab
W303 ρ°	MAT a, <i>ade2-1, his3-1,15, leu2-3,112, trp1-1, ura3-1</i>	Glerum lab
KL14 ρ°	MAT α , <i>met-6</i>	Glerum lab
CB11 ρ°	MAT a, <i>ade-1</i>	Glerum lab
EG103	MAT α , <i>his3-1,15, leu2-3,112, trp1-1, ura3-1, gal+</i>	Edith Gralla & Joan Valentine
EG103	MAT a, <i>his3-1,15, leu2-3,112, trp1-1, ura3-1, gal+</i>	This study
EG118	MAT α , <i>his3-1,15, leu2-3,112, trp1-1, ura3-1, SOD1::URA3</i>	Edith Gralla & Joan Valentine
EG118	MAT a, <i>his3-1,15, leu2-3,112, trp1-1, ura3-1, SOD1::URA3</i>	This study
BY4741	MAT a, <i>his3Δ0, leu2Δ0, met15Δ0, ura3Δ0</i>	Glerum lab

Table 2.2 Media used in this study.

Media	Components	Application
YPD	1% yeast extract, 2% peptone, 2% dextrose	General <i>S. cerevisiae</i> growth medium
YPGal	1% yeast extract, 2% peptone, 2% galactose	General <i>S. cerevisiae</i> growth medium
EG	1% yeast extract, 2% peptone, 2% ethanol, 2% glycerol	Medium containing non-fermentable carbon sources, for testing mitochondrial defects
WO	0.67% nitrogen base without amino acids + (NH ₄) ₂ SO ₄ , 2% glucose	Minimal growth media, for strain verification
KAc	1% potassium acetate, 0.05% glucose	Sporulation media
2% agar added to any media to make plates		

Every 4 months, frozen yeast strains were patched onto YPD plates from an -80°C stock and then restreaked onto a fresh YPD plate. Replica plating was performed on WO media to confirm strains had the correct auxotrophies (0.5 mg of each amino acid per plate), and strains were also mated with either KL14 or CB11 to confirm colonies were ρ^+ . Strains were stored on YPD plates at 4°C for up to 4 weeks and then restreaked on new plates. Note: The EG118 strain requires methionine and lysine supplementation to grow on minimal media (Liu *et al*, 1992).

2.1.1 Mating and sporulation

EG103 and EG118 (MAT α) were mated with W303 (MAT a) to form diploid patches on YPD. Auxotrophies of diploid patches were verified by replica plating onto WO, then diploids were replica plated onto KAc and incubated at RT until tetrads were visible under the microscope (7 days). Glusulase (15 μ L) was added to 1 mL of sterile dH₂O containing a loopful of spores and incubated at RT for 15 mins, followed by washing twice in sterile dH₂O and resuspension in 1 mL of dH₂O. 50 μ L of spores (1:100 dilution) were plated onto WO plates to select for colonies with the correct genotype. After this, 150 colonies with the correct genotype were patched onto YPD and verified for mating type (MAT a) by replica plating onto WO + 200 μ L of an overnight KL14 culture (for EG118, also added 0.5 mg of Met). Colonies with the correct mating type and genotype were further verified for ρ^o status and frozen down at -80°C.

2.2 Treatment with Cu Availability Reagents

Yeast strains from YPD plates were inoculated into 10 mL or 100 mL of YPD or YPGal and grown overnight at 30°C and 230 rpm. The next day, cultures were checked for contamination and optical density was measured at 600 nm (OD₆₀₀). For our experiments, we assumed that an OD₆₀₀ of 1.0 corresponded to 1×10^7 cells/mL. All cultures were diluted in fresh YPD or YPGal to a density of 1×10^6 cells/mL followed by addition of Cu availability reagents. Copper sulphate (CuSO₄) was diluted from a filter-sterilized 10% stock solution and bathocuproine disulphate (BCS) was made fresh every experiment as a 50 mM stock and filter sterilized. After addition of Cu availability reagents, cells were incubated in the dark for 18 hours and then collected for subsequent analyses.

2.3 Cell Viability

2.3.1 Spot plate assays

Overnight cultures of yeast strains were adjusted to a cell concentration of 10^7 cells/mL and then serially diluted ($10^0 - 10^{-4}$) in sterile dH₂O. Dilutions (5 μ L) were spotted onto YPD plates and incubated at 30°C for 1 day. Patches were replica plated onto either YPD or EG plates with CuSO₄ (0.01 – 0.4 %), BCS (10 μ M – 5mM), or HU (50 – 100 mM) and incubated in the dark at 30°C for 2 days then scored for growth.

2.3.2 Trypan blue staining

W303 cultures were treated with Cu availability reagents as described above (Section 2.2). Cells were then diluted (1:1) with 0.4 % Trypan blue solution (Sigma-Aldrich, Oakville, Canada) and visualized and counted under the microscope with a hemacytometer. At least 10 of the 25 sections on the hemacytometer were counted for each condition, and cells were classified as viable for their ability to exclude Trypan blue. Viability was scored as a percentage by dividing the number of viable cells by the total cells counted.

2.4 Suppressor Screen

The suppressor screen was performed to isolate mutants that were able to grow on a non-fermentable carbon source (EG) with 500 μ M BCS (Figure 4.6). 10^5 , 10^6 , or 10^7 cells of an overnight W303 culture were plated onto EG plates containing 500 μ M BCS and incubated in the dark at RT for 15 days. Four colonies were classified as suppressors: they were patched onto YPD plates and then restreaked onto YPD to isolate single colonies. Colonies were checked for the correct auxotrophies and stored at -80°C.

To verify colonies were able to grow on EG + BCS, the W303 strain and the suppressors were streaked onto YPD, and then replica plated onto EG with BCS concentrations ranging from 10 μ M – 1 mM. EG plates were incubated for 2 days at 30°C in the dark and growth of suppressors was compared to the W303 strain.

2.5 Subcellular Fractionations

For subcellular fractionations, protein concentrations were determined using the Folin-Ciocalteu reagent (Lowry *et al*, 1951). Before concentration determination, whole cell lysate samples were diluted 1:40, post-mitochondrial supernatant (PMS) samples were diluted 1:50, and mitochondrial samples were diluted between 1:100-1:120.

2.5.1 Whole cell lysate (WCL) preparation

Mitochondrial mutants and the W303 strain were grown in the presence or absence of Cu availability reagents as described above (Section 2.2). Cells (40 mL) were harvested and resuspended in lysis buffer (10 mM Tris-HCl pH 8.0, 1% Triton-X-100, 1 mM EDTA, 1 x Protease inhibitor cocktail, 1 mM PMSF, 140 mM NaCl) at a ratio of 0.8 g of cells to 1 mL of lysis buffer. Cell suspensions were transferred to tubes containing 0.5 mm glass beads (beads made up 25% of tube volume) and lysed using the BioSpec Mini-Beadbeater-24 (ThermoFisher Scientific, Mississauga, Canada). Lysing consisted of 8 cycles of 30 seconds in the bead beater and 30 seconds on ice. After lysis, homogenates were incubated on ice for 5 minutes and then centrifuged at 16,000g (1 minute, RT). The supernatant (whole cell lysate) was aliquoted and stored at -80°C.

2.6.2 Isolation of mitochondria

Mitochondria and PMS (cytosolic) fractions were prepared using differential centrifugation as described previously (Banting & Glerum, 2006). Cells were collected from 800 mL of media and incubated in digestion buffer (1.2 M sorbitol, 75 mM NaP_i pH 7.5, 1 mM EDTA, 1% β-mercaptoethanol, 9.9U/mL zymolyase) for 160 minutes (untreated) or 120 minutes (Cu-treated) followed by washing in 1.2 M sorbitol and resuspension in 4 mL STE (0.5 M sorbitol, 20 mM Tris pH 7.5, 0.5 mM EDTA) per gram of wet weight. Homogenization of cells was done using a Waring blender (20 seconds) or Dounce homogenizer (35 strokes) and homogenates were treated with 1 mM PMSF. Differential centrifugation was carried out by a low speed spin at 1500g (10 minutes, 4°C) and high-speed spin at 17,000g (15 minutes, 4°C). After the first high-speed spin 5mL of supernatant were collected and saved as the cytosolic fraction. Mitochondrial pellets were then washed

twice (20,000g, 15 min, 4°C) with 40 mL STE and resuspended in 200 µL of 10 mM Tris pH 7.5. Mitochondrial and PMS fractions were aliquoted and stored at -80°C.

2.7 RNA Isolations

RNA was isolated using the Geneaid Yeast Total RNA Kit (Geneaid Biotech, Taipei, Taiwan). After treatment with Cu availability reagents (Section 2.2), 1.5 mL of culture was transferred to a 1.5 mL RNase-free tube and digested for 30 minutes with 200 U of zymolyase. Cells were lysed and transferred to a column where they were treated immediately with DNase according to the manufacturer's instructions. Columns were washed once in wash buffer and twice in 70% ethanol before RNA was eluted into 50 µL of RNase free water. All RNA samples were measured with a Nanodrop 3300 (Thermo Fisher, MA, USA) to determine their concentrations.

RNA Gels: RNA was run on agarose gels before cDNA synthesis to determine integrity. All glassware and lab materials used were treated with 0.1% DEPC for 12 hours and then autoclaved. Gel electrophoresis equipment was soaked in 3% hydrogen peroxide overnight. 1 µL of ethidium bromide (1 mg/mL) was added to 500 ng of RNA (diluted in RNase-free dH₂O to a final volume of 10 µL) and loaded onto a 1% agarose gel in 1X MOPS buffer (0.2M MOPS, 0.05M sodium acetate, 0.01M EDTA). Gels were run for 90 minutes at 80V then visualized with UV light.

2.8 Quantitative PCR (qPCR)

2.8.1 Nuclear DNA (nDNA) preparation and primer optimization

Optimization of primers was performed by running PCR on nuclear DNA (nDNA) and confirming the presence of a single product at the correct molecular weight. nDNA was isolated with the QIAGEN Genomic DNA Kit (QIAGEN, Hilden, Germany). 20 mL of W303 cells were harvested (5,000g, 5 min, RT) and digested with zymolyase (250 U), lysed, and treated with RNase A (100 mg/mL stock) and Proteinase K (20 mg/mL stock) before being transferred to a column according to the manufacturers instructions. Columns were washed twice and DNA was eluted into 5 mL of the Qiagen elution buffer. DNA was collected by addition of 3.5 mL isopropanol and centrifugation (10,000g, 15 min, 4°C) and resuspended in 50 µL dH₂O. DNA was precipitated by addition of 100% ethanol (7 volumes)

and sodium acetate (3M stock, 40 μ L) and incubated at -20°C for 30 minutes. DNA was collected by centrifugation (16,000 g, 1 min, RT) and excess ethanol was removed using a speed vacuum. The final DNA pellet was resuspended in 50 μ L TE (10 mM Tris pH 7.5, 1 mM EDTA) and measured with the Nanodrop 3300 (Thermo Fisher, MA, USA).

Primers were designed using NCBI PrimerBLAST. nDNA (50 – 500 ng) was subject to PCR using 13 sets of primers (Table 2.3) on the PTC-200 machine (GMI Laboratory Solutions, MN, USA) to confirm the correct product and to optimize annealing temperature. The PCR mixture contained primers (200 nM each), Taq polymerase (0.125 μ L, Invitrogen), dNTPs (200 nM), 10X PCR buffer (Invitrogen), and MgCl₂ (1.5 mM) PCR cycles were as follows: (1) 95°C, 4 minutes (2) 95°C, 20 s (3) 53 – 60°C, 30 s (4) 68°C, 2 minutes (5) Go to 2, 39X (6) 68°C, 2 minutes. PCR products (2 – 5 μ l) were run on 1% agarose gel in 1X TBE buffer (tris, boric acid, EDTA) for 60 minutes at 100V then visualized with UV light.

Table 2.3 Primers used in this study

Sequences are listed from 5' to 3'.

Target	Primer Sequences	Product Length
<i>ACT1</i>	CTGCCGGTATTGACCAAACCT CGGTGATTTCCTTTTGCATT	144 bp
<i>CCS1</i>	TGACCACGAACGATACATAC CACGCTCATTATTTGTTGCT	143 bp
<i>COX4</i>	ATTGGTCCCTGGTGCTAAAGAGGG CCCTCCCTGGACGAATCTAATGG	135 bp
<i>COX11</i>	CCTGAGATGAATGCAGATGA TGAGTTGTCTTTCCCTTGTGT	90 bp
<i>COX17</i>	GAGTGCGAGGACAAACCTAAGCC CGAAGCCATAACCC TTCATGCAC	160 bp
<i>CTR1</i>	GCAGCATGAATATGGACGCC TTGACGACATAGTCGACGCC	177 bp
<i>CUP1</i>	CATGTAGCTGCCCAACGG CATTTCCCAGAGCAGCATG	94 bp
<i>CUP2</i>	CAATCTTGATTTGGCTTCCC TATATGCGCTTCCCTGTTTCA	92 bp
<i>MAC1</i>	AACACTCTCCCAAAGCTCCG ATAGGCTCCTGTTGAAGCCG	106 bp
<i>PIM1</i>	CATCCAGTCGATCGGATTCT AATAAGGGCCGTCTGGCTAT	112 bp
<i>SCO1</i>	CTGAAGTTGTCAAGAAGTGC CTGCTTAATGGTTTCTTGCC	146 bp
<i>SOD1</i>	AACGTGGGTTCACATTCAT CACCATTTTCGTCCGTCTTT	156 bp
<i>TDH2</i>	CCATGGGCTTCTCTAAACA GCGTTGGAAACAATCTTCAA	194 bp

2.8.2 cDNA synthesis

Synthesis of cDNA from total RNA was performed using the SensiFAST cDNA synthesis Kit (Froggabio, Toronto, Canada). RNA (1 μg), 5X TransAmp buffer (4 μL), and reverse transcriptase (1 μL) were used to synthesize cDNA on the CFX96 Real-Time PCR Detection System (BioRad Laboratories, Mississauga, Canada) with the following cycles: (1) 25°C, 10 minutes (2) 42°C, 15 minutes (3) 85°C, 5 minutes.

2.8.3 RT-qPCR

All qPCR reactions were performed with the Ssofast EvaGreen Supermix (BioRad Laboratories, Mississauga, Canada). Reactions consisted of cDNA (50 ng), primers (50 nM), and the 2X EvaGreen master mix. Each reaction was done in technical triplicate and for every set of primers a negative control without cDNA was also run in technical triplicate. qPCR cycles were as follows: (1) 95°C, 30 s (2) 95°C, 5 s (3) 60°C, 5 s (4) 55°C – 57°C, 15 s (5) Plate read (6) Go to 2, 39X, (7) 65°C – 95°C 0.5s/cycle, plate read. Reactions were monitored on the CFX96 Real-Time PCR Detection System and Cq values were obtained using the CFX Manager Software (BioRad Laboratories, Mississauga, Canada). Data was omitted if the Cq value of the negative control was below 35 cycles. An example qPCR curve is shown in Figure 2.1.

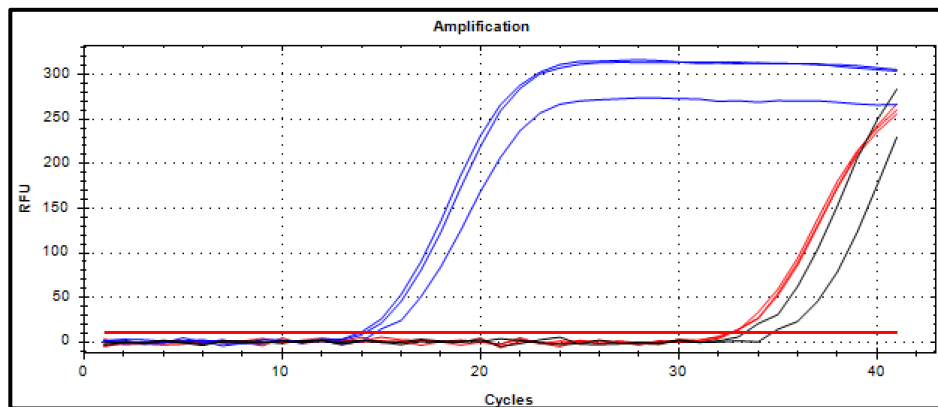


Figure 2.1 Sample qPCR curve

The blue lines represent the amplification curves for a gene of interest. Y-axis is the relative fluorescence units (RFU) and the x-axis is the cycle number.

2.8.4 Analysis & Statistics

All qPCR data is presented as the relative fold change ($\Delta\Delta\text{Cq}$) of the gene of interest compared to the *ACT1* control gene. To obtain the $\Delta\Delta\text{Cq}$ value, the differences of Cq values

between the gene of interest and the *ACT1* control in the no treatment condition and the treatment condition (i.e 0.1% Cu) were calculated and further analyzed according to the method by Livak & Schmittgen (2001). The $\Delta\Delta Cq$ values for treatment conditions were compared to the wild type value using a one-way ANOVA (Microsoft Excel). Statistically significant values were further tested through performing a Tukey HSD test to determine which treatment conditions were significant from the no treatment control.

2.9 Western Blotting

2.9.1 SDS-PAGE and Western blotting

Protein samples (mitos: 25 μ g, cytosol: 25 μ g, WCL: 60 μ g) were diluted in Tris (10 mM pH 6.8) and 1 μ L of 100 mM PMSF was added immediately. Samples were then solubilized in 4X loading buffer (4% SDS, 4% β -mercaptoethanol, 40% glycerol, 200 mM Tris pH 6.8, 0.08% bromophenol blue) and loaded into a gel (10% gel for Rad53 blots, 12% gel for all others). Samples were not boiled if the following Western blot was for detection of a membrane protein. All other samples were boiled at 95°C for 5 minutes and loaded immediately. Gels were run for 70 minutes at 150V.

The Transblot Turbo transfer system (BioRad Laboratories, Mississauga, Canada) was used to transfer proteins onto nitrocellulose membranes. Prior to transfer, membranes and gels were soaked in transfer buffer (20% Transblot turbo buffer, 20% ethanol) for 30 seconds. If the size of the protein of interest was below 50 kDa, the Low MW setting (5 minutes) was used; otherwise the high MW setting was used (10 minutes).

Membranes were stained with Ponceau S (2% Ponceau S, 30% TCA, 30% sulfosalicylic acid) for 5 minutes on the rocker (Setting 4), rinsed with dH₂O and imaged to ensure equal loading. Membranes were incubated with blocking buffer (10 mM Tris pH 8, 1 mM EDTA, 150 mM NaCl, 0.1% Triton-X-100, 1.5% milk) for 1 hour (RT) then treated with primary antibodies diluted with blocking buffer (see Table 2.4) for 1 hour (RT). Following this, membranes were washed three times in blocking buffer without milk (10 minute washes), and treated with secondary antibodies diluted in blocking buffer (see Table 2.4) for 1 hour (RT). Membranes were then washed three times with secondary wash solution (10 mM Tris pH 8, 1 mM EDTA, 1 M NaCl, 0.1% Triton-X-100) and rinsed in dH₂O before imaging. Immediately prior to imaging, membranes were incubated with 500 μ L Clarity™

(BioRad Laboratories, Mississauga, Canada) in the dark for 2 minutes. Imaging was done using a ChemiDoc MP (BioRad Laboratories, Mississauga, Canada).

Table 2.4 List of antibodies used in this study

Primary Antibodies				
Antigen	Host	Clonality	Dilution	Source
α -Aco1	Rabbit	Polyclonal	1:1000	Bulteau lab
α -Act1	Mouse	Monoclonal	1:1000	Thermo Fisher
α -Cox2	Mouse	Monoclonal	1:1000	Abcam
α -Cox4	Mouse	Monoclonal	1:1000	Abcam
α -Cox11	Rabbit	Polyclonal	1:500	Glerum lab
α -Cox17	Rabbit	Polyclonal	1:500	Glerum lab
α -Cyc1	Rabbit	Polyclonal	1:400	Promokine
α -DNP	Rabbit	Monoclonal	1:150	Thermo (Oxyblot)
α -Lon	Rabbit	Polyclonal	1:1000	Suzuki lab
α -Por1	Mouse	Monoclonal	1:10,000	Molecular Probes
α -Rad53	Rabbit	Polyclonal	1:1000	Abcam
α -Rnr3	Rabbit	Polyclonal	1:500	Antibodies online
α -Sco1	Rabbit	Polyclonal	1:500	Glerum lab
α -Sdh2	Rabbit	Polyclonal	1:1000	Lemire Lab
α -Sod1	Rabbit	Polyclonal	1:500	Antibodies online
Secondary Antibodies				
α -mouse IgG	Goat	Polyclonal	1:5000 - 1:10,000	Thermo Fisher
α -rabbit IgG	Goat	Polyclonal	1:300 -1:10,000	Abcam

2.9.2 Analysis

Raw data from Western blots was processed and analyzed using the ImageLab software Version 5.2.1. Densitometry was performed on Western blots where the signal for the no treatment control was clear. For the analysis, the relative intensity of the control was compared to the intensity of the bands for the treatment conditions. If the protein of interest was more different from the no treatment sample than the control protein (Por1 for mitos, Act1 for cytosol and WCL), the protein of interest was considered to be significantly different in that treatment condition.

2.9.3 Oxyblot

To assess oxidative modification of proteins, the EMD Millipore Oxyblot Protein Oxidation Detection Kit (Fisher Scientific, NH, USA) was used according to the manufacturer's protocol. Protein samples (mitos & cytosol: 25 μ g, WCL: 20 μ g) were diluted in 10 mM Tris pH 7 (5 μ L final volume) in duplicate and denatured with SDS (6%).

Carbonyl groups were modified after addition of derivitization solution (10 μ L) and incubation at RT for exactly 15 minutes. The derivitization control solution (10 μ L) was added to the second tube and treated in the same manner. After derivitization, neutralization solution (7.5 μ L) and 4X loading buffer (9.2 μ L) were mixed with protein samples and the solution was loaded into a 12% polyacrylamide gel. Gels were run at 100V for 120 minutes and transferred onto nitrocellulose using the Transblot Turbo System (described above) using the High MW setting (10 minutes). Blocking and antibody incubation were performed as described above, except the blocking buffer (1X PBS, 0.05% Tween, 1% BSA) and rinse buffer (1X PBS, 0.05% Tween) were different. Blots were imaged as described above using the ChemiDoc MP (BioRad Laboratories, Mississauga, Canada).

2.10 Enzyme Activity Assays

2.10.1 COX activity

COX activity was measured qualitatively using TMPD and quantitatively using a spectrophotometric assay. For the qualitative method, colonies from agar plates were permeabilized onto Whatman filter paper and briefly soaked in potassium phosphate buffer (0.04 M KPi pH 6.7, 0.05% Tween-20). Rewetted filter paper was treated with 1 mL of TMPD solution (1% TMPD in DMSO) for 5 minutes and colonies with COX activity formed a purple precipitate (McEwen *et al*, 1985).

COX activity was measured spectrophotometrically by recording the decrease of reduced cytochrome *c* at 550 nm for 60 seconds (Tzagoloff *et al*, 1975). Cytochrome *c* was reduced using a few crystals of sodium dithionite. Immediately prior to reading absorbance, 10 μ L of mitochondrial protein was solubilized with 1% deoxycholate (DOC) for 20 seconds and added to a cuvette containing 0.92 mL KPi buffer (20 mM KPi pH 7) and 80 μ L reduced cytochrome *c* (10 mg/mL in 20 mM Tris pH 7.5). To calculate specific activity, Beer's law was used with the reduced cytochrome *c* extinction coefficient (28 $\text{mM}^{-1} \text{cm}^{-1}$). Significance was calculated by using a one-way ANOVA followed by a Tukey HSD test.

2.10.2 SOD activity

SOD activity was measured in mitochondrial (24 μ g protein) and cytosolic (48 μ g protein) fractions using zymographic analysis as described previously (Beauchamp &

Fridovich, 1971). Protein fractions were diluted to 12 μL in Tris buffer (200 mM Tris pH 6.8), treated with 1 μL PMSF (100 mM) and 6 μL loading dye (250 mM Tris pH 6.8, 50% glycerol, 0.02% bromophenol blue), and run on a 10% non-denaturing polyacrylamide gel. Gels were incubated in the dark with NBT solution (2% nitroblue tetrazolium in 50 mM KPi pH 7) and riboflavin solution (0.02% riboflavin in 36 mM KPi pH 7) followed by development in the light for 1 hour. Imaging was done using white light in a BioRad ChemiDoc MP (Bio-Rad Laboratories, Mississauga, ON, Canada), and quantification was performed on the ImageLab 6.0.1 software (Bio-Rad Laboratories, Mississauga, ON, Canada) by comparing relative abundance of bands.

2.10.3 Aconitase activity

Aconitase activity was assayed as described by Bulteau et al (2005). Mitochondria (10 μL) were solubilized with 25 mM KH_2PO_4 pH 7.5 containing 0.05% Triton X-100 (10 μL) and added to 990 μL of assay buffer (10 mM KPi pH 7.5, 1 mM trisodium citrate, 0.6 mM MnCl_2 , 0.5 mM NADP^+ , 0.05% Triton-X-100). Activity was measured by observing NADP^+ reduction at 340 nm for 2 minutes after addition of isocitrate dehydrogenase (1.0 U/reaction). Specific enzyme activity was calculated using the NADPH extinction coefficient (6.2 $\text{mM}^{-1} \text{cm}^{-1}$). Significance was calculated by using a one-way ANOVA followed by a Tukey HSD test.

2.11 Cell Cycle

2.11.1 Sample preparation

Cultures were treated with Cu availability reagents as described above (Section 2.2). 2×10^7 cells were harvested (2,000g, 3 minutes, RT), washed in sterile dH_2O , and resuspended in fresh YPD (20mL). Alpha factor (10 $\mu\text{g}/\text{mL}$) and Cu availability reagents were added and cultures were incubated for 3 hours in the dark (30°C, 230 rpm). Visualizing cells under the microscope and seeing the “schmoo” morphology ensured successful arrest. Cells were harvested (2,000g, 5 minutes, RT), washed twice in pre-warmed YPD (20 mL), and resuspended in YPD (20 mL) with pronase (10 $\mu\text{g}/\text{mL}$) and Cu availability reagents. Cells were then incubated (30°C, 230 rpm) so they would enter the cell cycle synchronously. At 0, 40, 80, and 120 minutes after release cells (1.5 mL) were collected; at the 0 minute time

point two aliquots were collected and one served as the negative control. At each time point, cells were immediately washed in 1mL dH₂O (20,000g, 1 minute, RT), fixed in 1 mL of 70% ice cold ethanol, and stored at 4°C overnight.

Fixed cells were harvested (20,000g, 1 minute, RT), washed in dH₂O (500 µL), resuspended in 500 µL RNase A solution (0.80 µg/mL RNase A in 50 mM Tris pH 8) and incubated for 3 hours at 37°C. This was followed by an incubation with 500 µL Proteinase K solution (0.25 mg/mL Proteinase K in 50 mM Tris pH 7.5) at 50°C. Cells were collected (20,000g, 1 minute, RT), resuspended in 500 µL of the flow cytometry buffer (200 mM Tris pH 7.5, 200 mM NaCl, 78 mM MgCl₂, 1 µM SYTOX green), and transferred to BD Falcon tubes (BD Biosciences, Mississauga, Canada). For each sample, a negative control was prepared in the same buffer without SYTOX green.

2.11.2 Flow cytometry parameters

DNA content analysis was performed using the BD FACS Aria Fusion flow cytometer (BD Biosciences, Mississauga, Canada). Immediately prior to analysis, samples were vortexed for 10 seconds. The wild type negative control (unstained) and 0-minute time point sample (SyTOX stained) were used to set up parameters on the 488 nm laser, which were kept consistent for the remainder of the experiment. 20,000 events were collected per sample at a maximum flow rate of 1000 events per second.

2.11.3 Analysis using FACSDiva software

The FACSDiva 8.0.1 software was used for DNA content analysis. All events collected by the flow cytometer were included in the analysis. Chromatograms shown in this thesis are distributions of fluorescence intensity of the SyTOX green stain. For each sample (consisting of all time points), the 0-minute time point was used to determine the relative fluorescence intensity of the 1N and 2N peaks and the 40, 80, and 120-minute time points were analyzed according to those parameters. There were lots of events that displayed fluorescence intensities greater than the 2N peak; these were assumed to consist of clumps of cells and were omitted from the analysis.

Chapter 3: Impacts of Excess Cu

The mitochondrial Cu pool is thought to play an important role in control of Cu homeostasis in the cell (Baker *et al*, 2017a). However, the mechanisms by which mitochondria regulate Cu homeostasis and how mitochondrial dysfunction impacts non-mitochondrial cuproproteins remain under investigation. Many studies have looked at how changes in Cu levels impact cellular function. A recent large-scale screen in yeast concluded that Cu imbalance is associated with defective Fe homeostasis, NAD⁺ imbalance, and dysfunctions in arginine metabolism, glucose transport, and the pyridoxal phosphate pathway (Cankorur-Centinkaya *et al*, 2013). Our goal in this study was to evaluate how changes in extracellular Cu availability adversely impact mitochondria.

Specifically, we ensured that our cells are physiologically responding to changes in extracellular Cu, and we studied how excess Cu affects mitochondrial function. In a Wilson disease mouse model, Cu excess has been shown to result in upregulation of cell cycle proteins but lead to no change in oxidative stress proteins (Huster *et al*, 2007).

3.1 Optimization of Cu availability conditions in *S. cerevisiae*

3.1.1. Determining the appropriate concentrations of CuSO₄ and BCS

Before investigating whether mitochondrial cuproproteins are affected by changes in extracellular Cu levels, we wanted to ensure that the yeast cultures were physiologically responding to their changing extracellular environments. To mimic conditions of excess extracellular Cu we supplemented media with copper sulphate (CuSO₄), and for Cu deplete conditions we used bathrocuproine disulfate (BCS), which is a specific Cu chelator and will not bind other divalent cations. To optimize concentrations of CuSO₄, we considered the observation that 0.1% Cu is able to rescue a Ctr1 KO strain (Glerum *et al*, 1996a) and chose the concentrations 0.01% Cu and 0.1% Cu. For BCS, we chose concentrations ranging from 10 μM to 500 μM based on a previous report that had shown a physiological response in yeast to BCS in the range of 10 μM – 100 μM (Wood & Thiele, 2009).

To measure the cellular response to these chemicals, we looked at transcript levels for *CTR1* and *CUPI*. *CTR1* encodes a high affinity Cu transporter located on the plasma membrane and is transcriptionally upregulated in response to reduced cellular Cu (Wood &

Thiele, 2009). In contrast, the *CUP1* gene encodes the main metallothionein and is transcriptionally upregulated in response to Cu excess conditions. After yeast cultures were exposed to either CuSO₄ or BCS for 18 hours, RNA was isolated, and used for cDNA synthesis and qPCR analysis with primers specific for *CTR1* and *CUP1* genes (Figure 3.1). Transcript levels of *CTR1* and *CUP1* were normalized to *ACT1* transcript levels, which were used as a baseline. As expected, *CTR1* transcript levels significantly increased with increasing concentrations of BCS, and decreased with increasing concentrations of CuSO₄. *CUP1* transcript levels changed in the opposite way: they significantly increased in response to increasing CuSO₄ and decreased in response to BCS. The response of *CTR1* and *CUP1* transcript levels to 0.01% - 0.1% CuSO₄ and 10 μM – 500 μM BCS confirmed that the cells were physiologically responding to changing Cu concentrations in the extracellular environment, in keeping with current understanding.

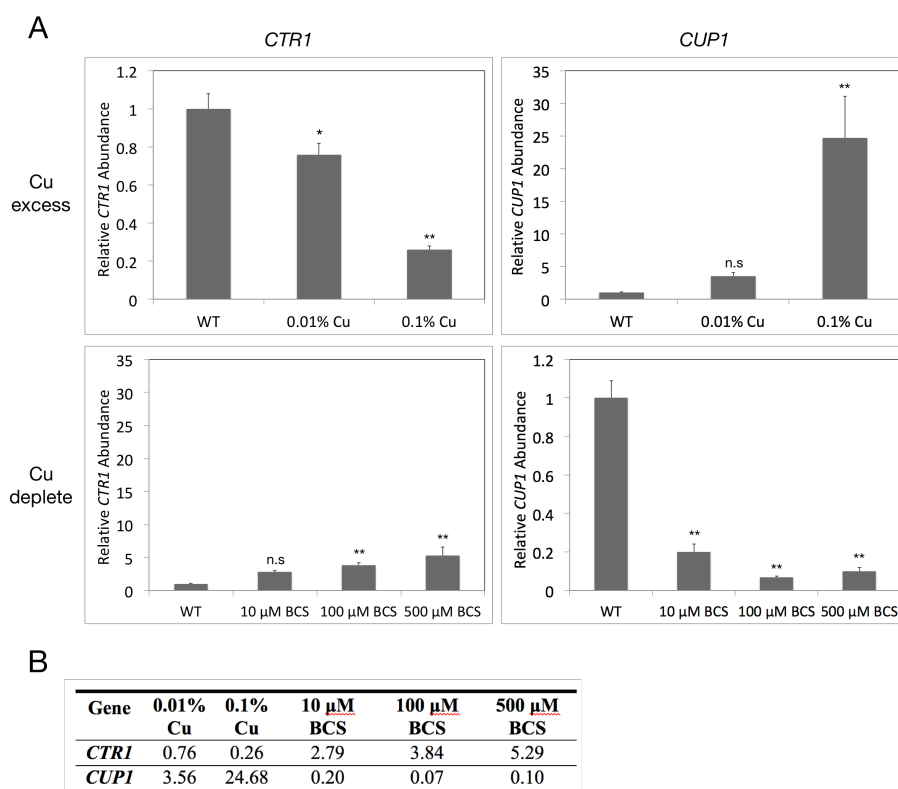


Figure 3.1 RT-qPCR of *CTR1* and *CUP1* in Cu excess and Cu deplete conditions

(A) Graphical representation of relative abundance of *CTR1* and *CUP1* compared to no treatment controls. RNA was isolated from yeast cells grown for 18 hours in the Cu condition stated. PCR was performed using cDNA on both the gene of interest and *ACT1* as a control. Values are representative of $\Delta\Delta Cq$ values. Three biological replicates were performed for each treatment condition. A one-way ANOVA was done to determine statistical significance: not significant = n.s, $p < 0.05 = *$, $p < 0.01 = **$. Error bars represent \pm SEM. (B) Raw $\Delta\Delta Cq$ values, representing the fold-change in each condition relative to *ACT1*.

3.1.2. Effect of Cu availability on cell viability

To ensure that Cu excess or Cu depletion conditions did not lead to a major growth defect, we took a two-pronged approach to test cell viability in the presence of Cu excess and depletion conditions. First, a spot plate assay was performed on plates with different concentrations of the chemicals to identify any growth defects (Figure 3.2-A). These results clearly demonstrate that the presence of either 500 μ M BCS or 0.15% Cu does not result in a growth defect in wild type yeast. In a second approach, wild type yeast were grown in liquid media in the presence or absence of BCS or Cu for 18 hours and the numbers of viable and non-viable cells were analyzed using the Trypan blue staining method (Figure 3.2-B). The difference in this alternative approach is that cells are not required to replicate in order to be considered viable. Therefore, counting viable cells using the Trypan blue approach will account for live cells that are unable to replicate. Our results displayed that at concentrations up to 5 mM BCS and 0.2% Cu, over 85% of cells are still viable. Taken together, these data indicated that the concentration range of Cu excess and depletion used are sufficient to initiate a physiological response but do not affect cell viability.

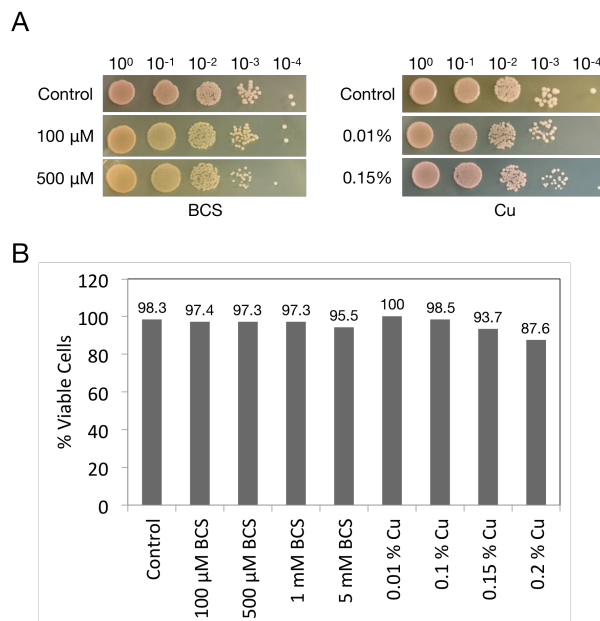


Figure 3.2 Cell viability analysis with CuSO₄ and BCS

(A) Ten-fold dilution series of WT yeast on YPD media with added chemicals. Cells were spotted onto plates and incubated for 48 hours at 30°C. (B) Viability analysis with the Trypan blue stain. Liquid cultures of yeast were grown for 18 hours with either CuSO₄ or BCS and cells were counted using a hemacytometer. A minimum of 500 cells was counted for at least two biological replicates for each treatment. Percentages are representative of unstained, viable cells (Hilker, unpublished).

3.1.3 Response of *MAC1* and *CUP2* to extracellular Cu changes

Mac1 and Ace1, Cu-responsive transcription factors in yeast, have activities dependent on the concentration of Cu bound to them (Keller *et al*, 2005). Measurement of Mac1 and Ace1 activity is normally performed indirectly by measuring transcript levels of *CTR1* and *CUP1*, two of their gene products (Nevitt *et al*, 2012). From the results in Figure 3.1, we saw changes in *CTR1* and *CUP1* transcript levels in both Cu excess and Cu depletion conditions, suggesting that activity levels of Mac1 and Ace1 are also affected by Cu availability conditions.

In an attempt to identify a relationship between transcript levels and activity, we analyzed whether *MAC1* and *CUP2* (Ace1) transcript levels changed in response to Cu excess or depletion conditions (Figure 3.3). *MAC1* transcript levels significantly increased with 0.1% CuSO₄ but did not significantly change with BCS. The increase of *MAC1* transcript levels corresponded to a decrease of *CTR1* transcription levels in 0.1% Cu, suggesting a disconnect between transcript and activity levels. We have seen a similar phenomenon in our studies of the yeast stationary phase (Dubinski *et al*, 2018). A likely explanation is that Mac1 binds high levels of Cu when it is inactive; in Cu excess conditions, the cell will transcribe high levels of *MAC1* so that it can bind free Cu, acting like a Cu sink, but the Mac1 protein will remain inactive. Therefore, the increase of *MAC1* transcript levels in Cu excess conditions is not surprising. *CUP2* transcript levels significantly increased with excess Cu and significantly decreased with increasing BCS (Figure 3.3), mirroring the changes we saw in *CUP1* transcript levels. Ace1 is activated when it binds high concentrations of Cu atoms (Keller *et al*, 2005), suggesting that transcript levels of *CUP2* are directly correlated with Ace1 activity levels. Overall, both *MAC1* and *CUP2* transcript levels change in response to Cu excess, but only *CUP2* responds to Cu depletion.

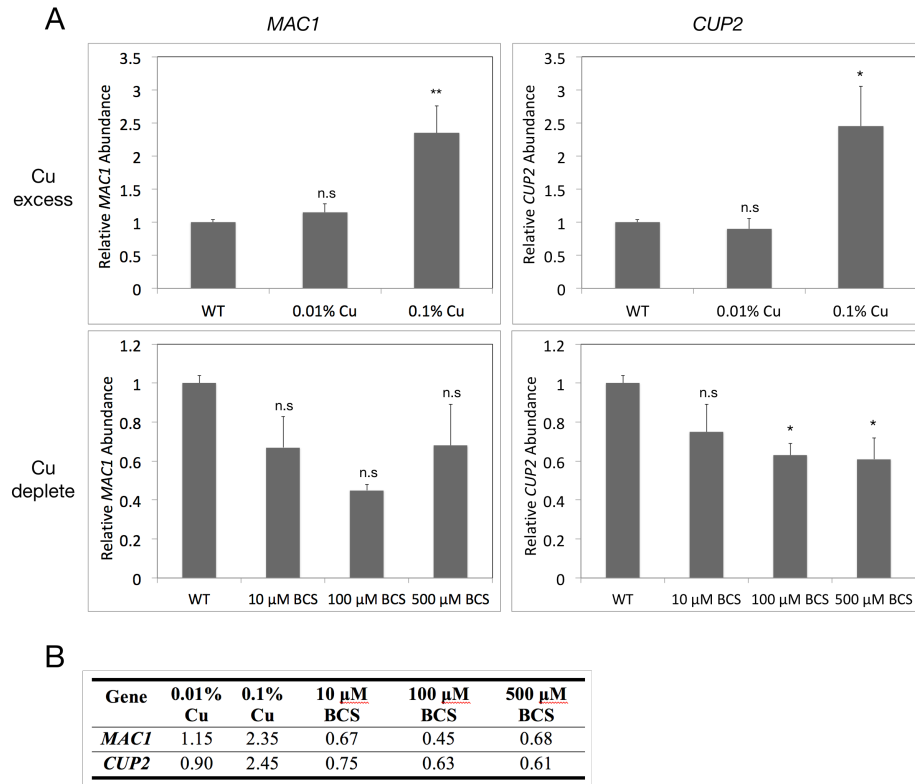


Figure 3.3 RT-qPCR of *MAC1* and *CUP2* in Cu excess and Cu deplete conditions

(A) Graphical representation of relative abundance of *MAC1* and *CUP2* compared to no treatment controls. RNA was isolated from yeast cells grown for 18 hours in the Cu condition stated. PCR was performed using cDNA on both the gene of interest and *ACT1* as a control. Values are representative of $\Delta\Delta Cq$ values. Three biological replicates were performed for each treatment condition. A one-way ANOVA was performed to determine statistical significance: not significant = n.s., $p < 0.05 = *$, $p < 0.01 = **$. Error bars represent \pm SEM. (B) Raw $\Delta\Delta Cq$ values, representing the fold-change in each condition relative to *ACT1*.

3.2 Mitochondrial Cuproproteins in Cu Excess conditions

3.2.1 COX in the face of Cu excess

For our analyses of COX in Cu excess conditions, we compared how COX assembly factors and subunits responded to CuSO_4 transcriptionally, how their protein levels are affected, and if this led to changes in activity of the holoenzyme. We began by looking at transcript levels of *COX17*, *SCO1*, and *COX11*, which are the three assembly factors with a well-defined role in Cu delivery to COX. To do this, we isolated RNA after treatment of wild type cells with CuSO_4 for 18 hours, followed by cDNA synthesis and qPCR analysis. Interestingly, we found no significant difference in the transcript levels of these genes after treatment with either 0.01% or 0.1% Cu after 18 hours (Figure 3.4), suggesting that regulation of these genes is not affected by Cu. The result that *COX17* transcript levels do not

change with changing Cu is in agreement with a large-scale screen that was done in attempt to identify genes important in Wilson disease (Cankorur-Centinkaya *et al*, 2013). We also investigated transcript levels for one of the nuclear-encoded subunits, *COX4*, as a means to control for a general COX assembly defect unrelated to Cu (Figure 3.4). Similarly to the COX assembly factors, increased extracellular Cu did not significantly affect *COX4* transcript levels. These results suggest that there are not likely to be Cu-responsive elements in the promoters of *COX17*, *SCO1*, *COX11* and *COX4*.

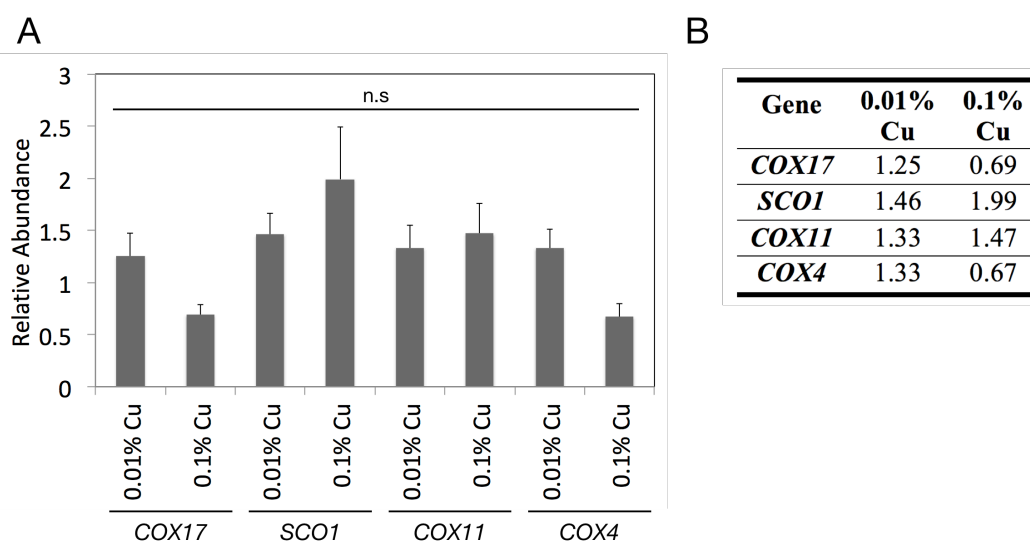


Figure 3.4 RT-qPCR of *COX17*, *SCO1*, *COX11* and *COX4* in Cu excess conditions

(A) Graphical representation of relative abundance of *COX17*, *SCO1*, *COX11* and *COX4*. RNA was isolated from yeast cells grown for 18 hours in YPD + CuSO₄. PCR was performed using cDNA on both the gene of interest and *ACT1* as a control. Values are representative of $\Delta\Delta Cq$ values. Three biological replicates were performed for each concentration. A one-way ANOVA was performed to determine statistical significance: not significant = n.s. Error bars represent \pm SEM. (B) Raw $\Delta\Delta Cq$ values, representing the fold-change in each condition relative to *ACT1*.

We next investigated how the protein levels of COX assembly factors and subunits responded to increases in extracellular Cu levels. Mitochondria were isolated by subcellular fractionation and 25 μ g of mitochondrial protein were separated by SDS-PAGE, transferred to nitrocellulose membranes and Western blotted with antibodies against COX assembly factors and subunits (Figure 3.5). As a control, we used Por1, a mitochondrial OMM protein that is commonly used to verify equal loading. To quantify the Western blots, we compared the relative intensity of the band representing the no treatment control to each treatment condition. From three biological replicates, we found that Por1 decreased by 20% in response to increased extracellular Cu (Figure 3.5). Therefore, we considered proteins that increased or

decreased more than 20% (lower than 0.8X or higher than 1.2X) to be affected by excess Cu. If protein levels changed by less than 20%, we defined them to be unaffected by increased Cu since they were similarly varied compared to our control.

In the presence of either 0.01% or 0.1% Cu, Cox17 protein levels are affected similarly, increasing by about 1.70X compared to the not treatment control. Sco1 protein levels are unaffected at 0.01% Cu when compared to the Por1 control, but are slightly affected at 0.1% Cu, increasing 32% relative to the no treatment control. Unexpectedly, Cox11 protein levels remained unchanged in the presence of excess Cu since they are vary to the same extent as the Por1 control, even though Cox11 plays a role in Cu delivery to Cox1, one of the core subunits. The divergent changes of these COX assembly factors to excess Cu are unexpected, as they are involved in the same pathway of Cu delivery to COX.

Investigation of both an mtDNA-encoded subunit and a nuclear-encoded subunit revealed differences in how these proteins respond to excess Cu levels. Cox2 is slightly increased in 0.1% Cu; however, Cox4 is substantially increased, with 3.65X more protein after treatment. It is likely that excess Cu has a stabilizing effect on Cox4 protein, since *COX4* transcript levels do not change in response to excess Cu. Although Cox4 does not bind Cu, the crystal structure reveals a zinc (Zn) atom (Coyne *et al*, 2007), suggesting that excess Cu may stabilize Zn-binding proteins. The electron donor cytochrome *c* (Cyc1) also increases in excess Cu conditions, which supports the increase we see in both Cu-related COX assembly factors and subunits and is logical since Cyc1 is an electron donor in the respiratory chain.

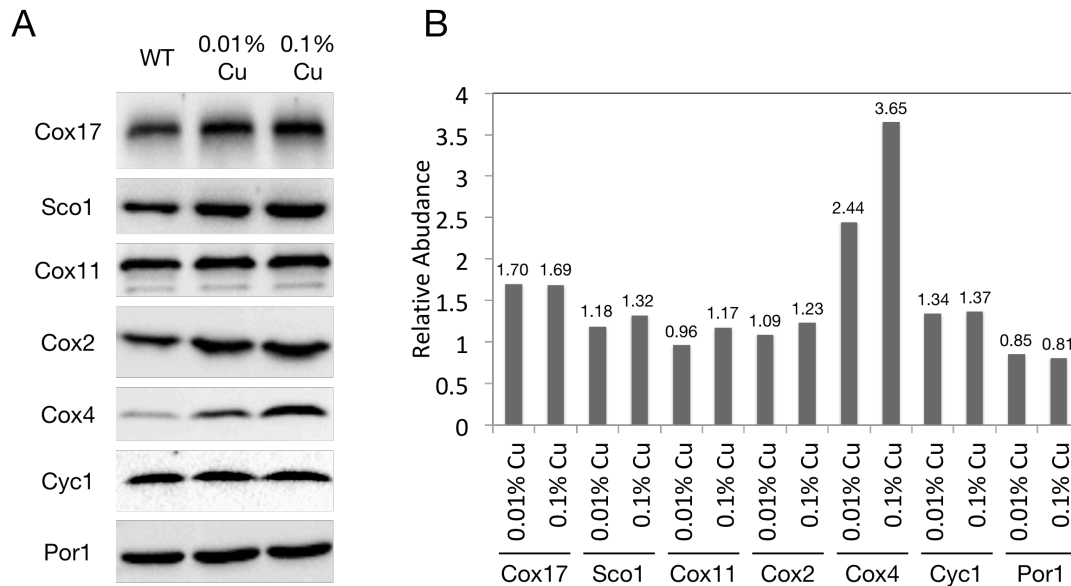


Figure 3.5 Mitochondrial protein levels in Cu excess conditions

(A) Representative Western blots of mitochondrial protein samples (25 μ g protein) using antibodies to proteins involved in COX assembly (Cox17, Sco1, Cox11), COX subunits (Cox2, Cox4), or other mitochondrial protein (Cyc1, Por1). All blots were stained with Ponceau S prior to immunoblotting to ensure equal loading across all lanes of the gel. (B) Quantification of protein levels on Western blots relative to the no treatment control. Por1 was used as the loading control. Using the changes in Por1 levels, any quantification above 1.2X or below 0.8X was considered to be significant. Quantification is the average of at least two separate subcellular fractionations.

Although Cox17 has a well-defined role in the mitochondria, approximately 40% of the protein is found in the cytosol (Beers *et al.*, 1997). Therefore, we wanted to compare changes of Cox17 protein levels in the mitochondria to those in the cytosol and in the cell as a whole. Interestingly, we found that Cox17 protein levels decreased in the cytosolic fraction in response to excess Cu, and this is accompanied by a decrease of Cox17 protein in cell lysates (Figure 3.6). Specifically, Cox17 protein levels decreased by 38% in the cytosol and 69% in cell lysates, in contrast to increasing 70% in the mitochondria. The fact that similar *COX17* transcript levels correlated with an decrease in total cellular Cox17 protein levels in Cu excess suggests that Cu might have an overall destabilizing effect on Cox17, but a stabilizing effect on the mitochondrial pool of the protein. Because the cell is exposed to excess Cu, we hypothesize that only the mitochondrial pool of Cox17 is binding Cu, explaining the stabilizing effect that is unique to the mitochondria.

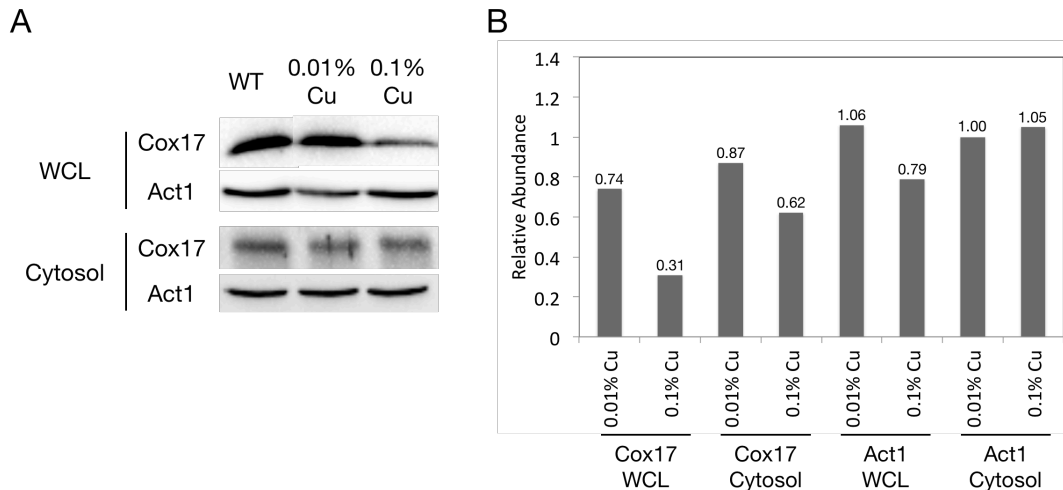


Figure 3.6 Cox17 protein levels in Cu excess conditions

(A) Representative Western blots of cytosolic protein samples (25 μg protein) and cell lysate protein samples (60 μg protein) using antibodies to Cox17 or Act1. All blots were stained with Ponceau S prior to immunoblotting to ensure equal loading across all lanes of the gel. (B) Quantification of protein levels on Western blots relative to the no treatment control. Act1 was used as the loading control. Using the changes in Act1 levels, any quantification above 1.21X or below 0.79X in cell lysates and above 1.05X or below 0.95X in the cytosol was considered to be significant. Quantification is the average of at least two separate subcellular fractionations.

To understand how changes in protein levels reflected in activity, we measured COX activity on isolated mitochondria after CuSO_4 treatment by recording the oxidation of cytochrome *c* at 550 nm. We found that the specific activity of COX significantly increased in response to excess Cu (Figure 3.7). Interestingly, COX activity was similar with 0.01% Cu and 0.1% Cu, indicating that a 10-fold difference in Cu does not have an effect on activity. This suggests that there may be a threshold of COX activity in the presence of excess Cu that is already met in an environment containing 0.01% Cu. Overall, the increase in COX activity is in agreement with our Western blots, which displayed increases in protein levels of Cox17, Sco1, Cox2, Cox4, and Cyc1, proteins that are all important for a fully functional COX. Contrary to our expectations, Cox11 protein levels were similar in excess Cu conditions compared to no treatment controls, even though other COX assembly factor protein levels and COX activity were increased.

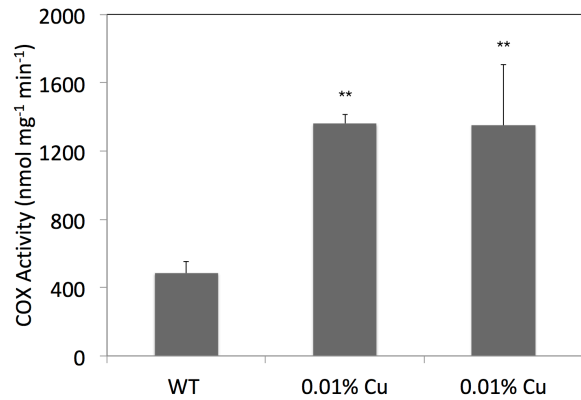


Figure 3.7 COX activities in Cu excess conditions

Mitochondrial fractions were tested for COX activity by measuring the oxidation of reduced cytochrome *c* at 550 nm for 60 seconds. The Student's T-Test was used between the WT and each treatment to determine statistical significance: $p < 0.01 = **$. Error bars represent \pm SEM of technical duplicates on three different biological replicates.

3.2.2 Sod1 in the face of Cu excess

We next investigated how Cu,Zn-Sod1 responds to excess extracellular Cu. Similarly to COX assembly factors and subunits, we started by assessing how Sod1 transcript levels changed in response to excess Cu. We also looked at *CCSI* transcript levels, given its role as Cu chaperone for Sod1 in yeast. We found that, after treatment with 0.1% Cu for 18 hours, transcript levels of both *CCSI* and *SOD1* were significantly increased by 3.24X and 2.54X, respectively (Figure 3.8). In contrast, treatment with 0.01% Cu revealed no significant changes in *CCSI* and *SOD1* transcript levels. The increase of *SOD1* transcript levels with 0.1% Cu is consistent with the finding that Ace1 activity results in upregulation of *SOD1* transcription (Nevitt *et al*, 2012). Because we know that *CCSI* is functionally related to *SOD1*, it is not surprising that *CCSI* transcript levels correlated with *SOD1* transcript levels.

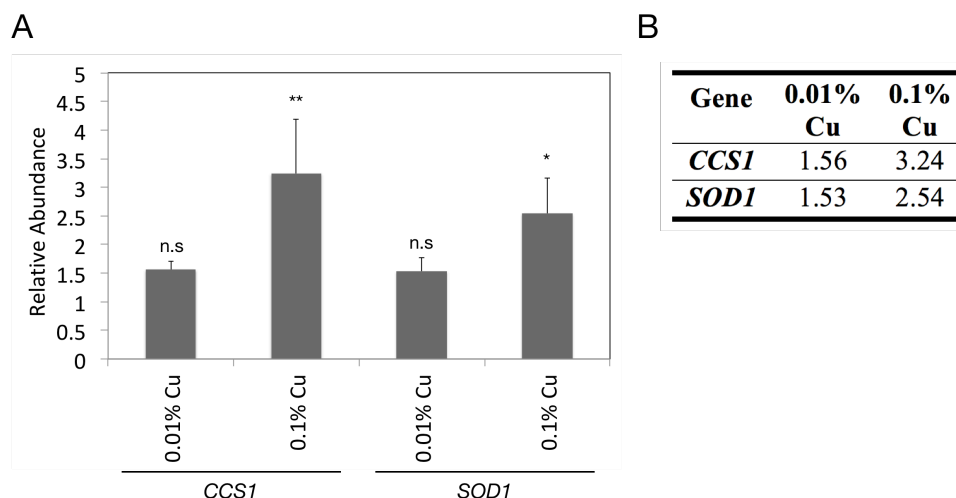


Figure 3.8 RT-qPCR of *CCS1* and *SOD1* in Cu excess conditions

(A) Graphical representation of relative abundance of *CCS1* and *SOD1*. RNA was isolated from yeast cells grown for 18 hours in YPD + CuSO₄. PCR was performed using cDNA on both the gene of interest and *ACT1* as a control. Values are representative of $\Delta\Delta Cq$ values. Three biological replicates were performed for each concentration. A one-way ANOVA was done to determine statistical significance: not significant = n.s, $p < 0.05 = *$, $p < 0.01 = **$. Error bars represent \pm SEM (B) Raw $\Delta\Delta Cq$ values, representing the fold-change in each condition relative to *ACT1*.

To evaluate if Sod1 responded to excess Cu at the protein and activity levels, we considered the Sod1 pools in both the mitochondria and the cytoplasm. Similarly to Cox17, Sod1 is dually localized to the mitochondria and cytosol; approximately 90% of Sod1 protein resides in the cytosol and the other 10% is found in the IMS of mitochondria (Valentine *et al*, 2005). Western blotting analysis of Sod1 in both mitochondrial and cytosolic fractions revealed an increase in protein levels after treatment of either 0.01% or 0.1% Cu (Figure 3.9). We used Por1 protein levels (Figure 3.5) as a loading control for mitochondria, and Act1 protein levels (Figure 3.6) as a loading control for the cytosol. Interestingly, at 0.01% Cu, the unchanged *SOD1* transcript levels did not correspond to the increase we observed in Sod1 protein levels, again suggesting altered protein stability.

Analysis of SOD activity in mitochondrial and cytosolic fractions was performed by running protein fractions on a non-denaturing gel followed by exposure to nitroblue tetrazolium (NBT) and riboflavin, which form superoxide (Beauchamp and Fridovich, 1971). The presence of active Sod1 or Sod2 will appear as a clear band on the gel that can be quantified after imaging. As seen in Figure 3.9, SOD activity increased with excess Cu treatment, which corresponded to the increased protein levels. Mitochondrial SOD activity consists of both Sod1 and Sod2 activity, and is increased 1.61X and 2.19X with treatment of

0.01% and 0.1% Cu respectively. Cytosolic SOD activity, which only consists of Sod1, increased by 1.51X and 1.80X with the two Cu treatment conditions. Overall, Sod1 protein and activity levels are increased in both compartments with excess extracellular Cu.

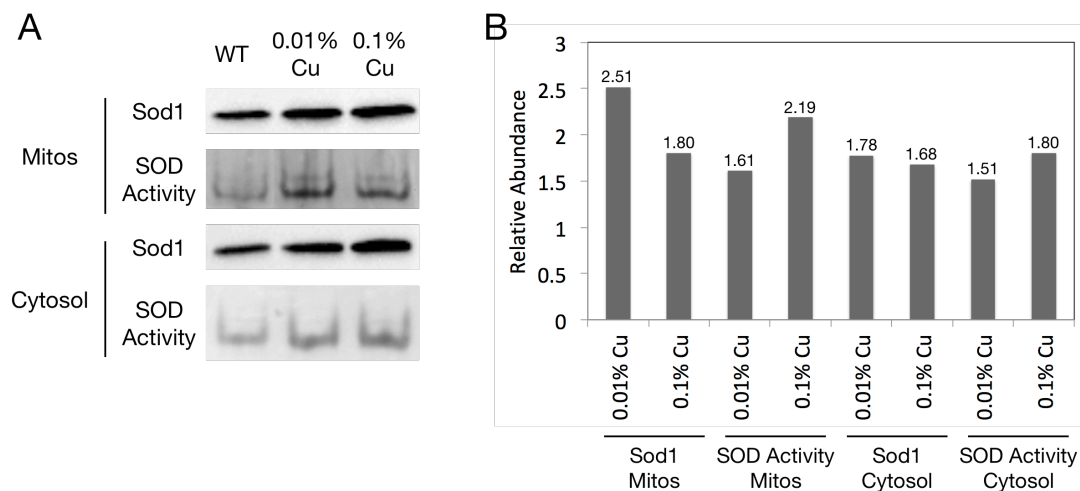


Figure 3.9 Sod1 protein and activity levels in Cu excess conditions

(A) Representative Sod1 Western blot (25 μ g protein) and SOD activity gel (48 μ g protein in mitochondria, 24 μ g protein in cytosol) using mitochondrial and cytosolic protein samples. SOD activity was measured in-gel using a well-established method (Beauchamp & Fridovich, 1971). (B) Quantification of protein and activity levels relative to the no treatment control. Por1 was used as the loading control for the Sod1 Western blot in the mitochondria, and Act1 for the cytosol. Using the changes in Por1 levels (Figure 3.5) or Act1 levels (Figure 3.6), we defined significant changes in levels of Sod1. Quantification of protein and activity levels is the average of at least two separate subcellular fractionations.

3.2.3 Non-Cu related mitochondrial functions in the face in Cu excess

Although COX and Sod1 are the main sources of mitochondrial Cu, we wanted to investigate if excess Cu affected other mitochondrial functions, unrelated to Cu. The increase we saw in COX activity suggests that there may be more flux through the respiratory chain. Therefore, we asked whether TCA cycle proteins Sdh2 and Aco1 are affected by treatment with excess Cu. Western blotting analysis revealed that Sdh2 protein levels increase at 0.01% Cu but remain constant at 0.1% Cu, while Aco1 protein levels are increased with both treatment conditions (Figure 3.10-A, 3.10-B). Sdh2 protein levels increasing at 0.01% Cu but not 0.1% Cu could suggest a dose-dependent response of the protein to CuSO₄, but more experiments would be needed to confirm this hypothesis.

Because of the differential response between Sdh2 and Aco1 protein levels, we cannot conclusively state how the TCA cycle behaves in response to excess Cu conditions. To further analyze flux through the TCA cycle, we measured mitochondrial Aco1 activity

using an indirect approach (Bulteau *et al*, 2005). We found that with Cu excess treatment conditions, regardless of concentration, Aco1 activity significantly increased (Figure 3.10-C), which is consistent with the increased protein levels. In contrast to Sdh2, Aco1 protein and activity levels responded similarly to both concentrations of Cu. Taken together, it is likely that TCA cycle flux is increased with excess Cu treatment, consistent with the increased flux we observed in the respiratory chain.

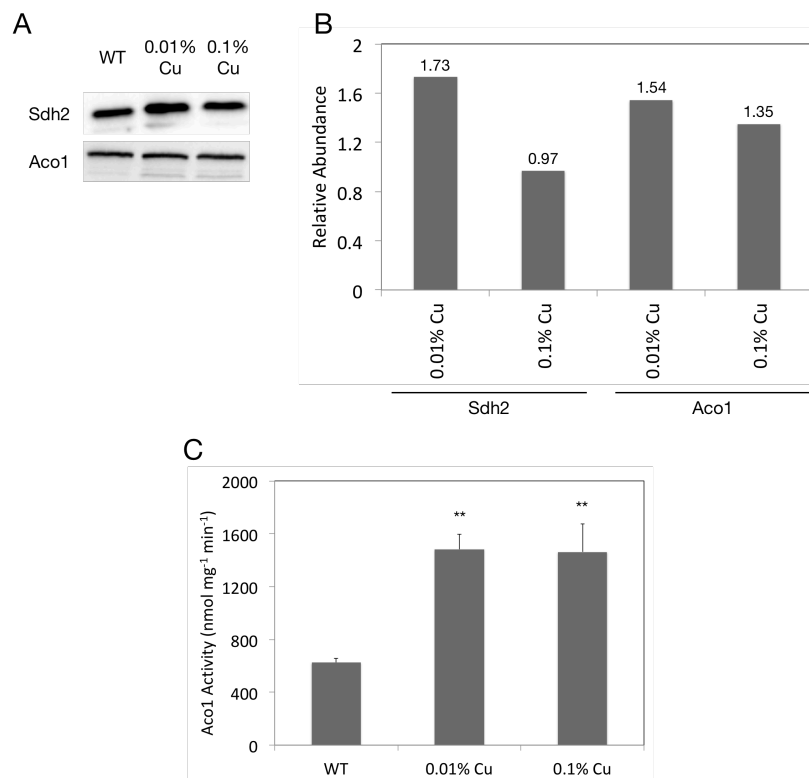


Figure 3.10 TCA cycle protein levels and Aco1 activity levels in Cu excess conditions

(A) Representative Western blots of mitochondrial protein samples (25 μ g protein) using antibodies to proteins in the TCA cycle (Sdh2, Aco1). Blots were stained with Ponceau S prior to immunoblotting to ensure equal loading across all lanes of the gel. (B) Quantification of protein levels on Western blots relative to the no treatment control. Por1 (Figure 3.5) was used as the loading control. Using the changes in Por1 levels, any quantification above 1.2X or below 0.8X was considered to be significant. Quantification is the average of at least two separate subcellular fractionations. (C) Aconitase activity was assayed from mitochondrial fractions using citrate as the substrate. NADPH production was measured over 60 seconds at 340 nm (Bulteau *et al*, 2003). Error bars represent \pm SEM of duplicates of three separate mitochondrial isolations.

In addition to being part of the TCA cycle, Aco1 activity is also regarded as a marker of oxidative stress in the mitochondria (Bulteau *et al*, 2005). Aco1 contains an iron-sulfur (FeS) centre that is extremely sensitive to oxidative damage. To define whether our increased Aco1 activity correlated with decreased oxidative stress, we used an Oxyblot, which allows visualization of oxidative damage by detection of protein carbonylation. Our results from cell

lysates displayed that, when treated with 0.1% Cu, there is less protein carbonylation relative to a no treatment control (Figure 3.11). However, both the cytosolic and mitochondrial fractions revealed increased protein carbonylation after exposure to excess Cu. This suggests that other cellular compartments, such as the nucleus, have decreased oxidative damage in excess Cu conditions. Taken together, we concluded that the increased Aco1 activity we see in the 0.1% Cu treatment is related to increased flux through the TCA cycle, and not a reflection of a decrease in oxidative damage.

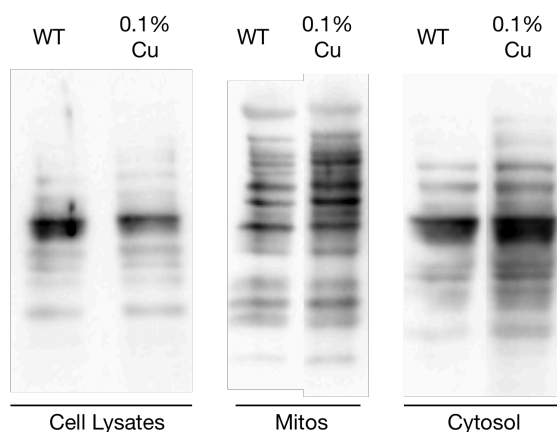


Figure 3.11 Oxidative damage in Cu excess conditions

Carbonylation of proteins, a common form of oxidative damage, was measured in cell lysates (20 μ g), mitochondria (25 μ g) and cytosolic (25 μ g) fractions after 18 hours of treatment with 0.1% CuSO₄, using the Millipore OxyBlot Kit. Oxidized proteins were conjugated with 2,4-dinitrophenylhydrazine (DNP) and then visualized by Western blotting using an anti-DNP antibody. Blots were done on two separate biological replicates (Soule, unpublished)

Because we saw increased levels of oxidative damage in the mitochondria in the Oxyblot, we wondered whether they were associated with changes in mitochondrial proteasomal machinery. Therefore, our final test of mitochondrial function was measurement of transcript and protein levels of the *PIMI* (Lon) gene, an abundant mitochondrial protease that degrades proteins that reside in the mitochondrial matrix or the IMM. Assessment of *PIMI* transcript levels was identical to measurement of other transcripts; qPCR was performed on cDNA using primers specific to the *PIMI* gene, and $\Delta\Delta$ Cq values were obtained by comparing *PIMI* gene expression to *ACT1* gene expression with increasing Cu concentration. We found that at a concentration of 0.01% Cu, *PIMI* expression is not significantly changed, but at 0.1% Cu, *PIMI* transcript levels significantly increased 3.35X compared to a no treatment control (Figure 3.12-A, 3.12-B). This indicated that exposure to 0.1% Cu does affect *PIMI* gene expression.

We next looked at Lon protein levels to identify if the increase in *PIMI* transcript levels were consistent with levels of the protein product. When compared to the Por1 control, we observed no significant changes in Lon protein levels after treatment with excess Cu. Specifically, Lon protein levels were 14% increased with 0.01% Cu and 3% decreased with 0.1% Cu, relative to the no treatment control (Figure 3.12-C). As a result, we concluded that the increased transcript levels of *PIMI* did not correlate with increased Lon protein levels. These preliminary results suggest that in response to excess Cu, the mitochondria do not greatly modify their protein degradation machinery.

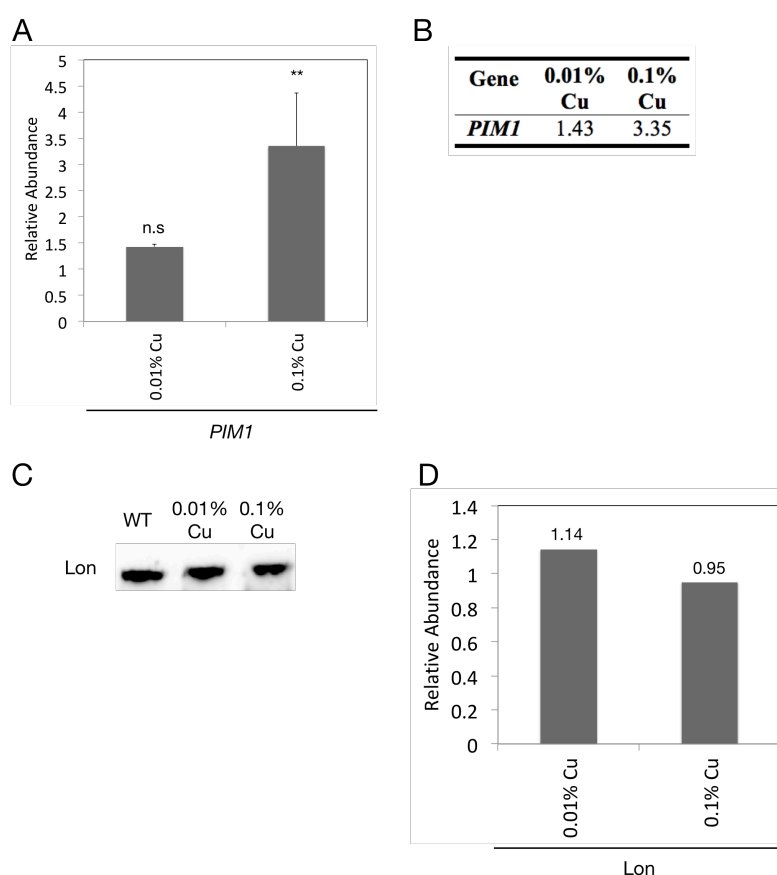


Figure 3.12 Analysis of mitochondrial Lon protease in Cu excess conditions

(A) Graphical representation of RT-qPCR data of *PIMI* in Cu excess conditions. RNA was isolated from yeast cells grown for 18 hours in YPD + CuSO₄. PCR was performed using cDNA on both the gene of interest and *ACT1* as a control. Values are representative of $\Delta\Delta Cq$ values. Three biological replicates were performed for each concentration. A one-way ANOVA was done to determine statistical significance: not significant = n.s, $p < 0.01 = **$. Error bars represent \pm SEM (B) Raw $\Delta\Delta Cq$ values, representing the fold-change in each condition relative to *ACT1*. (C) Representative Western blot of mitochondrial protein samples (25 μ g protein) using antibody to Lon. Blots were stained with Ponceau S prior to immunoblotting to ensure equal loading across all lanes of the gel. (D) Quantification of protein levels on Western blots relative to the no treatment control. Por1 (Figure 3.5) was used as the loading control. Using the changes in Por1 levels, any quantification above 1.2X or below 0.8X was considered to be significant. Quantification is the average of at least two separate subcellular fractionations.

3.3 Summary of Results

In order to study the impact of Cu availability on mitochondrial function, we established concentrations of CuSO₄ (0.01% and 0.1%) and BCS (10, 100, and 500 μM) that physiologically impacted the cell but did not cause a growth defect.

In Cu excess conditions, we saw a generalized increase in protein levels of COX subunits and COX assembly factors, as well as COX activity, but not transcript levels. One exception was Cox11 protein levels, which did not significantly increase with either 0.01% or 0.1% Cu treatment. Although Cox17 protein levels increased in the mitochondria with increasing concentrations of Cu, they decreased in both the cytosolic fraction and the whole cell lysate, suggesting that the mitochondrial pool of Cox17 is most important under Cu excess conditions.

At 0.1% Cu, both *CCSI* and *SOD1* genes were upregulated, which corresponded to the increase we observed in Sod1 protein levels and SOD activity compared to the no treatment control. Our analyses also revealed an increase in flux through the TCA cycle, higher mitochondrial oxidative damage, and upregulation of *PIMI* in Cu excess conditions. Interestingly, the upregulation of *PIMI* did not correspond to an increase in Lon protein levels in the mitochondria. Taken together, our results suggest that excess extracellular Cu leads to increased mitochondrial cuproprotein levels and flux through the respiratory chain, which is consistent with increased oxidative damage.

Chapter 4: Analysis of Cu Deficient Conditions

Similar to having too much Cu, deficiencies of the metal also have negative impacts on cellular and mitochondrial function. When Cu is depleted, cells must alter their regulation of Cu distribution, and cuproproteins will not be fully functional. Patient cells with mutations in certain proteins related to COX assembly can be rescued by Cu supplementation, suggesting that the defect results in Cu deficiency (Jaksch *et al*, 2001) (Ghosh *et al*, 2014). Therefore, we studied how partitioning of mitochondrial Cu changes under conditions in which the metal is limited or restricted.

Previous literature has reported that in *Chlamydomonas* during Cu deficiency, cells will down-regulate the Cu-containing plastocyanin and a Fe-containing protein, cytochrome c_6 , will take over its native function (Kropat *et al*, 2015). Similarly, in the pathogenic yeast *Candida albicans*, Cu deficiency results in repression of the *SOD1* gene in order to restore COX activity in the mitochondria (Broxton & Culotta, 2016). Taken together, these results suggest that in the absence of adequate levels of Cu, cells will actively downregulate other cuproproteins to lessen the negative effect on mitochondria. In this chapter, we examined how Cu deficiency impacts mitochondrial protein levels and function in *Saccharomyces cerevisiae*.

4.1 Mitochondrial Proteins in Cu Deplete Conditions

4.1.1 COX in the face of Cu deficiency

We were interested in how mitochondria responded to a generalized Cu deficiency since both COX and Sod1 rely on Cu for their functions. To analyze the impact of Cu deficiency on mitochondrial cuproproteins, we took a similar approach to our analysis of Cu excess conditions. We started by looking at COX and Sod1 pools, and then looked at the impacts of Cu deficiency on more generalized mitochondrial function. As described in section 3.1, for inducing extracellular Cu-specific deficiency we treated our cultures with 10 μ M, 100 μ M, or 500 μ M BCS, a Cu chelator. These concentrations of BCS were shown to induce a physiological response and yet have minimal negative impact on cell viability.

Analysis of transcript levels of *COX17*, *SCO1*, and *COX11* revealed no significant changes with cells treated with BCS compared to the control (Figure 4.1), as seen for Cu excess, further suggesting that these genes do not contain any Cu-responsive elements. We used transcript levels of *COX4* as a control, and observed an unexpected decrease in *COX4* transcript levels by 35% after exposure to 100 μ M and 500 μ M BCS for 18 hours, but they were not significantly different at 10 μ M BCS exposure. Our observation of down-regulation of one of the COX subunits may indicate a dysfunctional COX or defective COX assembly at higher concentrations of BCS.

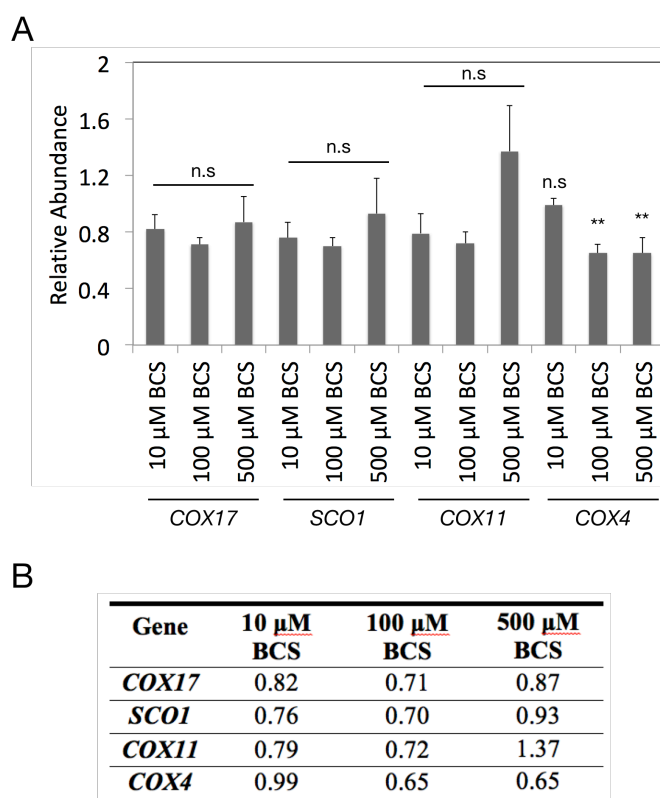


Figure 4.1 RT-qPCR of *COX17*, *SCO1*, *COX11* and *COX4* in Cu depletion conditions

(A) Graphical representation of relative abundance of *COX17*, *SCO1*, *COX11* and *COX4*. RNA was isolated from yeast cells grown for 18 hours in YPD + BCS. PCR was performed using cDNA on both the gene of interest and *ACT1* as a control. Values are representative of $\Delta\Delta$ Cq values. Three biological replicates were performed for each concentration. A one-way ANOVA was performed to determine statistical significance: not significant = n.s, $p < 0.01$ = **. Error bars represent \pm SEM. (B) Raw $\Delta\Delta$ Cq values, representing the fold-change in each condition relative to *ACT1*.

We next looked at how protein levels of COX assembly factors and subunits changed in response to Cu deficiency. As in Chapter 3, if protein levels of the protein of interest changed more than Por1 protein levels, we considered the change to be significant. At 500 μ M BCS, Cox17 protein levels increased while Sco1 and Cox11 protein levels decreased

compared to the control (Figure 4.2). However, after exposure to 10 μ M and 100 μ M BCS, Sco1 protein levels were unaffected while Cox11 protein levels decreased by 16%-57%. The differences seen with protein levels of Sco1 and Cox11 further supports differentiating behaviors of these two proteins, even though they have similar functions. The increase in Cox17 protein levels while cells experience a decrease in Sco1 and Cox11 protein levels at 500 μ M BCS, suggests that during Cu deficiency, the mitochondrial pool of Cox17 may have a secondary function.

In agreement with the decrease we observed in *COX4* transcript levels, the Cox4 protein was barely detectable at 500 μ M BCS. Specifically, Western blotting using antibodies against Cox4 revealed a 77% or 94% decrease in protein levels with 100 μ M BCS and 500 μ M BCS, respectively. Cox2, our representative mitochondrial subunit, also significantly decreased with increasing BCS concentrations. The decrease in Cox2 and Cox4 protein levels is consistent with a decreased level of Cyc1, the COX electron donor, which we also observed at 500 μ M BCS. Taken together, the loss of both nuclear and mitochondrial-encoded COX subunits suggests a loss of assembled COX in Cu deficient conditions.

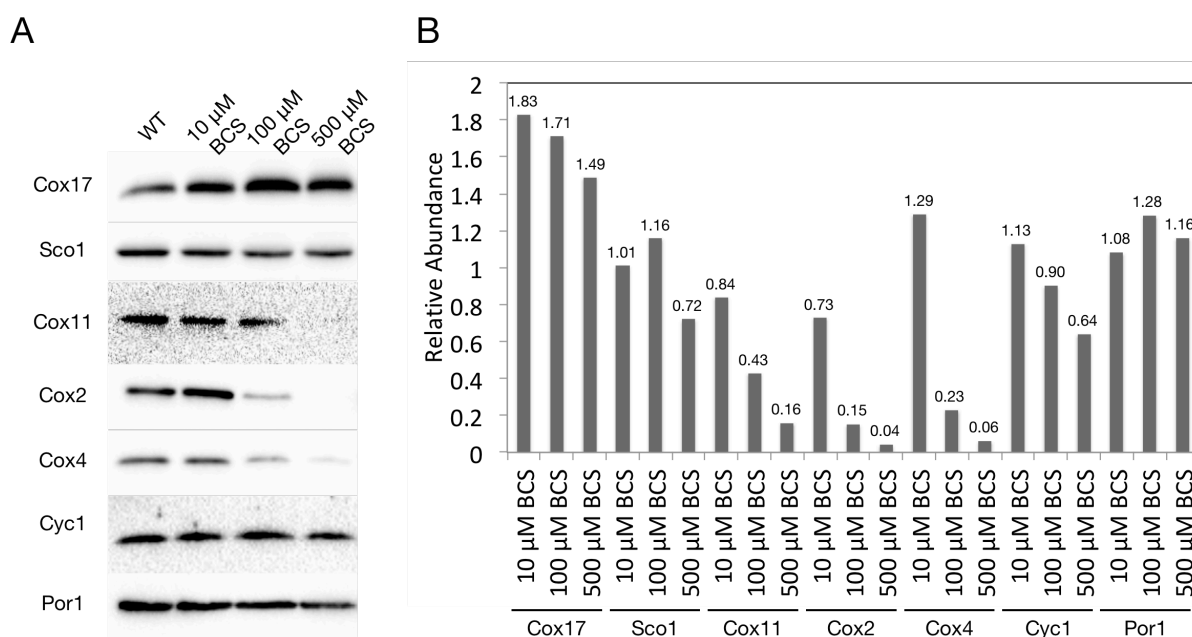


Figure 4.2 Mitochondrial protein levels in Cu depletion conditions
 (A) Representative Western blots of mitochondrial protein samples (25 μ g protein) using antibodies to proteins involved in COX assembly (Cox17, Sco1, Cox11), COX subunits (Cox2, Cox4), or other mitochondrial protein (Cyc1, Por1). All blots were stained with Ponceau S prior to immunoblotting to ensure equal loading across all lanes of the gel. (B) Quantification of protein levels on Western blots relative to the no treatment control. Por1 was used as the loading control. Using the changes in Por1 levels, any quantification above 1.28X or below 0.72X was considered to be significant. Quantification is the average of at least two separate subcellular fractionations.

Similarly to what we saw with excess Cu, Cox17 protein levels increased in the mitochondria from cells with Cu deficiency. We also performed Western blotting on whole cell lysate and cytosolic protein fractions to investigate whether total cell Cox17 pools or cytosolic protein levels changed in response to Cu depletion. In whole cell lysates, we observed a slight increase in protein levels at 10 μ M and 100 μ M BCS compared to the Act1 control, while after exposure to 500 μ M BCS the Cox17 protein level was virtually identical to the no treatment control (Figure 4.3). From three separate subcellular fractionations, we saw that cytosolic Cox17 protein levels were unchanged between the control and all of the BCS treatments. Overall, our results suggest that levels of Cox17 in the whole cell are unchanged in response to increasing concentrations of BCS. However, we observe a redistribution of Cox17; more Cox17 is transported into the mitochondria while the cytosolic pool remains constant.

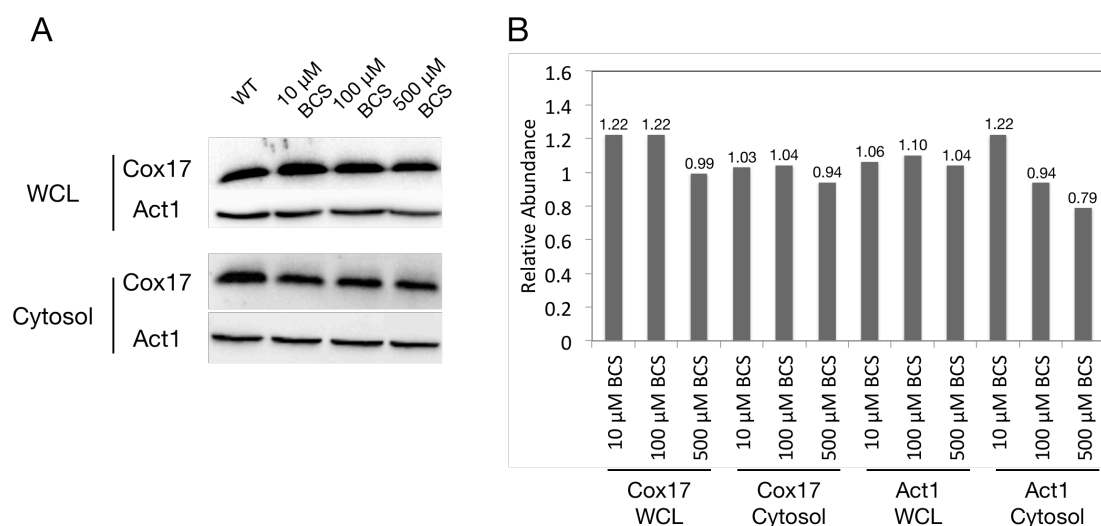


Figure 4.3 Cox17 protein levels in Cu deficiency

(A) Representative Western blots of cell lysate protein samples (60 μ g protein) and cytosolic protein samples (25 μ g protein) using antibodies to Cox17 or Act1. All blots were stained with Ponceau S prior to immunoblotting to ensure equal loading across all lanes of the gel. (B) Quantification of protein levels on Western blots relative to the no treatment control. Act1 was used as the loading control. Using the changes in Act1 levels, any quantification above 1.10X or below 0.90X in the cell lysates and above 1.21X or below 0.79X in the cytosol was considered to be significant. Quantification is the average of at least two separate subcellular fractionations.

Western blotting data on COX assembly factors and subunits showed that during Cu deficiency, we appeared to have a loss of assembled COX. Therefore, we hypothesized that increasing concentrations of BCS would correlate with a decrease in COX activity. After 18 hours of exposure to BCS, we isolated mitochondria and analyzed COX activities by

measuring the reduction of reduced cytochrome *c* over time (Figure 4.4). At 10 μM BCS, we did not observe any significant change in COX activity compared to the no treatment control, agreeing with the similar protein levels of Cox2 and Cox4 we saw between the no treatment sample and 10 μM BCS sample. At 100 μM BCS and 500 μM BCS, we observed a large decrease in COX activity, which was confirmed to be significant after performing the Student's T-test. Specifically, COX activity decreased from 470.7 $\text{nmol mg}^{-1} \text{min}^{-1}$ with no treatment to 179.3 $\text{nmol mg}^{-1} \text{min}^{-1}$ with 100 μM BCS and to 70.7 $\text{nmol mg}^{-1} \text{min}^{-1}$ with 500 μM BCS. This low rate of cytochrome *c* oxidation is likely due to auto-oxidation and therefore is not representative of COX activity. Therefore, we concluded that when subjected to Cu deficient conditions, COX is no longer assembled or functional. This contradicts results from the yeast *C. albicans*, where it is thought that during Cu deficiency, the cell restores COX activity with the minimal mitochondrial Cu present (Broxton & Culotta, 2016).

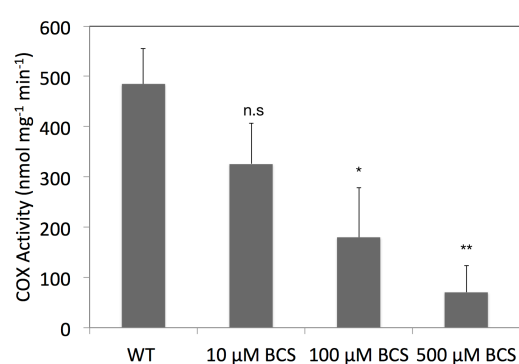


Figure 4.4 COX activities in Cu depletion conditions

Mitochondrial fractions were tested for COX activity by measuring the oxidation of reduced cytochrome *c* at 550 nm for 60 seconds. The Student's T-Test was used between the WT and each treatment to determine statistical significance: not significant = n.s, $p < 0.05 = *$, $p < 0.01 = **$. Error bars represent \pm SEM of technical duplicates on three different biological replicates.

The significant decrease in COX activity with increasing BCS concentration is not lethal in *S. cerevisiae*, as it is able to survive solely by glycolysis. This led us to ask whether we could recover COX function in a low Cu environment, if we forced the cells to use oxidative phosphorylation by growing the yeast on a non-fermentable carbon source. Strikingly, we observed that on EG medium with 500 μM BCS, wild type yeast could not survive. This demonstrated that even when forced to undergo mitochondrial respiration, *Saccharomyces* cannot shift its metabolism and therefore the carbon source change is lethal. For confirmation of the loss of COX activity when cultures grown in glucose are exposed to BCS, we also tested our spot plates for COX activity using a qualitative assay (McEwen *et*

al, 1985). Colonies were permeabilized onto Whatman filter paper and incubated with *N, N, N', N'*-tetramethyl-p-phenylenediamine dihydrochloride (TMPD). Specifically, oxidation of TMPD increases the rate of reaction between cytochrome *c* and COX, and this results in a blue precipitate visible on the filter paper. As expected, we observed COX activity using this method in our no treatment control, and the absence of COX activity when cells were exposed to BCS.

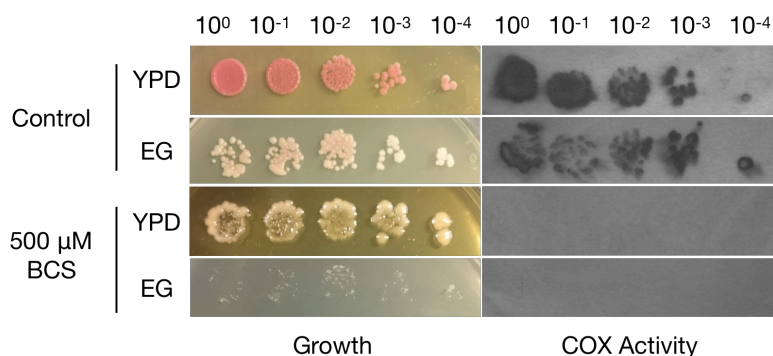


Figure 4.5 Analysis of yeast on non-fermentable carbon source during Cu deficiency

Spot plates of WT yeast were grown YPD and EG media in the absence and presence of 500 μM BCS for 2 days at 30°C. The COX activity was performed on colonies dried onto Whatman filter paper using 1% TMPD (McEwan et al, 1985).

As a first step towards identifying genes involved in the pathway that regulates cellular Cu distribution during low Cu conditions, we screened for suppressors that could grow on the non-fermentable carbon source. Overnight cultures of wild type yeast were plated onto EG + 500 μM BCS and left to grow until mutants arose. After 15 days, 4 mutants colonies were observed. They were streaked onto YPD and replica plated onto EG with different concentrations of BCS to confirm the suppressor phenotype (Figure 4.6). These patches were tested for COX activity by using the qualitative assay described above. We observed that after 2 days of growth at 30°C, suppressors grown on 100 μM BCS had increased COX activity compared to the wild type strain, which displayed minimal COX activity. At 500 μM BCS, neither the suppressors nor the wild type showed any growth, and therefore no COX activity. Genomic DNA preparation and sequencing of the suppressors should provide insights into the proteins that regulate mitochondrial Cu distribution in yeast.

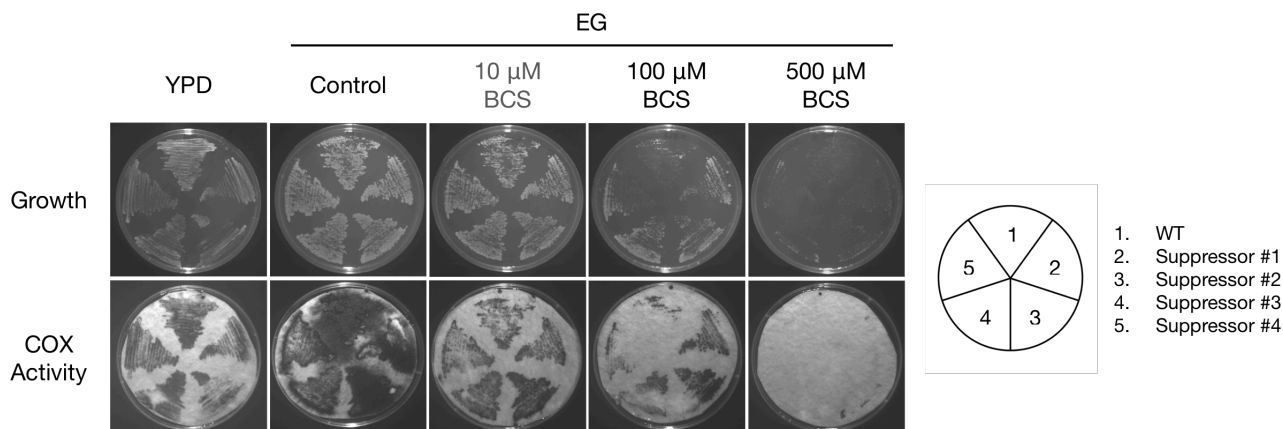


Figure 4.6 Analysis of suppressors isolated from plates containing EG + 500 μ M BCS
 Colonies were isolated after growth on EG + 500 μ M BCS for 15 days at RT, patched onto YPD, strain verified, and then restreaked. COX activity assay was performed as described (Figure 4.5).

4.1.2 Sod1 in the face of Cu deficiency

Since we observed that COX became inactive during increasing Cu depletion, we wondered if this also applied to the mitochondrial and cytosolic pools of Sod1. The distribution of SOD activity between these two compartments might provide insight into mitochondrial Cu import in Cu deficient conditions. Our initial analysis of *CCSI* and *SOD1* transcript levels in Cu deplete conditions revealed an increase in *CCSI* transcript at 500 μ M BCS, but no significant changes in *SOD1* transcript levels with any treatment of BCS (Figure 4.7). Specifically, *CCSI* transcript levels increased by 89% with 500 μ M BCS treatment while *SOD1* transcript levels increased by 3%, a non-significant change. Because *CCSI* transcript levels significantly changed with treatment of either excess Cu or BCS suggests that there is a Cu-responsive element on the gene.

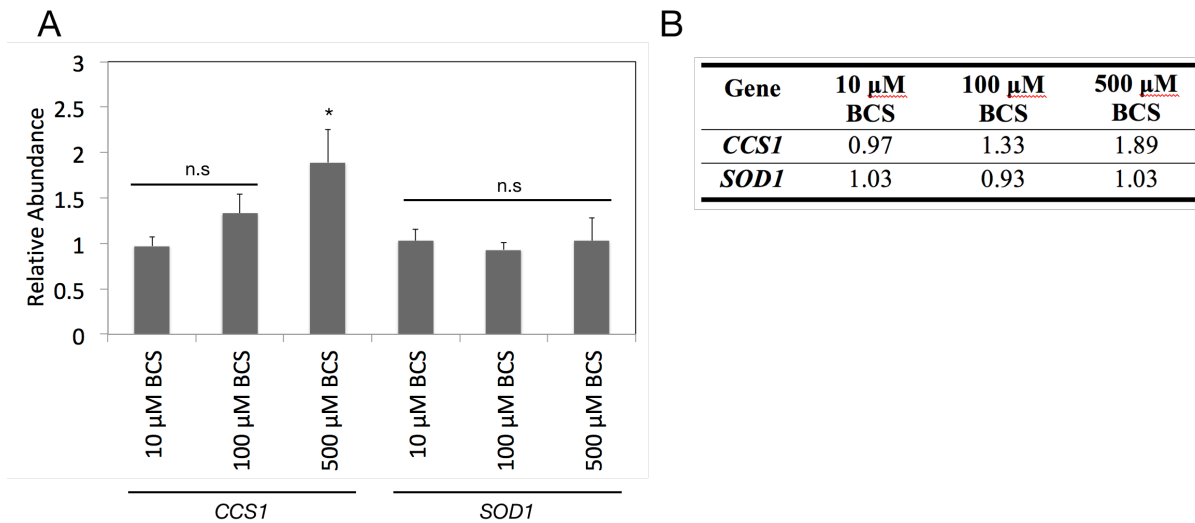


Figure 4.7 RT-qPCR of *CCS1* and *SOD1* in Cu deplete conditions

(A) Graphical representation of relative abundance of *CCS1* and *SOD1*. RNA was isolated from yeast cells grown for 18 hours in YPD + BCS. PCR was performed using cDNA on both the gene of interest and *ACT1* as a control. Values are representative of $\Delta\Delta Cq$ values. Three biological replicates were performed for each concentration. A one-way ANOVA was done to determine statistical significance: not significant = n.s, $p < 0.05$ = * Error bars represent \pm SEM (B) Raw $\Delta\Delta Cq$ values, representing the fold-change in each condition relative to *ACT1*.

We next analyzed how protein and activity levels of Sod1 changed at different concentrations of BCS. In the mitochondria, we observed that Sod1 protein levels were similar in the 500 μ M BCS sample and the control (Figure 4.8). Interestingly, Sod1 protein levels at 100 μ M were increased 3.03X compared to the control, suggesting that the response of mitochondrial Sod1 protein levels to BCS is dose-dependent. We had previously reported that Sod1 protein levels are not consistent with activity levels in mitochondrial mutants (Dubinski *et al*, 2018), so we asked whether mitochondrial Sod1 was active at 500 μ M BCS. Because Sod1 requires Cu to function, we assumed that the presence of Sod1 activity would be indicative of Cu being present at the active site. Surprisingly, SOD activity gels revealed consistency between protein and activity levels in the mitochondria, indicating that at 500 μ M BCS, our mitochondrial pool of Sod1 was present and active. Taken together, the loss of COX activity and retention of Sod1 activity after treatment with 500 μ M BCS strongly suggests a preferential distribution of Cu to Sod1 in mitochondria.

Compared to the no treatment sample, cytosolic Sod1 protein and activity levels are similar at 10 μ M BCS and gradually decrease at 100 μ M BCS (Figure 4.8). In contrast to the mitochondrial fraction, both Sod1 protein and activity levels were barely detectable in the cytoplasm at 500 μ M BCS. Since the cytosolic Sod1 pool consists of approximately 90% of

the protein, the similar transcript levels of *SOD1* likely correspond to a decrease in protein level, which suggests that cytosolic Sod1 protein is less stable when Cu is depleted. These results suggest that limiting Cu is only donated to the mitochondrial pool of Sod1 and not the cytosolic pool. Because we also observed loss of COX activity at 500 μ M BCS (Figure 4.4), our data suggest that during Cu deficiency, mitochondrial Sod1 activity is essential.

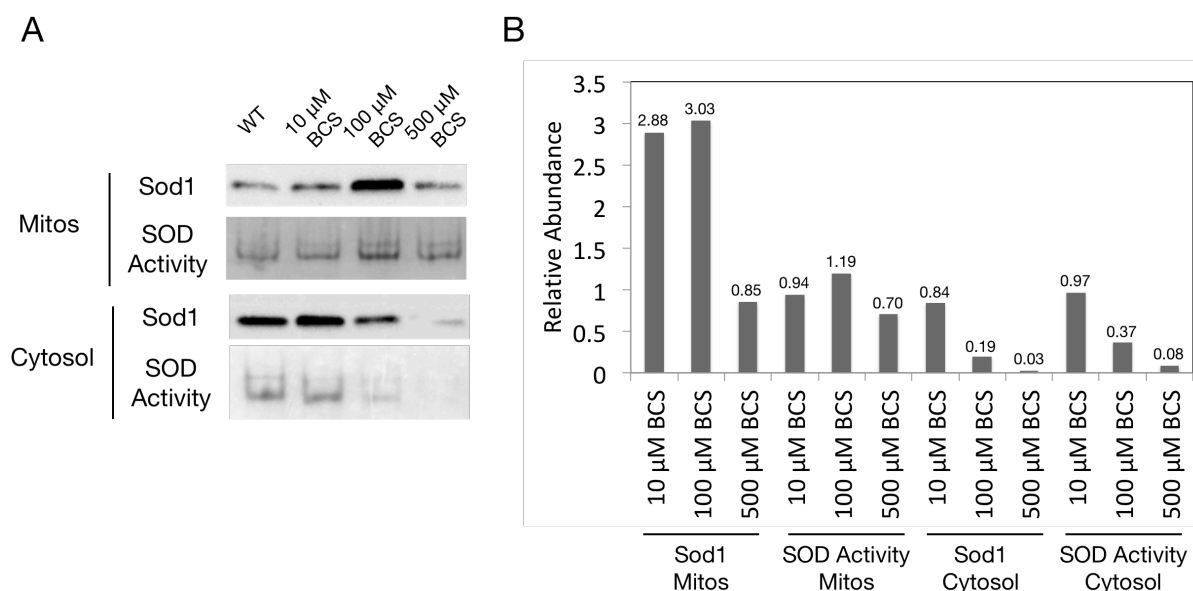


Figure 4.8 Sod1 protein and activity levels in Cu deplete conditions

(A) Representative Sod1 Western blot (25 μ g protein) and SOD activity gel (48 μ g protein for mitochondria, 24 μ g protein for cytosol) using mitochondrial and cytosolic protein samples. SOD activity was measured in-gel using a well-established method (Beauchamp & Fridovich, 1971). (B) Quantification of protein and activity levels relative to the no treatment control. Using the changes in Por1 levels (Figure 4.2) or Act1 levels (Figure 4.3), we defined significant changes in levels of Sod1. Quantification of protein and activity levels is the average of at least two separate subcellular fractionations.

4.1.3 Non-Cu related mitochondrial functions in the face in Cu deficiency

The lack of COX activity we observed at high concentrations of BCS led us to investigate how the TCA cycle behaved in these conditions. We performed the same analyses as for Cu excess conditions, which included protein levels of Sdh2 and Aco1 and measuring Aco1 activity. Using the Por1 protein levels changes as our control (Figure 4.3), we determined that the protein levels of both Sdh2 and Aco1 did not significantly change with any BCS treatment. On the other hand, Aco1 activity levels were higher at 100 μ M and 500 μ M BCS compared to the control, but remained similar after treatment with 10 μ M BCS. Interestingly, the Aco1 activity at 100 μ M BCS was higher than measured activity at 500 μ M BCS, which suggests a dose-dependent response to BCS and is reminiscent the pattern we

saw with Sod1 protein and activity levels with BCS. At 100 μM BCS, increased levels of Sod1 protein and activity suggest a decrease in mitochondrial ROS, which is in agreement with increased Aco1 protein levels, since they are sensitive to oxidative damage. Overall, the pattern we observed in TCA cycle protein levels and activity did not correlate with the significant decrease in COX activity. These preliminary data suggest that the loss of COX activity in Cu deficient conditions does not greatly influence flux through the TCA cycle.

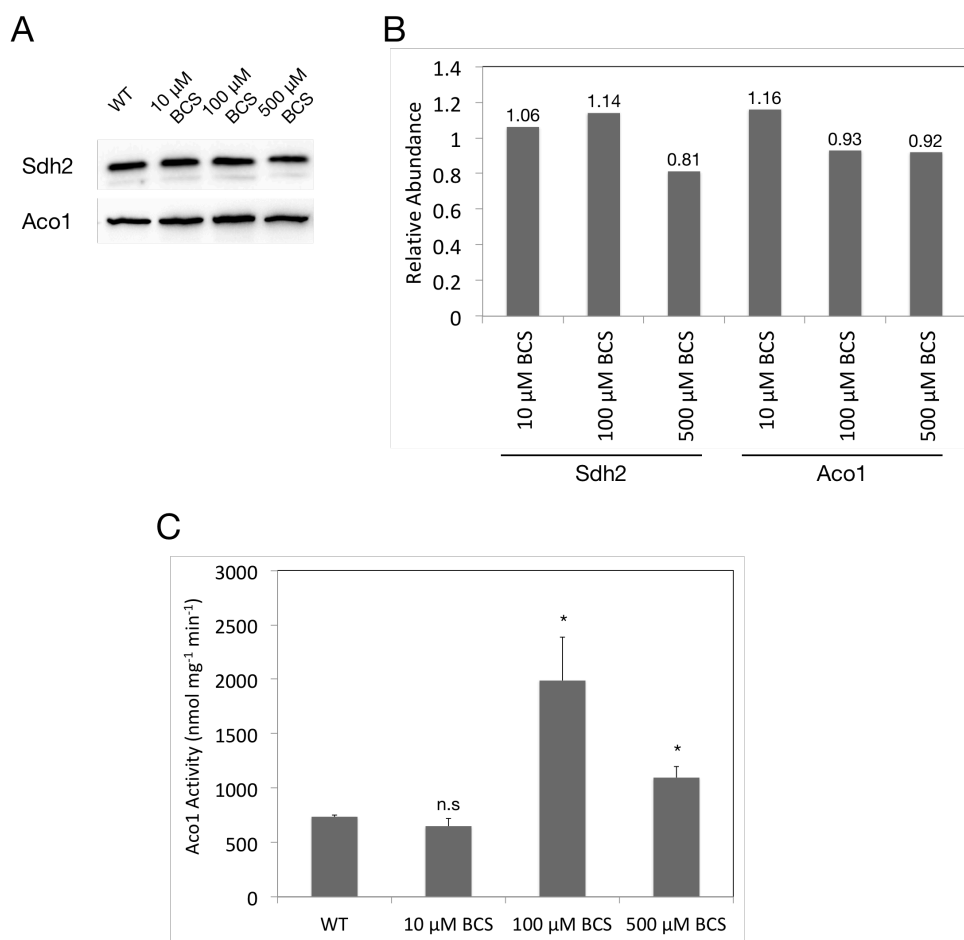


Figure 4.9 TCA cycle protein levels and Aco1 activity levels in Cu depletion conditions

(A) Representative Western blots of mitochondrial protein samples (25 μg protein) using antibodies to proteins in the TCA cycle (Sdh2, Aco1). Blots were stained with Ponceau S prior to immunoblotting to ensure equal loading across all lanes of the gel. (B) Quantification of protein levels on Western blots relative to the no treatment control. Por1 (Figure 3.5) was used as the loading control. Using the changes in Por1 levels, any quantification above 1.28X or below 0.72X was considered to be significant. Quantification is the average of at least two separate subcellular fractionations. (C) Aconitase activity was assayed from mitochondrial fractions using citrate as the substrate. NADPH production was measured over 60 seconds at 340 nm (Bulteau et al, 2003). Error bars represent \pm SEM of duplicates of three separate mitochondrial isolations.

Since increased Aco1 activity could imply either an increased flux through the TCA cycle or a decrease in oxidative stress, we asked if oxidative damage in mitochondria was

affected by treatment with 500 μ M BCS. We performed the Oxyblot with samples exposed to 500 μ M BCS for 18 hours and compared the status of oxidative damage to the no treatment control. In the mitochondria, we saw less oxidative damage in the 500 μ M BCS sample compared to the untreated sample (Figure 4.10). However, the whole cell lysates showed similar oxidative damage between the treated and untreated samples, and the cytosolic sample showed that the BCS-treated sample had increased oxidative damage compared to the control. In the mitochondria, the decrease in oxidative damage is in agreement with the increased Aco1 activity levels we observed. The retention of Sod1 activity in the mitochondria, but not in the cytosol, at 500 μ M BCS is also consistent with the differing levels of oxidative damage we observe in the two compartments. Overall, our Oxyblot analyses revealed that in the presence of BCS, oxidative damage is variable between compartments but is similar in the whole cell compared to the untreated control.

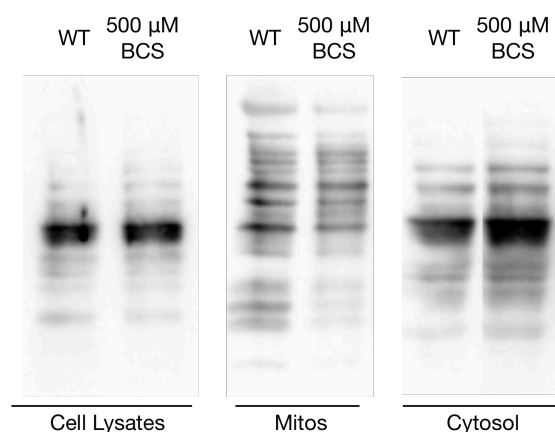


Figure 4.10 Oxidative damage in Cu depletion conditions

Carbonylation of proteins, a common form of oxidative damage, was measured in cell lysates (20 μ g), mitochondria (25 μ g) and cytosolic (25 μ g) fractions after 18 hours of treatment with 500 μ M BCS, using the Millipore OxyBlot Kit. Oxidized proteins were conjugated with 2,4-dinitrophenylhydrazine (DNP) and then visualized by Western blotting using an anti-DNP antibody. Blots were done on two separate biological replicates (Soule, unpublished).

In keeping with analyses in Cu excess conditions, our final assay in Cu deficient conditions was analyzing transcript and protein levels of *PIMI* (Lon), an important player in the mitochondrial proteasomal machinery. *PIMI* has an essential role in the degradation of Cox2, which we observed to have almost undetectable protein levels at 500 μ M BCS, and decreased protein levels at lower BCS concentrations. Therefore, we hypothesized that *PIMI* transcript levels and Lon protein levels are increased after BCS treatment compared to an untreated control. As expected, analysis of *PIMI* transcript levels revealed a significant

increase at 500 μM BCS, but no changes at the lower BCS concentrations (Figure 4.11-A, 4.11-B). The increase in transcript levels at 500 μM BCS was associated with no change in Lon protein levels, compared to the untreated sample. At 100 μM BCS, the unchanged *PIMI* transcript levels represented a slight decrease in Lon protein levels. At 10 μM BCS, the unchanged transcript levels were consistent with unchanged Lon protein levels. Overall, these results suggest that there is no obvious pattern between *PIMI* transcript levels and Lon protein levels in the face of Cu deficiency. One possibility is that the decrease we saw in Cox2, a mitochondrial-encoded subunit of COX, is likely due to decrease transcription of the *COX2* gene and not protein degradation, although we did not analyze other mitochondrial proteases.

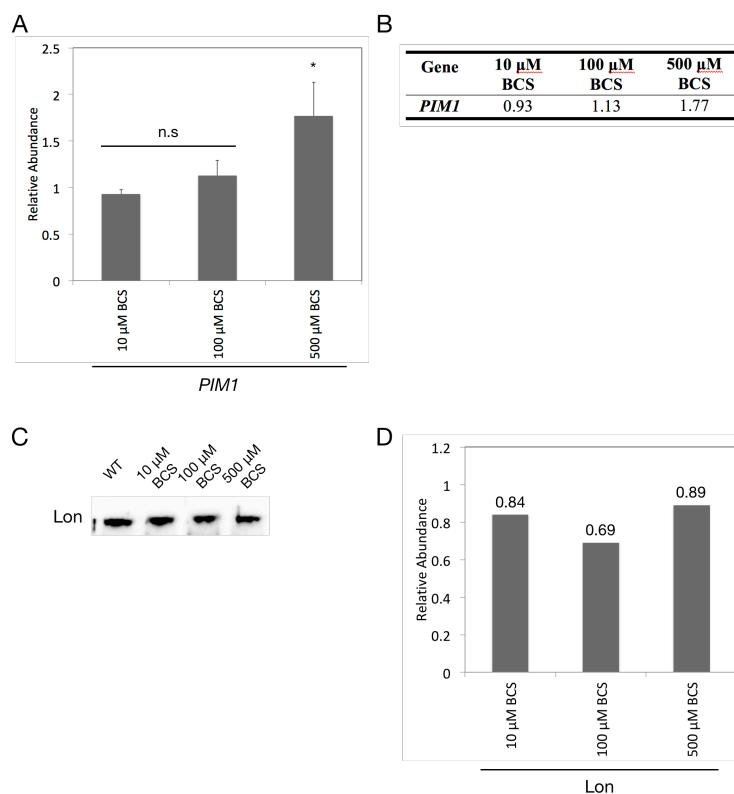


Figure 4.11 Analysis of mitochondrial Lon protease in Cu depletion conditions

(A) Graphical representation of RT-qPCR data of *PIMI* in Cu depletion conditions. RNA was isolated from yeast cells grown for 18 hours in YPD + BCS. PCR was performed using cDNA on both the gene of interest and *ACT1* as a control. Values are representative of $\Delta\Delta\text{Cq}$ values. Three biological replicates were performed for each concentration. A one-way ANOVA was done to determine statistical significance: not significant = n.s., $p < 0.05 = *$. Error bars represent \pm SEM (B) Raw $\Delta\Delta\text{Cq}$ values, representing the fold-change in each condition relative to *ACT1*. (C) Representative Western blot of mitochondrial protein samples (25 μg protein) using antibody to Lon. Blots were stained with Ponceau S prior to immunoblotting to ensure equal loading across all lanes of the gel. (D) Quantification of protein levels on Western blots relative to the no treatment control. Por1 (Figure 3.5) was used as the loading control. Using the changes in Por1 levels, any quantification above 1.28X or below 0.72X was considered to be significant. Quantification is the average of at least two separate subcellular fractionations.

4.2 Examining Cu Deficiency in Mitochondria with Galactose

The phenomenon of glucose repression in yeast occurs when glucose is used as the primary energy source, and results in repression of respiration and gluconeogenesis (Kayikci & Nielson, 2015). When using galactose as a carbon source, *S. cerevisiae* must convert it to glucose before it can enter glycolysis, and this process requires energy. Recent studies have proposed that Sod1 has a role in glucose repression in yeast through its interaction with yeast casein kinase 1 (Yck1), which is required for respiratory repression (Reddi & Culotta, 2013). Furthermore, Yck1 has been found to localize to the plasma membrane but translocates to the mitochondrial membrane during glucose repression and is dynamically tethered there by protein palmitoylation (Matic *et al*, 2018). We wondered if the preferential donation of Cu to mitochondrial Sod1 during Cu deficient conditions was related to glucose repression. Therefore, we asked if and how mitochondrial function was altered in Cu excess and Cu deficient conditions with galactose as the primary carbon source.

Before investigating changes in respiratory function with galactose in Cu deficient conditions, we wanted to confirm that altering Cu availability affected the cellular physiological response, similar to what we did in section 3.1. To measure the response, we incubated cells with galactose and CuSO₄ or BCS for 18 hours and then isolated RNA from cells. We found that *CTR1* and *CUPI* transcript levels, our controls that are expected to change with altered Cu availability, were significantly affected (Figure 4.12). *CTR1* transcript levels significantly decreased with excess Cu and increased with Cu deficiency, confirming that cells were transcriptionally responding to the changing Cu environment. In contrast, *CUPI* transcript levels significantly increased with excess Cu and decreased with limiting Cu. Interestingly, the changes in *CTR1* transcript levels were more pronounced with galactose, but the differences we observed in *CUPI* transcript levels were less obvious in galactose when compared to glucose (Figure 3.1). Overall, the differences detected in *CTR1* and *CUPI* transcript levels with changing Cu availability confirmed that cells were appropriately responding when they were grown in galactose as the primary carbon source.

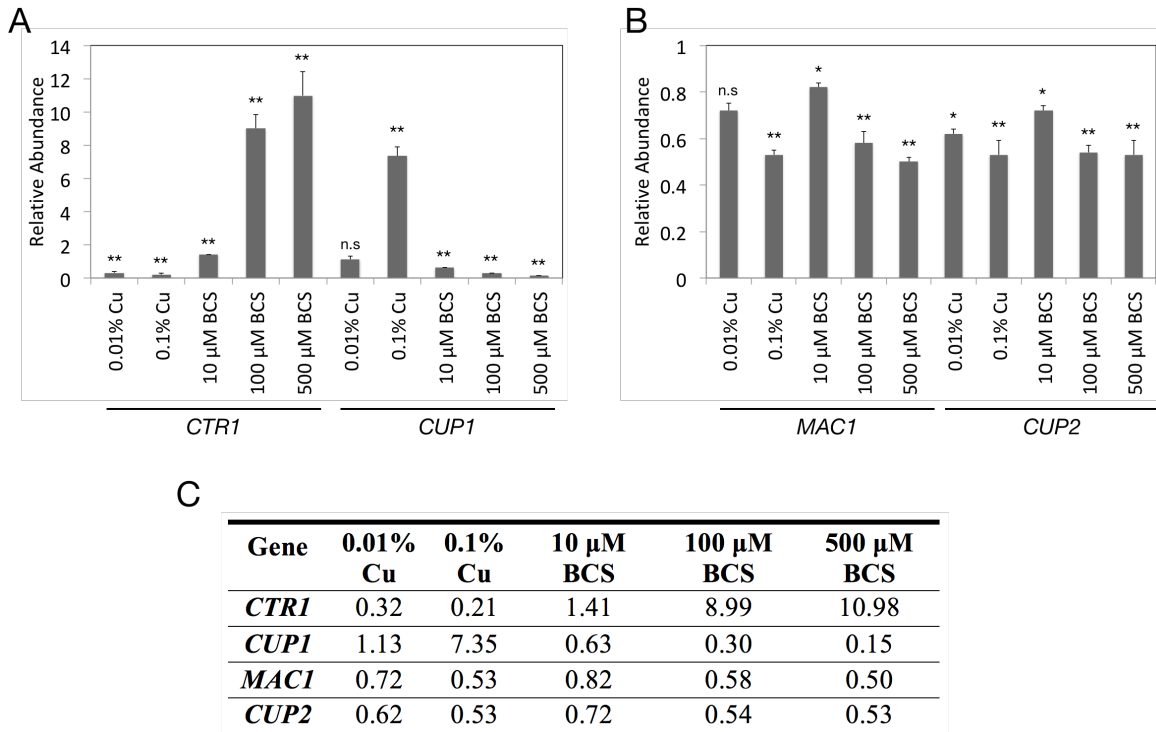


Figure 4.12 RT-qPCR of *CTR1*, *CUP1*, *MAC1*, and *CUP2* with galactose as a carbon source
 (A) Graphical representation of relative abundance of *CTR1* and *CUP1* compared to no treatment controls. RNA was isolated from yeast cells grown for 18 hours in the Cu condition stated. PCR was performed using cDNA on both the gene of interest and *ACT1* as a control. Values are representative of $\Delta\Delta Cq$ values. Three biological replicates were performed for each treatment condition. A one-way ANOVA was done to determine statistical significance: not significant = n.s, $p < 0.05 = *$, $p < 0.01 = **$. Error bars represent \pm SEM. (B) Graphical representation of relative abundance of *MAC1* and *CUP2* compared to no treatment controls. RT-qPCR and statistics were performed exactly as described in A. (C) Raw $\Delta\Delta Cq$ values, representing the fold-change in each condition relative to *ACT1*.

We also evaluated transcript levels of *MAC1* and *CUP2*, the Cu-responsive transcription factors in yeast. With galactose and excess Cu, qPCR analysis revealed a significant decrease in both *MAC1* and *CUP2* transcript levels (Figure 4.12). In glucose, we observed a significant increase in transcript levels of *MAC1* and *CUP2* with excess Cu (Figure 3.3), which was the first indication that cells respond differently to excess Cu based on carbon source. In galactose, we had observed a significant decrease in both *MAC1* and *CUP2* transcript levels in Cu deficient conditions, resembling the pattern we saw when using glucose. However, the small decrease we saw in *MAC1* transcript levels with glucose was not significant, even though it was significant in galactose. Taken together, these results highlight transcriptional differences in excess Cu conditions but suggest that transcript levels of *MAC1* and *CUP2* are not significantly altered by differing carbon sources during Cu deficiency.

In addition to examining the transcript levels depicted in Figure 4.12, we also measured transcript levels for *TDH2*, *COX17*, *SCO1*, *COX11*, *COX4*, *CCSI*, *SOD1*, and *PIMI*. These results are presented in Appendix A, as they were not immediately relevant to the main theme of this chapter.

4.2.2 Effect of carbon source on COX during Cu depletion

Our comparison between COX and Sod1 activity in glucose during Cu deficient conditions suggested that with limiting Cu, mitochondrial Sod1 is first in line for acquiring Cu. Since Sod1 has been proposed to have a role in glucose repression, we were curious whether Cu distribution during Cu deficiency changed with galactose as the primary energy source. Therefore, we performed a side-by-side analysis with a no treatment and 500 μ M BCS treated sample in glucose and galactose. For our analysis, we investigated COX assembly factor and subunit protein levels, COX activity levels, Sod1 protein and activity levels, and Lon, Sdh2, and Aco1 protein levels and Aco1 activity levels as described earlier.

The increase in Cox17 protein levels after treatment with 500 μ M BCS was similar between carbon sources, but exaggerated in galactose, as Cox17 protein levels increased 7.58X compared to the untreated sample. The trends between Sco1 and Cox11 protein levels were less noticeable: Sco1 protein levels were slightly decreased in glucose but similar in galactose, and Cox11 protein levels decreased in both carbon sources after BCS treatment. The two COX subunits, Cox4 and Cox2, were both barely detectable in either carbon source at 500 μ M BCS compared to the no treatment control. Lastly, Cyc1 protein levels slightly increased in glucose and were down by 51% in galactose following BCS exposure. Biological replicates of Cyc1 blots done in section 4.1 suggested that protein levels in glucose decrease at 500 μ M BCS, while these results suggest they slightly increase. Overall, it is likely that Cyc1 levels are not significantly changed at 500 μ M BCS as the changes we observed were minor.

As expected, our measurements of COX activities revealed more activity in the galactose control compared to the glucose control (Figure 4.13-C). This is due to glucose repression, which decreases mitochondrial respiration. However, after BCS exposure, COX activity was severely reduced in both carbon sources. In glucose, COX activity dropped 75% after treatment with BCS, while a 90% decrease in COX activity was found when galactose

was the carbon source. Taken together, the loss of COX subunit protein levels and the lack of COX activity we observed after treatment with 500 μM BCS occurs independent of carbon source.

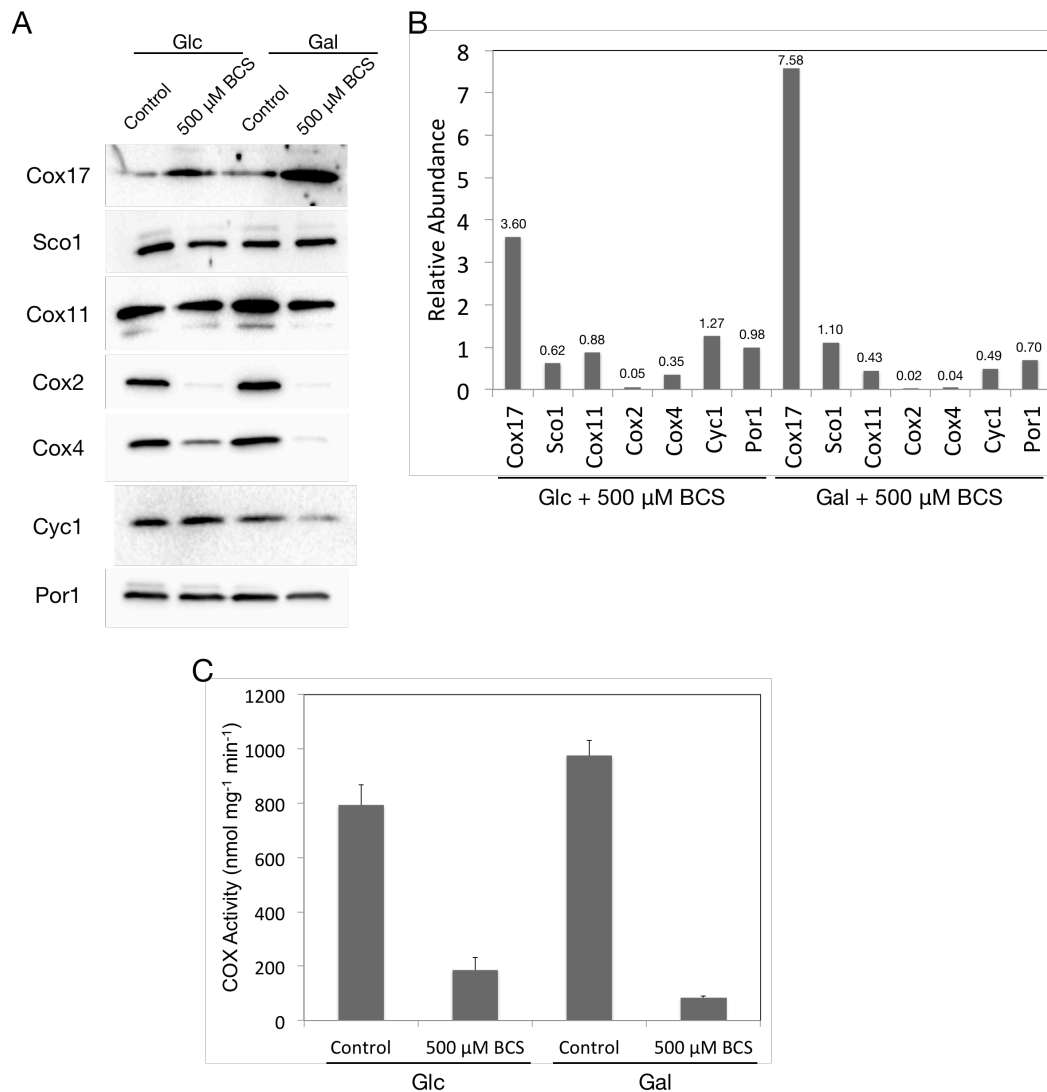


Figure 4.13 Mitochondrial protein levels and COX activities with glucose (Glc) and galactose (Gal) in Cu deficient conditions

(A) Representative Western blots of mitochondrial protein samples (25 μg protein) using antibodies to proteins involved in COX assembly (Cox17, Sco1, Cox11), COX subunits (Cox2, Cox4), or other mitochondrial protein (Cyc1, Por1). All blots were stained with Ponceau S prior to immunoblotting to ensure equal loading across all lanes of the gel. (B) Quantification of protein levels on Western blots relative to the no treatment control. Por1 was used as the loading control. Using the changes in Por1 levels, any quantification above 1.02X or below 0.98X for glucose and above 1.30X or below 0.7X of was considered to be significant. (C) Mitochondrial fractions were tested for COX activity by measuring the oxidation of reduced cytochrome *c* at 550 nm for 60 seconds. Each sample was run in duplicate and the error bars represent the range between replicates. All results in this figure are from one subcellular fractionation.

4.2.3 Effect of carbon source on mtSod1 during Cu depletion

Although we did not observe a major difference between carbon sources with respect to COX protein levels and activity, we sought to clarify whether Sod1 behaved similarly. We performed Western blotting and SOD activity assays on mitochondrial protein fractions in glucose and galactose, with and without treatment of 500 μ M BCS. The retention of Sod1 protein and activity levels with glucose was reproducible between the no treatment and 500 μ M BCS samples (Figure 4.14). Strikingly, the protein and activity levels of mtSod1 in cells grown in galactose were almost undetectable at 500 μ M BCS compared to the no treatment control. Specifically, Sod1 protein levels went down to 10% of control and activity levels went down by 65%, and these trends were reproducible in two separate subcellular fractionations. The decrease in Sod1 activity levels and the loss of COX activity suggest that in galactose, both major mitochondrial cuproprotein pools are lacking Cu. Because Sod1 has been suggested to play an essential role in glucose repression (Reddi & Culotta, 2013), these data suggest that the mitochondrial pool of Sod1 is likely important for this function.

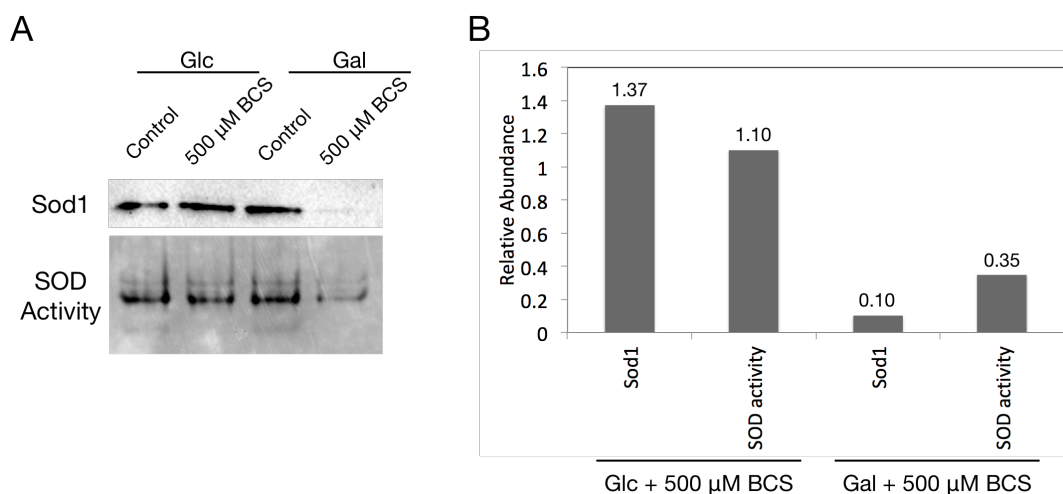


Figure 4.14 Sod1 protein and activity levels in glucose (Glc) and galactose (Gal)

(A) Representative Sod1 Western blot (25 μ g protein) and SOD activity gel (48 μ g protein) using mitochondrial protein samples. SOD activity was measured in-gel using a well-established method (Beauchamp & Fridovich, 1971). (B) Quantification of protein and activity levels relative to the no treatment control. Using the changes in Por1 levels (Figure 4.13) we defined significant changes in levels of Sod1. Quantification of protein and activity levels is from one subcellular fractionation.

4.2.4 Effect of carbon source on mitochondrial function during Cu deficiency

The major difference we see after changing the primary carbon source from glucose to galactose is the loss of Sod1 protein and activity in the mitochondria after exposure to 500 μ M BCS. While we observed that retention of Sod1 activity did not have a major affect on

TCA cycle function or mitochondrial proteasomal activity in glucose grown cells, we assayed Lon, Sdh2, and Aco1 protein levels as well as Aco1 activity in galactose after treatment with BCS. While *PIMI* transcript levels seem to be unaffected with BCS treatment in galactose (Appendix A), Lon protein levels increased with the treatment (Figure 4.15-A, 4.15-B). Increased Lon protein levels could explain the loss of Cox2 in galactose after BCS treatment. Our results regarding *PIMI* transcript levels and Lon protein levels highlight the lack of congruence in transcript and protein levels, which has been reported previously (Dubinski *et al.*, 2018).

In glucose, Sdh2 and Aco1 protein levels were similar at 500 μ M BCS compared to the no treatment control (Figure 4.15-A, 4.15-B), similar to our observations in Figure 4.9. However, after exposure to 500 μ M BCS in galactose, both Sdh2 and Aco1 protein levels decreased compared to the untreated sample. Therefore, we concluded that the Sod1 protein levels behaved similarly to the Sdh2 and Aco1 protein levels. In glucose, protein levels were similar with and without BCS treatment, but in galactose, protein levels decreased after treatment with BCS. Analysis of Aco1 activity showed that in galactose, the decrease in protein levels of Aco1 from the no treatment control to the 500 μ M BCS sample correlated with a decrease in Aco1 activity levels (Figure 4.15-C). Taken together, these data show a correlation between electron transport and TCA cycle activity in galactose in Cu deficient conditions, but display a disconnect between the two pathways in glucose when Cu is limiting.

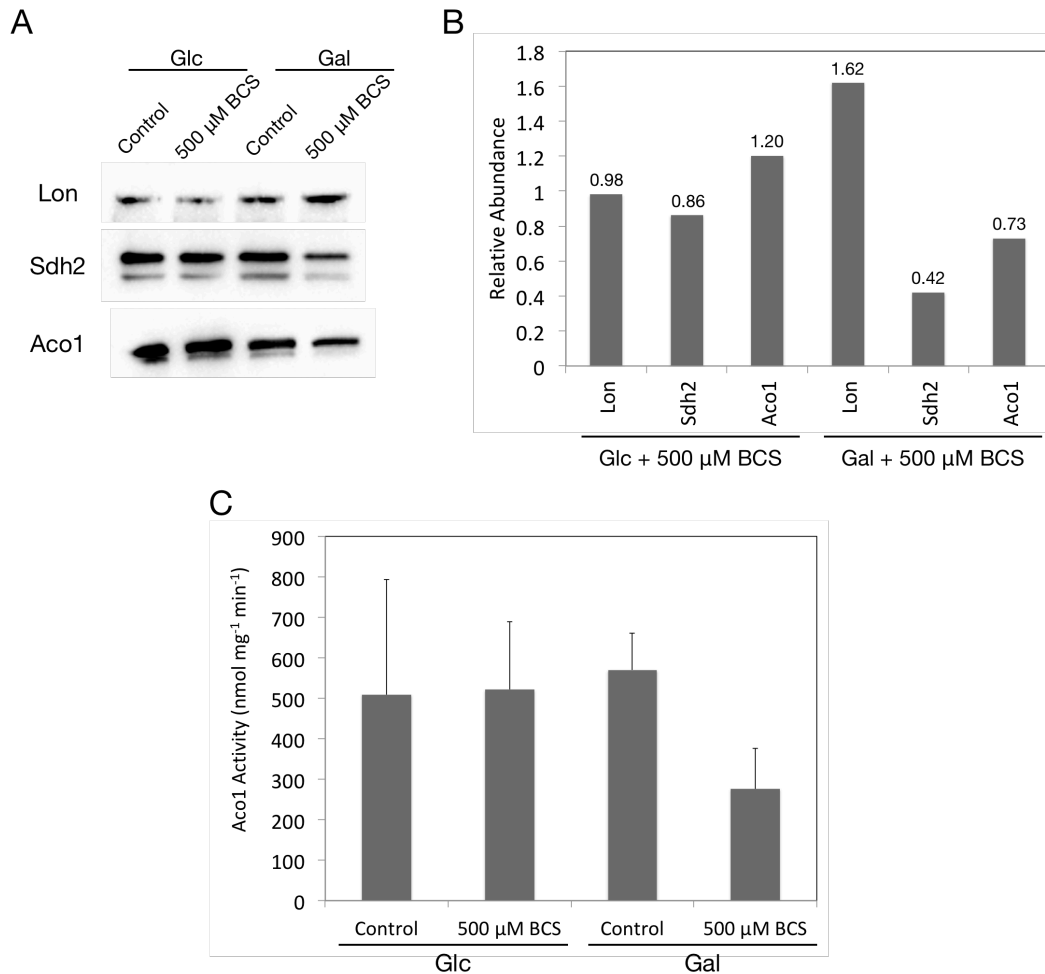


Figure 4.15 TCA cycle analysis in glucose (Glc) and galactose (Gal)

(A) Representative Western blots of mitochondrial protein samples (25 μ g protein) using antibodies to proteins in the TCA cycle (Sdh2, Aco1). Blots were stained with Ponceau S prior to immunoblotting to ensure equal loading across all lanes of the gel. (B) Quantification of protein levels on Western blots relative to the no treatment control. Por1 (Figure 4.13) was used as the loading control. (C) Aconitase activity was assayed from mitochondrial fractions using citrate as the substrate. NADPH production was measured over 60 seconds at 340 nm (Bulteau et al, 2003). Error bars represent \pm range of duplicates from one subcellular fractionation.

4.3 Summary of Results

When extracellular Cu is limiting, cells are forced to prioritize Cu distribution between all cuproproteins. Our first indication that COX was not a priority during Cu deficiency was that we observed a decrease in *COX4* transcript levels. We found that, after exposure to 500 μ M BCS, Cu appeared to be preferentially donated to mtSod1. Interestingly, although we observed a loss of COX activity during Cu depletion, we observed an increase of mitochondrial Cox17 protein levels while the levels in the cytosol and in the whole cell remained constant. Furthermore, the increase in mitochondrial Cox17 protein levels was

accompanied by no change in Sco1 protein levels and a decrease in Cox11 protein levels, even though these proteins all work together in Cu delivery to COX. The patterns we observed in mitochondrial COX and Sod1 activities corresponded to minimal effects on the TCA cycle or proteasomal activity, and a decrease in mitochondrial oxidative damage.

To check if glucose repression was affecting Cu distribution during depletion, we tested similar parameters using galactose as our primary carbon source. We showed that when cells are grown in galactose, they still physiologically respond to changes in extracellular Cu. Changing the carbon source to galactose did not affect the loss of COX activity we observed in glucose, but it did result in decreased levels of TCA cycle proteins and decreased Aco1 activity after cells were exposed to 500 μ M BCS. Most importantly, the change of carbon source to galactose coincided with a loss of mtSod1 protein and activity levels, demonstrating that both mitochondrial cuproprotein pools are inactive with galactose and BCS treatment.

Chapter 5: Cu Availability and Cell Cycle Progression

Our investigation of mitochondria under changing Cu conditions highlighted differences between Cu excess and deficiency. Preliminary results had shown that the Cox17 KO, Sco1 KO, and Cox11 KO strains exhibited a generalized problem with cell cycle progression (Camasta, 2017). In contrast, other COX assembly mutants unrelated to Cu, the Cox15 KO and Cox4 KO, did not show the same problem. Therefore, we hypothesized that cell cycle delay we observed might be due to Cu imbalance in the cell. To support this, there are known cell cycle defects in the Sod1 mutant, which also has problems with Cu homeostasis (Carter *et al*, 2005). In this chapter, we explore the mechanism behind the cell cycle defect seen in certain COX assembly mutants, and investigate cell cycle progression in wild type yeast exposed to Cu excess or Cu deficient conditions.

5.1 COX Assembly Mutants and Cell Cycle

Our initial analysis of cell cycle progression in mitochondrial mutants was undertaken because we saw abnormalities in budding indices during stationary phase in a subset of COX assembly mutants (Glerum lab, unpublished). We were interested to see if the anomalies in budding indices correlated with a cell cycle defect in COX assembly mutants. By using synchronized cultures and flow cytometry analysis, we found a cell cycle defect in our cuproprotein mutants (Cox17 KO, Sco1 KO, Cox11 KO), which we defined as a generalized cell cycle delay (Camasta, 2017).

The cell cycle progression issue in the COX assembly mutants was thought to be associated with an increased oxidative stress baseline in those mutants, due to the fact that the respiratory chain is one of the major producers of ROS in the cell. In addition, oxidative stress has been reported to be associated with cell cycle defects (Shapira *et al*, 2004). Therefore, we were interested to test sensitivity of the mitochondrial mutants to hydroxyurea (HU), a DNA damaging agent that has recently been proposed to also cause oxidative stress (Singh & Xu, 2017). At first, we tested for growth defects at a concentration of 240 mM HU, where the wild type strain appeared to have a growth defect (Camasta, 2017). Results did show a differential response by the cuproprotein mutants, suggesting they are more sensitive to the HU insult (Camasta, 2017).

To get a better picture of the HU sensitivities of the wild type strain and the COX assembly mutants, we performed spot plate assays with lower concentrations of HU. We used the Rad53 Sml1 double KO as a control, as it is known to display a major growth defect when exposed to low concentrations of HU (Desany *et al*, 1998). At 50 mM and 100 mM HU, which we saw caused a major growth defect in the Rad53 Sml1 double KO strain, we saw no growth defect in either the wild type strain or the COX assembly mutants (Figure 5.1-A). These results suggested that the cell cycle defect seen in the cuproprotein mutants was not as severe as the one in the Rad53 Sml1 double KO. Since HU is known to interfere with dNTP production and cause oxidative stress, doing these experiments in hypoxic conditions would allow for differentiation of the underlying cause of the growth defect.

To mechanistically understand the cause of the cell cycle defect in the cuproprotein mutants, we compared protein levels of Rad53 in the wild type strain and the COX assembly mutants. Rad53 is essential for cell cycle control in yeast and has two major functions: halting cell cycle progression in the presence of DNA damage and initiating a pathway that leads to a spike in dNTP pool production (Barnum & O'Connell, 2014).

Western blotting analysis of Rad53 in the COX assembly mutants revealed similar protein levels across the majority of the mutants (Figure 5.1-B, 5.1-C). One exception was in the Cox11 KO, where Rad53 protein levels decreased slightly compared to the Act1 loading control. Overall, the Rad53 protein levels are in agreement with our previous data (Camasta, 2017). It is important to note that although the Rad53 protein levels are similar between the wild type strain and most of the mitochondrial mutants, they do not give an indication of activity, which is done using a phosphorylation assay. Preliminary data from collaborators indicates that the Cox11 KO also has a problem with Rad53 activity (Duncker lab, unpublished). The fact that Rad53 seems to have lower activity in the Cox11 KO should mean there is no delay in cell cycle since Rad53 halts the cell cycle and generates an imbalance in the dNTP pools.

Because Rad53 also has an impact on dNTP pools, we performed Western blotting to detect protein levels of Rnr3 in the wild type strain and mitochondrial mutants (Figure 5.1-B, 5.1-C). Rnr3 is one of the four RNR subunits and is thought to be a good marker for dNTP pools. Consistent with a decrease in Rad53 protein levels and activity, we found that Rnr3 protein levels in the Cox11 KO are lower than protein levels seen in the wild type strain. In

contrast, the levels of Rnr3 in all other mitochondrial mutants were not different from the wild type strain or from each other. Overall, the cell cycle delay seen in the Cox17 and Sco1 KO strains does not appear to be associated with changes in Rad53 or Rnr3 protein levels. However, the cell cycle defect in the Cox11 KO is correlated to decreased Rad53 and Rnr3 protein levels, as well as decreased Rad53 activity.

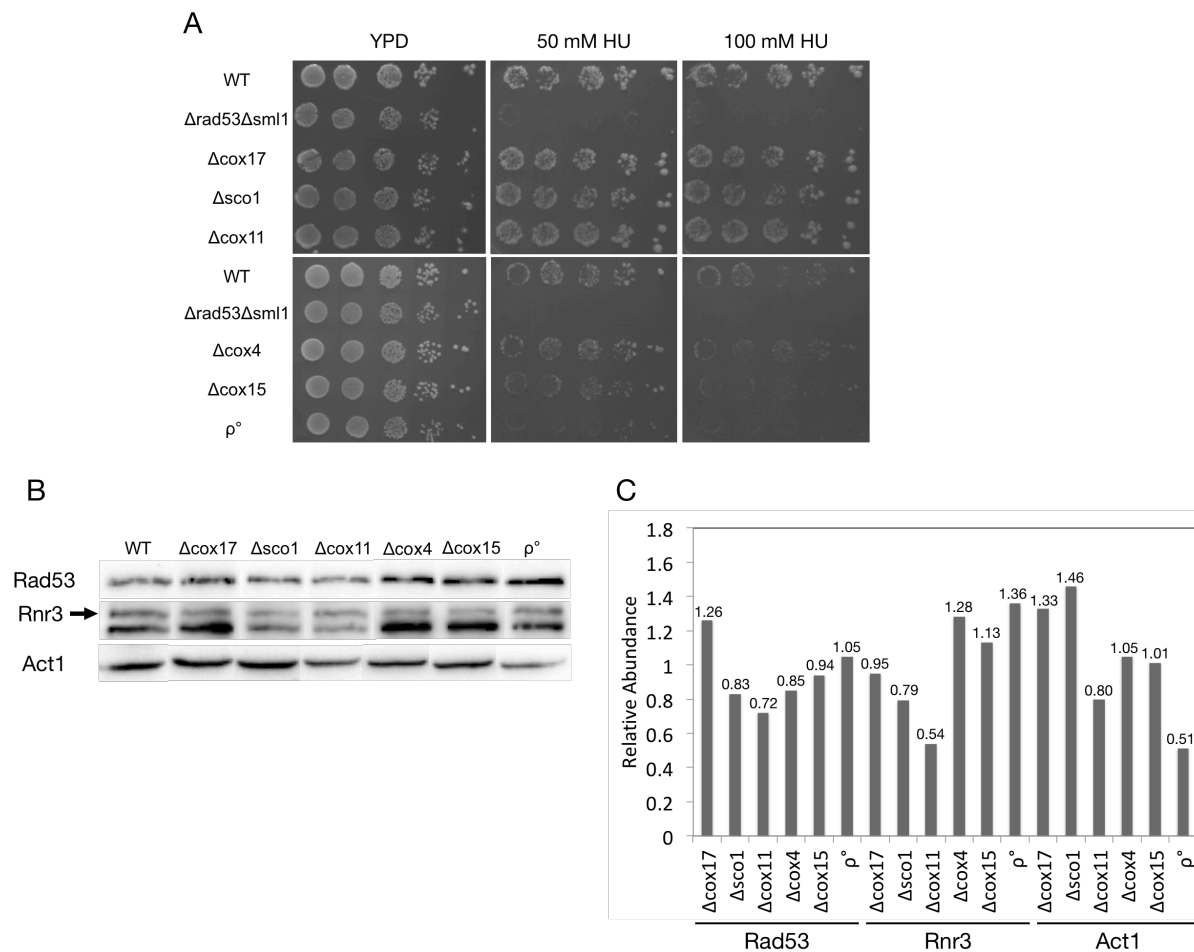


Figure 5.1 Analysis of cell cycle in COX assembly mutants

(A) Spot plates of COX assembly mutants on YPD + hydroxyurea (HU). Plates were incubated at 30°C for 2 days and imaged. (B) Western blots of cell lysate protein samples (60 μg) using antibodies against Rad53, Rnr3, and Act1. Blots were cropped from two separate gels. (C) Quantification of Western blots relative to the WT strain. Act1 was used as a loading control. These experiments were done on one protein isolation. Tyler Soule helped perform the Western blots in (B).

5.2 Cu Availability and Cell Cycle Progression

The differences in Rad53 and Rnr3 protein levels in the Cox17, Sco1, and Cox11 KO strains suggested that the cell cycle defect in the Cox17 and Sco1 KO occurs by a different mechanism from that of the Cox11 KO. However, all three of these proteins are involved in

Cu delivery to COX, suggesting that they all have imbalanced cellular Cu levels. Therefore, we wanted to ask whether Cu imbalance affected cell cycle progression and if under these treatment conditions, we could reproduce the generalized cell cycle delay we saw in the cuproprotein mutants.

Similar to our previous analyses with the mitochondrial mutants, cell cycle progression was tested with a flow cytometry approach. First, we incubated our cells for 18 hours in the same concentrations of CuSO₄ and BCS as used throughout this study and were optimized in section 3.1. Cells were then transferred to new media and exposed to the mating hormone α -factor, which arrests them in G1 phase. After this, cells were released into fresh YPD containing either excess or limiting Cu, allowing them to synchronously enter the cell cycle so progression could be monitored. Aliquots were collected at 0, 40, 80, and 120 minutes after release and were stained with Sytox Green to measure DNA content. From the literature, the average yeast cell cycle should take 125 +/- 9 minutes, with the G1-S phase taking approximately 54 minutes (Shaw *et al*, 1998). Therefore, at the 120-minute time point, we should expect to see slight return of the 1N peak as some cells have completed cytokinesis.

The results for cell cycle progression with excess Cu treatment are shown in Figure 5.2. In the no treatment control, we observed that almost all cells had duplicated their DNA after 40 minutes, because of the absence of the G1 peak and the presence of the G2 peak. At the 120-minute time point in the WT, we started to see slight return of the G1 peak, as expected. The sample treated with 0.01% Cu looked similar to the no treatment control, indicating that this treatment has little effect on cell cycle progression. However, the sample treated with 0.1% Cu seemed to have a major cell cycle defect. Specifically, the G1 peak was present at all time points, suggesting that after treatment with 0.1% Cu some cells are stuck in G1 and cannot replicate their DNA. There is also a sub-G1 peak to the left of the G1 peak that represents cells containing less than 1N DNA. Reports in the literature suggest that these cells are apoptotic (Burhans *et al*, 2003), since high Cu concentrations cause oxidative stress, which likely leads to DNA damage and apoptosis. Taken together, these results show a cell cycle defect after treatment with 0.1% Cu, but not at the lower concentration of 0.01% Cu.

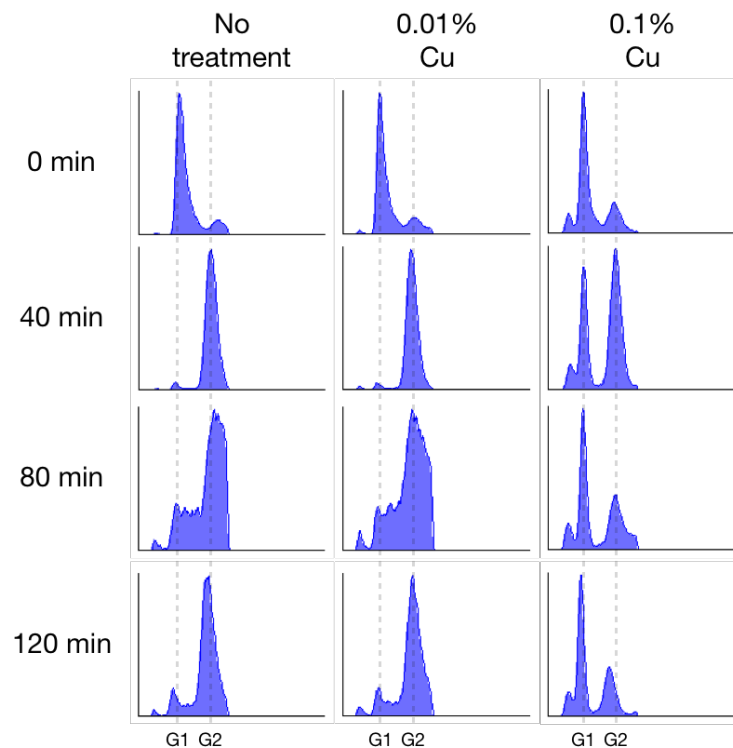


Figure 5.2 Cell cycle analysis after treatment with excess Cu

Chromatograms representative of cell cycle progression. Cells were arrested in G1 by treatment with α -factor and then released into fresh media with excess Cu and collected at 40-minute intervals for 120 minutes. Subsequent staining with SyTOX Green and processing through flow cytometry resulted in the chromatograms shown here. The G1 peak denotes cells with 1N DNA and the G2 peak denotes cells with 2N DNA. The y-axis represents frequency and the x-axis represents fluorescence intensity. These experiments were repeated 3 times. Tyler Soule obtained these results.

Using the same flow cytometry approach, we also monitored cell cycle progression of wild type yeast after treatment with BCS. Exposure to BCS likely resembles problems in Cu concentration in the Cox17, Sco1, and Cox11 KO strains, as it has been shown that a Sco1 KO mouse has Cu deficient tissues (Baker *et al*, 2017b). Because these KO strains are the ones in which we observed a cell cycle delay, identifying a defect in a generalized Cu deficiency could provide important clues to the mechanism causing the delay in the cuproprotein mutants.

After exposure to BCS, cell cycle progression appeared to be similar between the BCS-treated samples and the control (Figure 5.3). At the 40-minute time point, the no treatment control and all the BCS treatment conditions had a prominent G2 peak, indicating that cells are all progressing through the cell cycle at a comparable pace. Similarly, at the 120-minute time point, the G1 peak seems to be returning in all of the samples. Even though

we clearly showed that BCS treatment impacts mitochondrial function in Chapter 4, the cell cycle analysis shown here suggests that BCS treatment does not affect cell cycle progression.

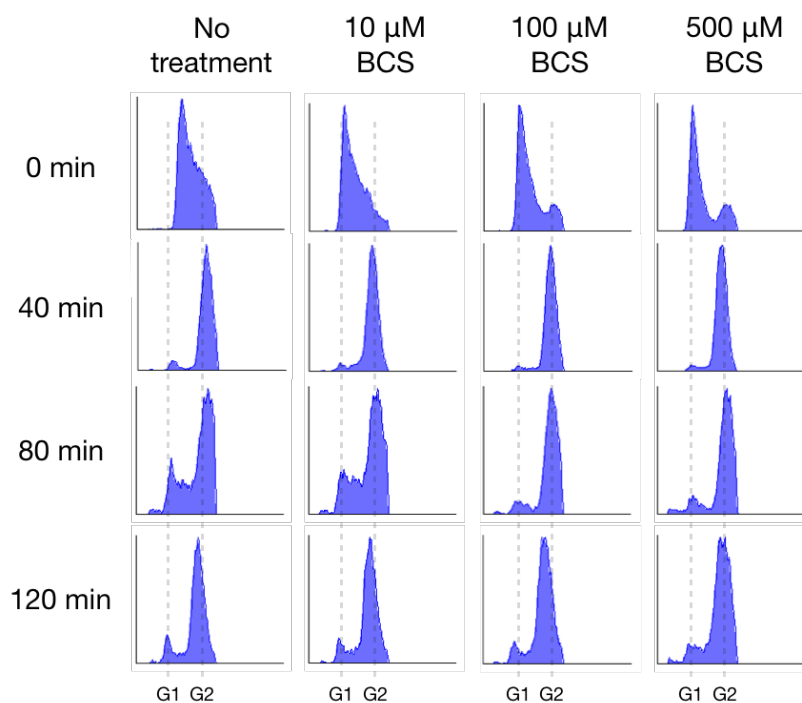


Figure 5.3 Cell cycle analysis after treatment with BCS

Chromatograms representative of cell cycle progression. Cells were arrested in G1 by treatment with α -factor and then released into fresh media with BCS and collected at 40-minute intervals for 120 minutes. Subsequent staining with SyTOX Green and processing through flow cytometry resulted in the chromatograms shown here. The G1 peak denotes cells with 1N DNA and the G2 peak denotes cells with 2N DNA. The y-axis represents frequency and the x-axis represents fluorescence intensity. These experiments were repeated 3 times. Tyler Soule obtained these results.

The fact that Cu excess conditions but not Cu deficiency affects cell cycle progression led us to ask whether there were any changes in Rad53 protein levels after changing Cu availability. Therefore, we performed Western blotting on whole cell lysates after treatment with either Cu or BCS. We found that after exposure to excess Cu, Rad53 protein levels were decreased in both treatment conditions compared to the control (Figure 5.4). This was unexpected, since we observed a defect in cell cycle progression only in the sample treated with 0.1% Cu. The decrease in Rad53 protein levels associating with cells stuck in the G1 phase is contradictory, given that increased Rad53 activity is required to introduce a cell cycle delay. Alternatively, the decrease in Rad53 protein levels could suggest that dNTP pools are lower, which is why we saw cells that cannot progress through DNA replication

(Figure 5.2). As we expected, Rad53 protein levels are unaffected across BCS treatments (Figure 5.4), which is in agreement with the normal cell cycle progression we saw in these treatment conditions.

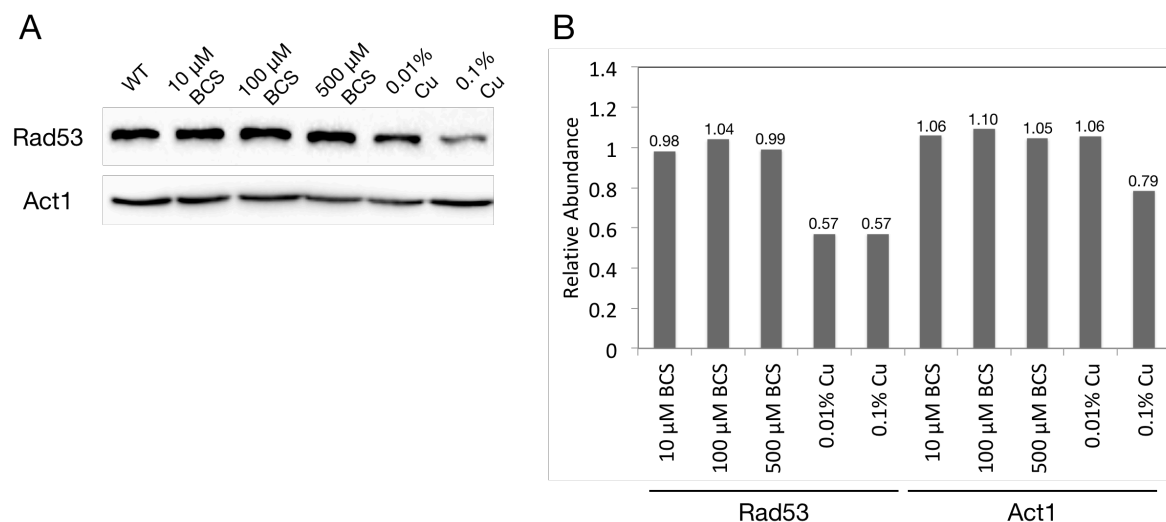


Figure 5.4 Rad53 protein levels with different Cu availability conditions

(A) Western blots of cell lysate protein samples (60 μg) using antibodies against Rad53 and Act1. (B) Quantification of Rad53 protein levels relative to the no treatment control. Act1 was used as the loading control. These experiments were done on one protein isolation.

One major difference we observed in Section 4.2 when changing carbon source from glucose to galactose was the absence of mitochondrial Sod1 after treatment with 500 μM BCS. A previous study has reported that Sod1 plays a role in cell cycle progression through an interaction with Rad53 (Dong *et al*, 2013). The fact that a Sod1 KO yeast strain exhibits a cell cycle delay (Carter *et al*, 2005) further illustrates that the presence of Sod1 is likely necessary for normal cell cycle progression. This prompted us to test whether a strain grown in galactose with 500 μM BCS showed a cell cycle defect, since Sod1 is not present in either the mitochondria or cytosol under these conditions (Section 4.2).

For this experiment, we used our glucose data as a control since we previously saw that BCS did not affect cell cycle progression when grown in glucose as a carbon source (Figure 5.3). Our results using glucose as the carbon source were extremely similar to those in Figure 5.3, demonstrating that the data are reproducible (Figure 5.5). When comparing our no treatment controls in the two different carbon sources, we saw that at the 120-minute time point the G1 peak return is much more noticeable when cells are grown in galactose,

suggesting that cells grown in these conditions have different cell cycle timing and may have a shorter G2/M phase. Cells exposed to 500 μM BCS displayed two minor differences when compared to the galactose no treatment control. First, at the 40-minute time point, there seemed to be more cells that have not progressed to the G2 phase in the BCS treated sample, suggesting a minor cell cycle delay. However, comparison of the chromatograms at 120 minutes displayed a larger G1 peak in the BCS treated sample. Taken together, treatment with BCS using galactose as a carbon source may result in a delayed G1 phase, but an accelerated pathway through mitosis.

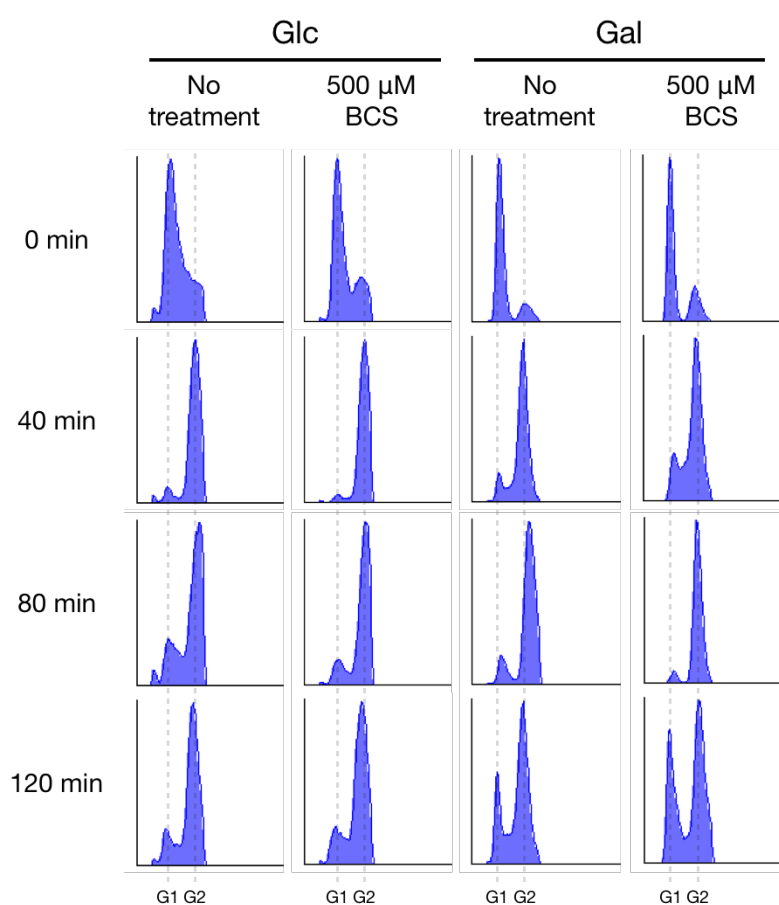


Figure 5.5 Cell cycle analysis with different carbon sources

Chromatograms representative of cell cycle progression. Cells were arrested in G1 by treatment with α -factor and then released into fresh media with BCS and collected at 40-minute intervals for 120 minutes. Subsequent staining with SyTOX Green and processing through flow cytometry resulted in the chromatograms shown here. The y-axis represents frequency and the x-axis represents fluorescence intensity. The G1 peak denotes cells with 1N DNA and the G2 peak denotes cells with 2N DNA. These experiments were done once.

5.3 Summary of Results

We began investigation of cell cycle by further analyzing mitochondrial cuproprotein mutants we previously showed to have a cell cycle defect. We found that at lower concentrations of HU, our mitochondrial mutants do not display a growth defect compared to the Rad53Sml1 double KO control. Because the Cox11 KO presents with lower Rad53 and Rnr3 protein levels compared to the wild type strain, we propose that the Cox11 cell cycle delay is based on decreased dNTP production and therefore decreased replication rates. In contrast, the Cox17 and Sco1 KO strains have similar Rad53 and Rnr3 protein levels.

Our analysis of cell cycle progression in generalized Cu problems revealed that with 0.1% Cu, many cells are unable to progress past replication, and this is associated with a decrease in Rad53 protein levels. On the other hand, treatment with 0.01% Cu resulted in no obvious cell cycle defect but a decrease in Rad53 protein levels. Taken together, our results show that all BCS treatment conditions did not affect cell cycle progression or Rad53 protein levels.

Lastly, we observed changes in cell cycle progression between carbon sources. Our preliminary results may suggest that BCS affects cell cycle progression in galactose, which would allow us to further investigate if and how mitochondrial Sod1 plays a role in cell replication.

Chapter 6: Discussion

The impacts of excess and limiting levels of Cu have been thoroughly studied at the system and organ levels in humans because of the debilitating clinical phenotypes seen in Wilson and Menkes diseases. Cu imbalance has also been observed in patients with mitochondrial defects and neurodegenerative disorders, highlighting the importance of Cu homeostasis in cells. However, the subcellular effects of exposure to changes in Cu concentrations are largely unexplored; as the locus for important cuproproteins and a storage space for Cu, mitochondria are considered to be central players in cellular Cu homeostasis. Additionally, recent reports have proposed a link between Cu homeostasis and cell cycle control. Therefore, our goal in this study was to analyze how excess or limiting levels of extracellular Cu impact mitochondrial function.

6.1 Existence of a Mitochondrial Matrix Cu Pool

In 2004, a non-proteinacious ligand (CuL) in the mitochondrial matrix was proposed to house the majority of mitochondrial Cu (Cobine *et al*, 2004). CuL exists as a soluble anionic complex and functions to store Cu, but the structure of CuL has not been clearly defined. Additionally, it has been suggested that CuL is the source of Cu for the mitochondrial cuproproteins COX and Sod1 (Cobine *et al*, 2006). The current understanding in the field is that the pool acts as a storage space for Cu, in the case that there is a problem with Cu concentrations in the surrounding environment (Horn & Barrientos, 2008). In Cu excess conditions, mitochondria could operate as a Cu sink to prevent toxicity of the metal in the cytosol, while in Cu deplete conditions the pool could provide a source of Cu to maintain functionality of cuproproteins (Dodani *et al*, 2011). Our data from this study provide insight into the behavior of the proposed matrix Cu pool with varying Cu availability.

In Wilson disease models, which are defined to have excess Cu, mitochondria are Cu overloaded resulting in severe structural and functional defects (Zischka & Lichtmannegger, 2014). One report suggested that there is an upper limit of Cu storage space in mitochondria, and that Cu transport to the CuL in the matrix is constitutive (Baker *et al*, 2017a). If the mitochondria are a main Cu storage location, we expect that cells will upregulate mitochondrial cuproproteins to compensate for the increased levels of Cu in the

mitochondria. However, our results show no change in transcript levels for *COX17*, *SCO1*, *COX11*, or *COX4* under excess Cu conditions. On the other hand, we do observe that Cox2 and Cox4 protein levels and COX activity are significantly increased at 0.01% and 0.1% Cu compared to the control, which suggests that COX is stabilized with higher levels of cellular Cu. COX activity values are 1359 nmol mg⁻¹ min⁻¹ and 1350 nmol mg⁻¹ min⁻¹ with 0.01% and 0.1% Cu, compared to 560 nmol mg⁻¹ min⁻¹ in the control. We do detect upregulation of *CCSI* and *SOD1* after treatment with excess Cu, which corresponds to higher mitochondrial Sod1 protein levels and a 1.6X increased SOD activity with 0.01% Cu and a 2.19X increase with 0.1% Cu. Finally, our results reveal higher levels of mitochondrial oxidative damage with 0.1% Cu, compared to a slight decrease in oxidative damage at the level of the whole cell. Overall, increases in activities of mitochondrial cuproproteins and more oxidative damage are consistent with the existence of a Cu pool located in the mitochondrial matrix that is responsible for Cu storage when the metal is in excess.

During Cu deficiency, the CuL is proposed to serve as an important source of Cu to ensure function of cuproproteins. Therefore, as we increase the concentration of BCS, we expect a threshold of mitochondrial cuproprotein activity once the mitochondria are depleted of Cu. In limiting Cu conditions, we selectively lose function of cytosolic Sod1, but not mtSod1, which is in agreement with the existence of the CuL. This is also consistent with the Cu pool in the matrix being the storage for Cu when the metal is depleted. We also see an increase in transcript levels of *CTRI* after BCS treatment, suggesting that some Cu is entering the cell through the plasma membrane. On the other hand, as we increase the concentration of BCS, the SOD activities in the mitochondria are 94%, 120%, and 70% with 10 μM, 100 μM, and 500 μM BCS compared to the control. In contrast, COX activity gradually decreases from 470 nmol mg⁻¹ min⁻¹ to 71 nmol mg⁻¹ min⁻¹, the latter resembling auto-oxidation, as BCS concentration increases to 500 μM. The potential reasons for the retention of SOD activity in the face of decreasing COX activity at 500 μM BCS will be discussed in detail in section 6.4. However, the trends we observe with SOD and COX activities contradict the proposal that the CuL is the source of Cu for these enzymes. There is more SOD activity at 100 μM BCS than 10 μM BCS, when the 100 μM BCS treatment should negatively impact mitochondrial Cu concentrations. We also observe a gradual decrease in COX activity instead of a threshold, which we would expect if the mitochondrial

pool were to be completely depleted of Cu. We still do not understand the mechanism in which Cu is delivered to Sod1 and COX, and whether this delivery mechanism is constitutive or inducible would impact the activities of these proteins under Cu deficiency.

The severe defect in mitochondrial cuproprotein function that is present with limiting Cu in galactose as the primary carbon source casts doubt on the existence of a mitochondrial Cu pool being the primary source of Cu for IMS residents. In the first description of the mitochondrial Cu pool, the authors found that carbon source does not influence the amount of mitochondrial Cu (Cobine *et al*, 2004). This indicates that if the CuL in the matrix were the primary source of Cu for Sod1 and COX, we would expect to see the same trends both in glucose or galactose. Our results reveal that in galactose, SOD activity is at 35% of control levels after exposure to 500 μ M BCS, which is much lower than the activity we observe when glucose is the primary carbon source. The trends in COX activities between glucose and galactose with limiting Cu are consistent with each other. The divergent trends we observe between glucose and galactose do not fit with the current proposal that the CuL is unaffected by carbon source. Overall, our results do not contradict the existence of a Cu pool in the mitochondrial matrix, but do contradict the hypothesis that the CuL is the source of Cu for Sod1 and COX in the IMS. The system of regulation of mitochondrial cuproprotein pools is poorly understood and our data suggest the need to reconsider the current model.

6.2 Cox17: the outlier among COX assembly factors

Cox17 is dually localized between the mitochondria and the cytosol, with 60% existing in the mitochondria and 40% residing in the cytosol (Beers *et al*, 1997). Its accepted function is in the mitochondrial IMS for delivery of Cu to Sco1 and Cox11. However, there has yet to be a defined function for the cytosolic pool of Cox17. Fumarase is an example of a protein that is only known for its mitochondrial function, yet is dually localized to the mitochondria and the cytosol; this is known to arise from incomplete uptake of fumarase into the mitochondria (Maxfield *et al*, 2004). It has been proposed that this is also the case for Cox17 (Maxfield *et al*, 2004), although other results suggest that cytoplasmic pool of Cox17 may have an alternate role. Surprisingly, site-directed mutagenesis of the Cox17 amino acid sequence revealed relatively few mutations that led to a detectable respiration defect (Punter & Glerum, 2003) suggesting that amino acid substitutions with no effect on COX activity

may, in fact, affect secondary pathways. In addition, it has been reported that a Cox17 KO has defective Mac1 activity in low Cu conditions, similar to the Sod1 KO, suggesting that both Cox17 and Sod1 are required for induction of Ctr1 (Wood & Thiele, 2009). This observation may be related to the fact that Cox17 has the ability to form poly-copper clusters, which consist of dimeric Cox17 in the cytosol or tetrameric Cox17 in the mitochondria (Heaton *et al*, 2001).

In addition to published experiments, our observations from studying COX assembly mutants, which are unable to assemble functional COX and are therefore respiration deficient, similarly suggest that Cox17 participates in other pathways. Firstly, *COX17* transcript levels increase in several other COX assembly mutants when compared to a respiratory competent strain (Dubinski, unpublished). In comparison, the *COX4* gene, which encodes a subunit of COX, has a decrease in transcript levels in the same COX assembly mutants when compared to a respiratory competent strain. Increased *COX17* transcript levels in the face of decreased *COX4* transcript levels in COX assembly mutants suggests that upregulation of the *COX17* gene does not correlate with its role in COX assembly (Dubinski, unpublished). Additionally, bioinformatics analysis reveals that a subset of nematodes and trematodes that have a functional COX do not contain a *COX17* gene, indicating that these organisms do not require Cox17 for respiration (Collington, unpublished). Taken together, our recent observations point to the existence of an alternate function for Cox17. For many years, we have been focused on defining a secondary function for the cytosolic pool of Cox17. Although a function for cytosolic Cox17 may exist, the results presented in this study strongly suggest a secondary function unrelated to COX assembly for the mitochondrial pool of Cox17.

Our results in limiting Cu conditions reveal a 1.49X increase in Cox17 protein levels after exposure to 500 μ M BCS. However, this increase is unrelated to the function of Cox17 in COX assembly, since Cox2 and Cox4 protein levels decrease significantly and COX activity decreases to 71 nmol mg⁻¹ min⁻¹ in the same conditions. In galactose and Cu deplete conditions, Cox17 protein levels also increase in the mitochondria by 7.36X compared to the no treatment sample, which is more prominent compared to glucose. We think this is due to activity of Puf3, an RNA binding protein that binds to the 3'UTR of Cox17 and degrades it in glucose, but not galactose (Miller *et al*, 2014). Puf3 binding to Cox17 in galactose only is

also in agreement with our results that *COX17* transcript levels are increased with 100 μ M and 500 μ M BCS in galactose (Appendix A).

In excess Cu, Cox17 protein levels are also increased in the mitochondria. Since COX activity, Sco1 protein levels, and Cox11 protein levels are also increased, we could propose that Cox17 is present because it needs to help with the COX delivery pathway. However, there is direct evidence that does not support this hypothesis. When Cox17 was first described, it was shown that addition of 0.1% and 0.4% Cu recovered the COX defect seen in the Cox17 KO (Glerum *et al*, 1996a). Since Cox17 was absent in these experiments, they clearly demonstrate that there is an alternate pathway that can donate Cu to Sco1 and Cox11. Surprisingly, the increase of Cox17 protein levels in mitochondria is accompanied by a decrease in Cox17 protein levels in the whole cell. Cox17 is not downregulated in Cu excess conditions even though there is less protein present, which means that excess Cu affects Cox17 stability in the whole cell. Taken together, our data presented here demonstrate an increase in mitochondrial Cox17 protein levels during both Cu excess and depletion, suggesting that mitochondrial Cox17 may be serving an alternative function when Cu homeostasis has been disrupted.

There has been one report of an alternate function for mitochondrial Cox17 in helping to maintain integrity of the mitochondrial contact site and cristae organizing system (MICOS) by interaction with Mic60 (Chojnacka *et al*, 2015). However, other than Cox17, there are no other connections between MICOS and Cu homeostasis. Although Cox17 likely does not shuttle Cu directly across the OMM, it still may have a role in mitochondrial Cu import. One hypothesis is that Cox17 could be the starting point for Cu delivery for both mtSod1 and COX. Once GSH enters the mitochondria with Cu (see section 1.4.3), GSH donates Cu to Cox17, and Cox17 might then be responsible for trafficking Cu towards Sod1 and COX.

Imbalance in cellular Cu homeostasis may also activate the apoptotic pathway because of Cu toxicity or improper cuproprotein function, and in this scenario Cox17 may function as a pro-apoptotic protein. The yeast apoptosis inducing factor 1 (Aif1), a mitochondrial resident, is an important player in the caspase-independent yeast apoptotic pathway. Mechanistically, it translocates from mitochondria to nuclei during apoptotic induction and promotes DNA damage in preparation for apoptosis (Madeo *et al*, 2009). Aif1

shows similarities to Cox17 as it resides in the IMS and is imported into mitochondria *via* the Mia40/Erv1 pathway (Hangen *et al*, 2015). Our lab has shown that a Cox17 KO is unable to undergo apoptosis when induced with either hydrogen peroxide or ultraviolet light, an observation unique to the Cox17 KO but absent in other COX assembly mutants or the respiratory competent wild-type strain (Dubinski, unpublished), suggesting that Cox17 may have a role in apoptotic induction.

Looking at the data presented in this thesis, apoptosis could occur during Cu excess conditions as we observe an increase in oxidative damage in both mitochondrial and cytosolic compartments, which suggests there is more DNA damage. During excess Cu, we also observe a decrease in Cox17 protein levels in WCL, but an increase in mitochondria. The decrease we observe in cytosolic Cox17 protein levels display disconnect with what we observed for whole cell protein levels, since the decrease in the whole cell is larger than the decrease in the cytosol. This suggests that Cox17 could exist in other cellular compartments, such as the nucleus. Preliminary evidence from nuclear isolations in steady state conditions reveals that Cox17 protein is not present in the nucleus (Dubinski, unpublished). However, Cox17 may translocate to the nucleus during apoptotic induction, and would not be present there during steady-state conditions. Additionally, Cox17 could potentially interact with XIAP in human cells, which presents another connection between Cox17 and apoptosis (Mufti *et al*, 2007).

Lastly, the secondary function of Cox17 could be more important in quiescent cells. Until recently, research regarding COX assembly has been done in yeast cells growing exponentially. When glucose has been depleted, yeast cells enter the stationary phase, which is characterized by low transcript abundance, high levels of antioxidant defense, and elevated aerobic respiration (Werner-Washburne *et al*, 1993) (Allen *et al*, 2006). Analysis of *ACT1* transcript levels in a wild-type strain show a significant decrease from exponential to stationary phase. Contrary to expectations, *COX17* transcript levels are not downregulated in yeast at stationary phase (Dubinski, unpublished). Since wild-type yeast have different mitochondrial physiology and a distinct oxidative damage profile at stationary phase when compared to exponential phase (Dubinski *et al*, 2018), the alternative role of Cox17 may be related to a pathway that is more prominent at stationary phase.

6.3 Comparison of behavior of Sco1 and Cox11

Sco1 and Cox11 are both IMM residents that function to deliver Cu to COX, and accept Cu from Cox17 (Hornig *et al*, 2004). More recently, Sco1 and Cox11 have been proposed to play roles in redox metabolism. The Sco1 crystal structure reveals a thioredoxin-like fold (Williams *et al*, 2005), and both the Sco1 and Cox11 KO strains display hypersensitivity to exogenous hydrogen peroxide (Banting & Glerum, 2006), suggesting that these proteins may have a role in responding to ROS. In 2011, an in depth study was performed comparing the Sco1 and Cox11 KO strains in yeast to further understand their peroxide sensitivity (Veniamin *et al*, 2011). The peroxide sensitivity in the Sco1 KO is recovered by overexpression of Sco2 or Cox11, but overexpressing Sco1 or Sco2 does not recover the peroxide sensitivity in the Cox11 KO. On the other hand, overexpression of Ctt1, the catalase in the mitochondrial matrix, recovers the peroxide sensitivity in both the Sco1 and Cox11 KO. Interestingly, when Sco1 KO loses mtDNA, it is no longer hypersensitive to peroxide, but this is not the case in the Cox11 KO (Veniamin *et al*, 2011). This article highlights that the nature of the peroxide sensitivity differs between the Sco1 and Cox11 KO strains.

In this study, we find that increasing or decreasing concentrations of extracellular Cu do not transcriptionally affect the *SCO1* and *COX11* genes. After treatment with 0.1% Cu, Sco1 protein levels increase slightly while Cox11 protein levels are unaffected. In 500 μ M BCS, *SCO1* and *COX11* transcript levels are unaffected, but there is a slight decrease in Sco1 protein levels while Cox11 protein is virtually absent. In lower concentrations of BCS, Sco1 protein levels remain similar and Cox11 protein levels are lower. The similar Sco1 protein levels corresponding to a decrease in COX activity suggest that the role of mitochondrial Sco1 during Cu depletion could be associated with its role in redox metabolism or its recently identified role in Cu homeostasis, and highlights a difference between the roles of Sco1 and Cox11.

Sco1 could be involved in breakdown of ROS in the mitochondria. Even though the Sco1 KO is sensitive to peroxide, it displays no growth defect when exposed to paraquat (PQ), a superoxide generator, or menadione (MD), which also generates ROS (Banting & Glerum, 2006) (Kocabey *et al*, 2018). However, a Sco1/Sod1 double KO drastically enhances the sensitivity to these chemicals that was seen in the Sod1 KO, suggesting that Sod1 and Sco1

may work together in the IMS to detoxify ROS. Together with our finding that cells maintain Sco1 protein levels in Cu depletion conditions, we propose that Sco1 and Sod1 can work together to break down superoxide in the mitochondria. This hypothesis is also consistent with the increase in Sco1 protein levels during Cu excess conditions, as we also observe an increase in Sod1 protein levels.

Mutations in Sco1 are known to be associated with clinical presentation of mitochondrial disorders (Leary *et al*, 2007). It is important to note that the yeast and human versions of Sco1 were thought to arise independently and therefore are considered paralogs. Another reason Sco1 protein levels might remain constant during Cu depletion is because of the role of Sco1 in Cu homeostasis in mammalian systems. Sco1 is thought to have a role in controlling Cu homeostasis since a Sco1 KO in mice results in a tissue and allele specific Cu deficiency, which is due to a change in Cu efflux (Leary *et al*, 2007). Cu deficiency in Sco1 patient fibroblasts is rescued by KD of Atp7a, which verifies that differential regulation of Cu homeostasis in a Sco1 KO is due to increased Cu efflux by Atp7a (Leary *et al*, 2013). In the same article, the authors report that Cox19 was involved in signal transduction between Sco1 and Atp7a; they test COX assembly factors associated with Cu that are dually localized between the IMS and cytosol (Cox17, Cox19, Cox23).

Further work done to analyze signal transduction from mitochondrial Sco1 has revealed that signaling is tissue-specific and various signaling mechanisms occur (Hlyaniuk *et al*, 2015) (Baker *et al*, 2017b). Taken together, these results suggest a general Cu deficiency in Sco1 KO tissues but tissue-specific variation exists for the underlying cause of the deficiency. In yeast, we suggest that maintenance of Sco1 levels during Cu deficiency could be related to a signaling pathway where cellular Cu influx is increased.

We previously saw that both the Sco1 and Cox11 KO Strains have a cell cycle defect (Camasta, 2017). Here, we show that the cell cycle defect seen in the Cox11 KO is associated with decreased protein levels of Rad53 and Rnr3, while in the Sco1 KO these protein levels are similar to that seen in the wild type strain, distinguishing the two KO strains. Our studies with a subset of COX assembly mutants reveal that the Cox11 KO strain has the most severe growth defect and appears to have higher levels of oxidative stress compared to other mitochondrial mutants (Dubinski *et al*, 2018). In agreement with our findings, overexpression of Cox11 in wild type yeast leads to increased oxidative stress resistance

(Radin *et al*, 2018), suggesting that Cox11 is important for oxidative stress management. We suggest that the decreased Rad53 and Rnr3 protein levels are a result of increased oxidative stress in the Cox11 KO, and that this leads to a cell cycle defect. To support this, oxidative stress is known to cause cell cycle delays, as has been seen after exposure of cells to various ROS-generating agents (Shapira *et al*, 2004). The mechanistic explanation for the Sco1 KO cell cycle defect remains unknown. Although Sco1 and Cox11 have similar functions in COX assembly, our results regarding the mechanism behind the cell cycle delay seen in Sco1 and Cox11 KO strains is another example of differential phenotypes associated with the loss of these proteins.

6.4 Mitochondrial Cu Distribution with Limiting Cu

Our results with Cu depletion clearly demonstrate a preference for Cu to be delivered Sod1 over COX in the mitochondria (Figure 6.1). For function of Sod1 and COX, Cu is essential. Therefore, our observation that SOD activity is retained in 500 μ M BCS while COX activity significantly decreases shows that Sod1 has obtained Cu but COX has not. From our Western blotting data, we show that protein levels of subunits of COX, Cox2 and Cox4, are significantly lower after exposure to 500 μ M BCS. Therefore, the decrease in Cu is likely destabilizing the COX complex. When there are defects in COX assembly, we normally see absence of proteins that make up the catalytic core – Cox1, Cox2, and Cox3; however, nuclear-encoded subunits are still present (Glerum & Tzagoloff, 1998). In this study, we observe loss of both mitochondrial and nuclear encoded subunits, suggesting that the cell is not responding to defective COX assembly, but something else. Identification of mutated genes in the suppressor screen for growth on non-fermentable carbon sources with BCS will likely provide insight into the genes that are responsible for this process.

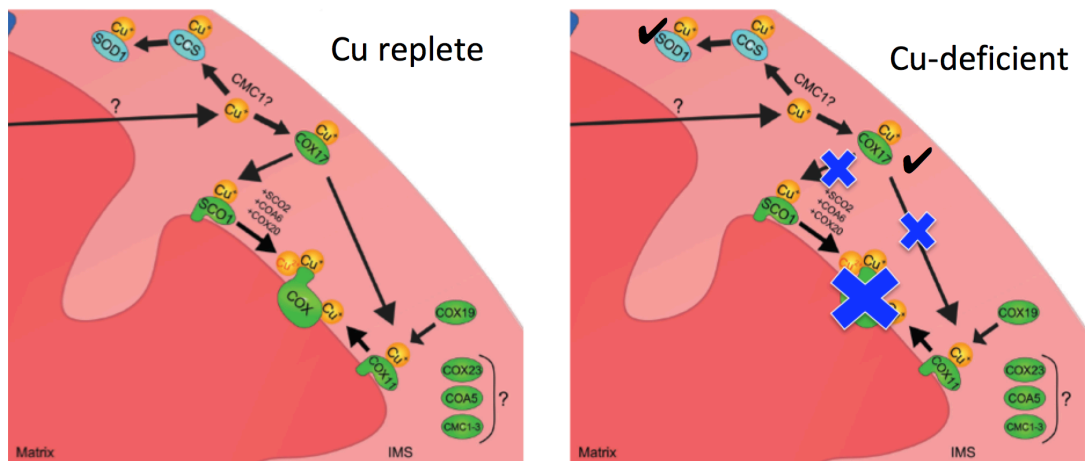


Figure 6.1 Model for Cells in Cu deficiency.

Cu is preferentially donated to mtSod1 in Cu deficient conditions (modified from Baker et al, 2017)

At 500 μM BCS, we are uncertain whether Cu is being directed towards COX *via* Cox17, but our results clearly demonstrate that Sod1 has Cu. Although we lack the antibody to detect Ccs1 protein levels in the mitochondria, the *CCSI* gene is upregulated in Cu deficient conditions and therefore is likely favoring the Cu donation to Sod1 in the mitochondria. Our analysis with BCS also reveals a disconnect between Sod1 transcript and protein levels. Cytosolic Sod1 protein levels make up approximately 90% of cellular Sod1, and they are decreased to 3% of control levels after treatment with 500 μM BCS. However, transcript levels of the *SOD1* gene remain constant after exposure to any BCS concentration, suggesting that protein stability of cytosolic Sod1 is greatly affected by BCS exposure. On the other hand, the mtSod1 pool is only slightly decreased after exposure to 500 μM BCS and therefore seems more stable during limiting Cu.

We first need to address how the mitochondrial and cytosolic pools of Sod1 differ after exposure to BCS. Because they house the electron transport chain, mitochondria generate higher amounts of ROS than other organelles. Although we see slightly lower oxidative damage in mitochondria after exposure to 500 μM BCS, this may be because mtSod1 levels are maintained and therefore are able to break down ROS or simply because there is less Cu present. This is in agreement with the fact that oxidative damage levels are higher in the cytosol, when there is no Sod1 present. Cytosolic Sod1 is likely getting degraded because Sod1 protein levels are barely detectable and *SOD1* transcript levels are maintained. However, if Sod1 enters mitochondria using the Mia40/Erv1 import pathway it is

known that Mia40 substrate take a longer time to enter mitochondria (Habich *et al*, 2019). Therefore, mitochondrial-target Sod1 must be protected in the cytosol so it does not get degraded like the cytosolic pool of Sod1. An exception to this could be if cytosolic Sod1 is not degraded until it is folded, because Sod1 targeted to mitochondria would be in an unfolded state. Previous work has illustrated that Sod1 can be modified by post-translation modifications, including phosphorylation and SUMOylation (Tsang *et al*, 2014) (Fei *et al*, 2006). One of these modifications could activate the proteasomal pathway, which ends with degradation of the cytosolic pool of Sod1. Lastly, mtSod1 would have a disulfide bond formed, which increases its affinity for Cu (Culik *et al*, 2018). This would provide more evidence regarding why the mtSod1 pool exists during Cu depletion conditions and how that pool gets Cu.

Once Cu goes to the IMS, it has two final destinations. Although COX is not assembled, both Cox17 and Sco1 are present during Cu deficient conditions. Therefore, Cu will be preferentially donated to one of the pathways. Since we observe 70% retention of SOD activity in the IMS during Cu depletion, we assume that Cu is first trafficked towards Sod1 before it goes towards COX *via* Cox17. Cmc1, a protein that has an as-yet defined role in COX assembly, was proposed to have a role in trafficking Cu towards one destination over the other (Horn *et al*, 2008). One possibility for the retention of Sod1 activity in mitochondria is because Sod1 is required for activation of Mac1, a Cu-responsive transcription factor that localizes to the nucleus (Wood & Thiele, 2009). As mentioned earlier, Mac1 is crucial for cell survival under low Cu conditions since its activation leads to increased production of Ctr1, a high affinity Cu transporter located on the plasma membrane. In conjunction with this finding, overexpression of Sod1, regardless of its Cu binding abilities, leads to an increase in cellular Cu levels (Tokuda *et al*, 2013). Sod1 localization and protein levels have also been associated with Cu dyshomeostasis in motor neuron cultures, further supporting the hypothesis that Sod1 functions in cellular copper homeostasis (Arciello *et al*, 2011) (Azzouz *et al*, 2000).

We propose that the main reason for the preferential Cu donation is purely based on chemical properties, and depends on the affinity of the candidate protein for Cu. One study done *in vitro* stated that Ccs1 has a higher affinity for Cu than Cox17, which would explain why we observe retention in Sod1 activity but a loss of COX activity (Banci *et al*, 2010). To

our knowledge, our result is the first demonstration of preferential Cu donation *in vivo* that is in agreement with the chemical affinity gradient. Moreover, GSH has an even lower affinity for Cu, further supporting the possibility that GSH is the responsible molecule for Cu import into mitochondria as feasible. Although our results are consistent with the chemical affinity for Cu described *in vitro*, they directly contradict other studies of Cu distribution in the presence of limiting amounts of metal.

The Culotta lab found that when depleting Cu in *Candida albicans*, a pathogenic fungus, cells downregulate Sod1 to maintain COX activity (Li *et al*, 2015) (Broxton & Culotta, 2016). These cells completely get rid of Sod1 in the mitochondria so there is no longer a competition between the Sod1 and COX pathways for Cu, which still supports the chemical affinity gradient (Banci *et al*, 2010). However, *C. albicans* also has a *SOD3* gene, which is purely cytosolic and uses Mn as its catalytic metal (Li *et al*, 2015). In this model system, the mitochondria would likely possess more ROS since they do not have Sod1 residing there. However, *C. albicans* also has an alternative oxidase (AOX), which acts as a final electron acceptor similar to COX. AOX has also been thought to reduce levels of oxidative stress in the mitochondria, which is further compensation for losing the mitochondrial pool of Sod1 (Ruy *et al*, 2006). Similar to this study, another study performed in the model organism *Chlamydomonas* shows that COX function is prioritized with limiting Cu, as other cuproproteins have more dispensable functions (Kropat *et al*, 2016). *Chlamydomonas* does not have a SOD enzyme that uses Cu, instead it contains Fe and Mn-Sod, changing the parameters of Cu distribution in this model system (Merchant *et al*, 2006). Interestingly, limiting Fe in *Chlamydomonas* leads to upregulation of the *MSD3* (Fe-Sod) gene, which leads to increased synthesis of the Mn-Sod gene (Page *et al*, 2012). In both *C. albicans* and *Chlamydomonas*, cells prioritize COX activity during Cu depletion, while in *S. cerevisiae* Cu is preferentially given to mtSod1. The differences we observe in Cu distribution in *S. cerevisiae* are likely associated with the presence of the AOX and the absence of Sod1 in *C. albicans* and *Chlamydomonas*.

When we change the primary carbon source to galactose, we see a significant drop in active Sod1 in mitochondria, in addition to lower Sod1 protein levels. We also see that at 100 μ M BCS in galactose, the *SOD1* gene is downregulated (Appendix A). We hypothesize that because of the role of Sod1 in glucose repression that is no longer necessary when galactose

is present (Reddi & Culotta, 2013). Sod1 is proposed to function in the cytosol to regulate glucose repression by interacting with Yck1 (Reddi & Culotta, 2013) and Pma1 (Baron *et al*, 2015). Specifically, the interaction between Sod1 and the C-terminal of Yck1 requires oxygen and glucose, and Yck1 stabilization means it can repress respiratory genes. The finding regarding Sod1 having a role in nutrient sensing is expanding as Sod1 interacts with mTORC1 in yeast to regulate ROS levels depending on levels of nutrients in the surrounding environment (Tsang *et al*, 2018). Interestingly, our results also show Sod1 depletion in the cytosol after exposure to BCS (Dubinski, unpublished). Another possibility is that *SOD1* is activated by glucose, a phenomenon that is seen with the *TOM22* gene (Gerberth *et al*, 2013). It should also be noted that a Sod1 KO in *S. cerevisiae* cannot grow in galactose, but the reasons behind this are unclear (Glerum, unpublished). Overall, our work regarding galactose remains preliminary and more data are needed to understand how carbon source affects the mitochondrial pool of Sod1.

6.5 Divergent Cell Cycle Phenotypes with Cu Availability

Based on preliminary experiments showing a cell cycle delay in COX assembly mutants, our aim of the cell cycle progression analysis in Cu excess and Cu deplete conditions was to observe whether the cell cycle delay we saw in the mitochondrial cuproprotein mutants was reproducible with Cu imbalance. The cell cycle defects we observe in excess Cu conditions are different than what we observed in the mitochondrial mutants as they reveal a subset of cells stuck in G1 phase. At the 40-minute time point, where all of the cells in the no treatment sample have completed S phase, we see two similar peaks in the 0.1% Cu sample representative of G1 and G2 phases. We also see that after treatment with 0.1% Cu, Rad53 protein levels are significantly decreased to 57% of control levels. Because Rad53 is known to have roles in dNTP pool control (Jossen & Bermejo, 2013), the decrease in Rad53 protein levels likely corresponds to lower dNTP concentrations in the cell. Another reason cells would halt replication is if there are high levels of DNA damage, and cells are extremely prone to mutations (Desany *et al*, 1998). Oxidative stress has been associated with cell cycle defects, suggesting that increased levels of oxidative stress likely play a role in cells being stuck in G1 (Shapira *et al*, 2004). Although we see higher oxidative damage in the mitochondria and cytosol, a more thorough investigation of activation of phosphorylation

cascades in response to DNA damage is necessary. Therefore, from our preliminary data we conclude that cells trapped in G1 phase cannot undergo replication because of decreased dNTP levels.

Another difference between the cell cycle traces in the samples with 0.1% Cu and the control is the presence of a sub-G1 peak in the samples with 0.1% Cu added. Sub-G1 peaks represent cells that have less than 1N DNA, and have been previously reported to be apoptotic cells (Burhans *et al*, 2003). Excess Cu can give rise to the Fenton reaction and causes oxidative stress, which is consistent with our observations that some cells are undergoing apoptosis. As we described in section 6.2, Cox17 may have a role in apoptosis during excess Cu conditions, and from the preliminary cell cycle analysis it appears that some of the cells in the population are apoptotic.

Although our cell cycle results with excess Cu did not mimic the cell cycle defect seen in the COX assembly mutants, literature has proposed that Cu deficiency is more physiologically representative of cuproprotein mutants (Baker *et al*, 2017b) (Maxfield *et al*, 2004). To our surprise, we observe no cell cycle defects between the no treatment sample and any sample treated with BCS. This suggests that the defects we see in the mitochondrial mutants are not associated with their lack of cuproproteins.

Because we observed a near absence of mtSod1 protein levels in galactose compared to retention of these protein levels in glucose, we tested whether cell cycle defects are observed with BCS when galactose was the primary carbon source. Although our results are preliminary, they reveal two distinct differences between carbon sources. Firstly, it appears that cells stay in the G1 phase for a longer period of time, but they go through the G2 phase more quickly. We think that the reason for changes in cell cycle progression we see between galactose and glucose with BCS is because of the presence or absence of mtSod1. Sod1 is a non-essential gene in aerobic organisms but is also found in anaerobic organisms (Chung, 2017), suggesting that it has roles unrelated to breaking down superoxide. Many novel roles of Sod1 unrelated to superoxide breakdown have been discovered in the model organism *Saccharomyces cerevisiae*, and several studies in mammalian systems support these findings.

Yeast Sod1 is thought to act as a transcription factor in response to peroxide-induced oxidative stress after it rapidly translocates to the nucleus (Tsang *et al*, 2014). This translocation is dependent on phosphorylation of ySod1 by a cascade involving Dun1 and

Cds1, and Sod1 must be fully metallated and dimerized for this process to occur (Tsang *et al*, 2014). Once in the nucleus, it is suggested that approximately 30% of Sod1 transcriptional targets are related to DNA damage stress and replication stress. It remains unclear whether Sod1 directly binds DNA or if this happens through interactions with other proteins. Because we know Sod1 is required for activation of Mac1, a well-defined transcription factor, one possibility could be that the upregulation of antioxidant genes during peroxide-induced stress is a result of an interaction involving Sod1 and Mac1. There is also more direct evidence that Sod1 helps regulate cell cycle and dNTP pools through its interactions with Rad53 (Dong *et al*, 2013) and Rnr (Das *et al*, 2018). In conjunction with this, wild type and mutant versions of Sod1 in humans have been found to affect apoptosis (Zhang *et al*, 2016), and this is likely through an interaction between Sod1 and Bcl-2, an anti-apoptotic protein (Pasinelli *et al*, 2004).

Our data suggest that the presence of mtSod1 could have a role in cell cycle regulation, as we observe no cell cycle defect when mtSod1 is present with glucose and BCS, but we do see abnormalities in galactose and BCS, where the major difference is the absence of mtSod1. Both the Ccs1 and Sod1 KO strains display a cell cycle defect (Carter *et al*, 2005), in agreement with our hypothesis. The cell cycle defect seen in the Sod1 KO is likely of a similar severity to the one seen in the Rad53 Sml1 double KO because the strains have similar sensitivities to the DNA damaging agent HU (Carter *et al*, 2005). We also see increase Rad53 protein levels in the Sod1 KO, illustrating that an important protein involved in cell cycle control is affected by loss of Sod1 (Dubinski, unpublished).

6.6 Conclusions and Future directions

In this study, we investigated mitochondrial function in Cu excess and limiting conditions. We hypothesized that changes in Cu availability would affect mitochondrial cuproprotein pools and lead to a cell cycle defect. Our results display significant changes to mitochondrial function with excess or limiting Cu, and we reveal a clear cell cycle defect after exposure to excess Cu.

Although mitochondrial Cu import is fundamental, the pathways surrounding the mechanism by how this works are still under debate. Our results cast doubt on the CuL in the matrix being a main Cu source for IMS residents. Recently, Mrs3, a Fe transporter, was

described to participate in import of Cu to the mitochondrial matrix (Vest *et al*, 2016), which is another mechanism illustrating the well-known intersection between Cu and Fe regulation. Assaying mitochondrial cuproprotein function in excess or limiting Fe conditions would provide insight on subcellular cross-talk between the metals. Similarly, two of the proteins that were assayed, Sod1 and Cox4, also bind Zn. Studying cuproprotein function in mitochondria in the presence or absence of Zn would broaden our understanding of metal homeostasis in mitochondria.

Because mutations in COX assembly factors lead to diverse clinical phenotypes, recent studies have been suggesting alternate functions of these proteins unrelated to COX assembly (Veniamin *et al*, 2011) (Chojnacka *et al*, 2015). We find that the mitochondrial pool of Cox17 is increased with both excess and limiting Cu, and propose that this finding is related to a secondary role of mitochondrial Cox17 in mitochondrial Cu import or apoptosis. To test the hypothesis that Cox17 plays a role in apoptosis, future work will focus on uncovering a relationship between Cox17 and Aif1 and performing immunofluorescence microscopy to track the location of Cox17 during apoptotic induction. This study also highlights divergence in Sco1 and Cox11 functions because of the differential behaviors we observe between these proteins with changing Cu. Our work supports the hypothesis that Sco1 and Sod1 work together to break down ROS in the mitochondria (Kocabay *et al*, 2018).

In Cu deplete conditions our results reveal that COX activity significantly decreases while mitochondrial Sod1 activity is maintained. These data directly contradict studies done in the organisms *Candida albicans* and *Chlamydomonas* and we propose that this is because of the presence of an AOX in these systems and the absence of mtSod1 in Cu deficiency. Growing cells on a non-fermentable carbon source in the presence of BCS is lethal, indicating that cells cannot recover COX function for survival. We isolate four suppressors able to grow on EG + 500 μ M BCS, which can now be sequenced and may provide insight on which genes are involved in regulating mitochondrial Cu distribution.

Changing the primary carbon source to galactose results in loss of both COX and Sod1 function in the mitochondria in limiting Cu conditions. Although we find that exposure to BCS has no apparent cell cycle defect in glucose, we see a defect in Cu deplete conditions with galactose. We hypothesize that the mitochondrial pool of Sod1 is important for normal cell cycle progression, and that loss of this protein pool results in a cell cycle defect. Future

experiments will be aimed at further characterizing the cell cycle defect we see in galactose during Cu deficiency, which will be followed by trying to reproduce the defect in a Sod1 KO or in other carbon sources, such as raffinose. Ultimately, the interactions between Sod1 with Rad53 (Dong *et al*, 2013) and Rnr3 (Das *et al*, 2018) will be explored in detail and provide mechanistic insight towards the function of Sod1 in yeast cell cycle control.

Studies of Cu homeostasis in *Saccharomyces cerevisiae* have provided essential contributions towards our understanding of Cu metabolism and cuproprotein functions in mammalian systems. Continuation of studies regarding Cu homeostatic pathways in yeast, such as this one, is imperative to expand our knowledge of these basic biological mechanisms and for understanding how dysfunction of these pathways plays a role in disease.

References

- Aich, A., Wang, C., Chowdhury, A., Ronsör, C., Pacheu-Grau, D., Richter-Dennerlein, R., ... Rehling, P. (2018). COX16 promotes COX2 metallation and assembly during respiratory complex IV biogenesis. *ELife*, 7, 1–18. <http://doi.org/10.7554/eLife.32572>
- Alberts, B., Johnson, A., Lewis, J., Morgan, D., Raff, M., Roberts, K., & Walter, P. (2015). *Molecular Biology of the Cell*.
- Allen, C., Büttner, S., Aragon, A. D., Thomas, J. A., Meirelles, O., Jaetao, J. E., ... Werner-Washburne, M. (2006). Isolation of quiescent and nonquiescent cells from yeast stationary-phase cultures. *Journal of Cell Biology*, 174(1), 89–100. <http://doi.org/10.1083/jcb.200604072>
- Arciello, M., Capo, C. R., Annibale, S. D., Cozzolino, M., Ferri, A., Carri, M. T., & Rossi, L. (2011). Copper depletion increases the mitochondrial-associated SOD1 in neuronal cells. *BioMetals*, 24(2), 269–278. <http://doi.org/10.1007/s10534-010-9392-3>
- Azzouz, M., Poindron, P., Guettier, S., Leclerc, N., Andres, C., Warter, J. M., & Borg, J. (2000). Prevention of mutant SOD1 motoneuron degeneration by copper chelators in vitro. *Journal of Neurobiology*, 42(1), 49–55. [http://doi.org/10.1002/\(SICI\)1097-4695\(200001\)42:1<49::AID-NEU5>3.0.CO;2-7](http://doi.org/10.1002/(SICI)1097-4695(200001)42:1<49::AID-NEU5>3.0.CO;2-7)
- Baker, Z. N., Cobine, P. A., & Leary, S. C. (2017). The mitochondrion: a central architect of copper homeostasis. *Metallomics*, 9, 1501–1512. <http://doi.org/10.1039/C7MT00221A>
- Baker, Z. N., Jett, K., Boulet, A., Hossain, A., Cobine, P. A., Kim, B. E., ... Leary, S. C. (2017). The mitochondrial metallochaperone SCO1 maintains CTR1 at the plasma membrane to preserve copper homeostasis in the murine heart. *Human Molecular Genetics*, 26(23), 4617–4628. <http://doi.org/10.1093/hmg/ddx344>
- Banci, L., Bertini, I., Ciofi-baffoni, S., Hadjiloi, T., Martinelli, M., & Palumaa, P. (2008). Mitochondrial copper (I) transfer from Cox17 to Sco1 is coupled to electron transfer. *Proceedings of the National Academy of Sciences*, 105(19), 6803–6808.
- Banci, L., Bertini, I., Ciofi-Baffoni, S., Kozyreva, T., Zovo, K., & Palumaa, P. (2010). Affinity gradients drive copper to cellular destinations. *Nature*, 465(7298), 645–648. <http://doi.org/10.1038/nature09018>
- Banting, G. S., & Glerum, D. M. (2006). Mutational Analysis of the *Saccharomyces cerevisiae* Cytochrome c Oxidase Assembly Protein Cox11p. *Eukaryotic Cell*, 5(3), 568–578. <http://doi.org/10.1128/EC.5.3.568>
- Barnum, K. J., & O'Connell, M. J. (2014). Cell Cycle Regulation by Checkpoints. *Methods in Molecular Biology*, (1170), 29–40. http://doi.org/10.1007/978-1-4939-0888-2_2
- Baron, J. A., Chen, J. S., & Culotta, V. C. (2015). Cu/Zn superoxide dismutase and the proton ATPase Pma1p of *Saccharomyces cerevisiae*. *Biochemical and Biophysical Research Communications*, 462(3), 251–256. <http://doi.org/10.1016/j.bbrc.2015.04.127>

- Barros, M. H., Johnson, A., & Tzagoloff, A. (2004). COX23, a homologue of COX17, is required for cytochrome oxidase assembly. *Journal of Biological Chemistry*, 279(30), 31943–31947. <http://doi.org/10.1074/jbc.M405014200>
- Beauchamp, C., & Fridovich, I. (1971). Superoxide Dismutase: Improved Assays and an Assay Applicable to Acrylamide Gels. *Analytical Biochemistry*, 287, 276–287.
- Beers, J., Glerum, D. M., & Tzagoloff, A. (2002). Purification and Characterization of Yeast Sco1p, a Mitochondrial Copper Protein. *Journal of Biological Chemistry*, 277(25), 22185–22190. <http://doi.org/10.1074/jbc.M202545200>
- Beers, J., Glerum, D. M., & Tzagoloff, A. (1997). Purification, characterization, and localization of yeast Cox17p, a mitochondrial copper shuttle. *Journal of Biological Chemistry*, 272(52), 33191–33196. <http://doi.org/10.1074/jbc.272.52.33191>
- Blachly-Dyson, E., Song, J., Wolfgang, W. J., Colombini, M., & Forte, M. (1997). Multicopy suppressors of phenotypes resulting from the absence of yeast VDAC encode a VDAC-like protein. *Molecular and Cellular Biology*, 17(10), 5727–38. <http://doi.org/10.1016/j.fishres.2013.07.001>
- Blomberg, M. R. A., & Siegbahn, P. E. M. (2014). Proton pumping in cytochrome c oxidase: Energetic requirements and the role of two proton channels. *Biochimica et Biophysica Acta - Bioenergetics*, 1837, 1165–1177. <http://doi.org/10.1016/j.bbabi.2014.01.002>
- Bode, M., Woellhaf, M. W., Bohnert, M., Laan, M. v. d., Sommer, F., Jung, M., ... Herrmann, J. M. (2015). Redox-regulated dynamic interplay between Cox19 and the copper-binding protein Cox11 in the intermembrane space of mitochondria facilitates biogenesis of cytochrome c oxidase. *Molecular Biology of the Cell*, 26(13), 2385–2401. <http://doi.org/10.1091/mbc.E14-11-1526>
- Boulet, A., Vest, K. E., Maynard, M. K., Gammon, M. G., Russell, A. C., Mathews, A. T., ... Cobine, P. A. (2018). The mammalian phosphate carrier SLC25A3 is a mitochondrial copper transporter required for cytochrome c oxidase biogenesis. *Journal of Biological Chemistry*, 293(6), 1887–1896. <http://doi.org/10.1074/jbc.RA117.000265>
- Brady, G. F., Galban, S., Liu, X., Basrur, V., Gitlin, J. D., Elenitoba-Johnson, K. S. J., ... Duckett, C. S. (2010). Regulation of the Copper Chaperone CCS by XIAP-Mediated Ubiquitination. *Molecular and Cellular Biology*, 30(8), 1923–1936. <http://doi.org/10.1128/MCB.00900-09>
- Broxton, C. N., & Culotta, V. C. (2016). An adaptation to low copper in *Candida albicans* involving SOD Enzymes and the alternative oxidase. *PLoS ONE*, 11(12), 1–16. <http://doi.org/10.1371/journal.pone.0168400>
- Bulteau, A.-L., Lundberg, K. C., Ikeda-Saito, M., Isaya, G., & Szwedda, L. I. (2005). Reversible redox-dependent modulation of mitochondrial aconitase and proteolytic activity during in vivo cardiac ischemia/reperfusion. *Proceedings of the National Academy of Sciences*, 102(17), 5987–5991. <http://doi.org/10.1073/pnas.0501519102>

- Burhans, W. C., Weinberger, M., Marchetti, M. A., Ramachandran, L., D'Urso, G., & Huberman, J. A. (2003). Apoptosis-like yeast cell death in response to DNA damage and replication defects. *Mutation Research - Fundamental and Molecular Mechanisms of Mutagenesis*, 532(1–2), 227–243. <http://doi.org/10.1016/j.mrfmmm.2003.08.019>
- Calabrese, G., Morgan, B., & Riemer, J. (2017). Mitochondrial Glutathione: Regulation and Functions. *Antioxidants & Redox Signaling*, 27(15), ars.2017.7121. <http://doi.org/10.1089/ars.2017.7121>
- Camasta, Raffaele (2017). Cytochrome c Oxidase Deficiency: Study of Aberrant Phenotypes and their Connection to Secondary Functions of Assembly Factors. *UW Space*. <http://hdl.handle.net/10012/12726>
- Cankorur-Cetinkaya, A., Eraslan, S., & Kirdar, B. (2016). Transcriptomic response of yeast cells to ATX1 deletion under different copper levels. *BMC Genomics*, 17(1), 1–14. <http://doi.org/10.1186/s12864-016-2771-6>
- Cankorur-Cetinkaya, A., Eraslan, S., & Kirdar, B. (2013). Transcriptional remodelling in response to changing copper levels in the Wilson and Menkes disease model of *Saccharomyces cerevisiae*. *Molecular BioSystems*, 9(11), 2889. <http://doi.org/10.1039/c3mb70276f>
- Carmona-Gutierrez, D., Eisenberg, T., Büttner, S., Meisinger, C., Kroemer, G., & Madeo, F. (2010). Apoptosis in yeast: Triggers, pathways, subroutines. *Cell Death and Differentiation*, 17(5), 763–773. <http://doi.org/10.1038/cdd.2009.219>
- Carroll, M. C., Girouard, J. B., Ulloa, J. L., Subramaniam, J. R., Wong, P. C., Valentine, J. S., & Culotta, V. C. (2004). Mechanisms for activating Cu- and Zn-containing superoxide dismutase in the absence of the CCS Cu chaperone. *Proceedings of the National Academy of Sciences*, 101(16), 5964–5969. <http://doi.org/10.1073/pnas.0308298101>
- Carter, C. D., Kitchen, L. E., Au, W., Babic, C. M., & Basrai, M. A. (2005). Loss of SOD1 and LYS7 Sensitizes *Saccharomyces cerevisiae* to Hydroxyurea and DNA Damage Agents and Downregulates MEC1 Pathway Effectors. *Molecular and Cellular Biology*, 25(23), 10273–10285. <http://doi.org/10.1128/MCB.25.23.10273>
- Chen, C.-C., Chen, Y.-Y., Tang, I.-C., Liang, H.-M., Lai, C.-C., Chiou, J.-M., & Yeh, K.-C. (2011). Arabidopsis SUMO E3 Ligase SIZ1 Is Involved in Excess Copper Tolerance. *Plant Physiology*, 156(4), 2225–2234. <http://doi.org/10.1104/pp.111.178996>
- Chojnacka, M., Gornicka, A., Oeljeklaus, S., Warscheid, B., & Chacinska, A. (2015). Cox17 protein is an auxiliary factor involved in the control of the mitochondrial contact site and cristae organizing system. *Journal of Biological Chemistry*, 290(24), 15304–15312. <http://doi.org/10.1074/jbc.M115.645069>
- Chung, W.-H. (2017). Unraveling new functions of superoxide dismutase using yeast model system: Beyond its conventional role in superoxide radical scavenging. *Journal of Microbiology*, 55(6), 409–416. <http://doi.org/10.1007/s12275-017-6647-5>

- Cobine, P. A., Ojeda, L. D., Rigby, K. M., & Winge, D. R. (2004). Yeast Contain A Non-proteinaceous Pool of Copper in the Mitochondrial Matrix. *Journal of Biological Chemistry*, 279(14), 14447–14455. <http://doi.org/10.1074/jbc.M312693200>
- Cobine, P. A., Pierrel, F., Bestwick, M. L., & Winge, D. R. (2006). Mitochondrial matrix copper complex used in metallation of cytochrome oxidase and superoxide dismutase. *Journal of Biological Chemistry*, 281(48), 36552–36559. <http://doi.org/10.1074/jbc.M606839200>
- Corson, L. B., Strain, J. J., Culotta, V. C., & Cleveland, D. W. (1998). Chaperone-facilitated copper binding is a property common to several classes of familial amyotrophic lateral sclerosis-linked superoxide dismutase mutants. *Proceedings of the National Academy of Sciences of the United States of America*, 95(11), 6361–6366. <http://doi.org/10.1073/pnas.95.11.6361>
- Coyne, H. J., Ciofi-baffoni, S., Banci, L., Bertini, I., Zhang, L., George, G. N., & Winge, D. R. (2007). The Characterization and Role of Zinc Binding in Yeast Cox4. *Journal of Biological Chemistry*, 282(12), 8926–8934. <http://doi.org/10.1074/jbc.M610303200>
- Cruz, R. Dela, Jeong, M., & Winge, D. R. (2016). Cox1 mutation abrogates need for Cox23 in cytochrome c oxidase biogenesis. *Microbial Cell*, 3(7), 275–284. <http://doi.org/10.15698/mic2016.07.511>
- Culik, R. M., Sekhar, A., Nagesh, J., Deol, H., Rumfeldt, J. A. O., Meiering, E. M., & Kay, L. E. (2018). Effects of maturation on the conformational free-energy landscape of SOD1. *Proceedings of the National Academy of Sciences*, 115(11), E2546–E2555. <http://doi.org/10.1073/pnas.1721022115>
- Culotta, V. C., Klomp, L. W. J., Strain, J., Casareno, R. L. B., Krems, B., & Gitlin, J. D. (1997). The Copper Chaperone for Superoxide Dismutase. *Journal of Biological Chemistry*, 272(23), 23469–23473. <http://doi.org/10.1074/jbc.272.23.23469>
- Cwerman-Thibault, H., Augustin, S., Lechauve, C., Ayache, J., Ellouze, S., & Sahel, J.-A. (2015). Nuclear expression of mitochondrial nd4 leads to the protein assembling in complex I and prevents optic atrophy and visual loss. *Methods & Clinical Development*, (January), 1–15. <http://doi.org/10.1038/mtm.2015.3>
- Dancis, A., Haile, D., Yuan, D., & Klausner, R. (1994). The *Saccharomyces cerevisiae* Copper Transport Protein (Ctr1p). *The Journal of Biological Chemistry*, 269(41), 25660–25667.
- Dancis, A., Roman, D. G., Anderson, G. J., Hinnebusch, A. G., & Klausner, R. D. (1992). Ferric reductase of *Saccharomyces cerevisiae*: molecular characterization, role in iron uptake, and transcriptional control by iron. *Proceedings of the National Academy of Sciences of the United States of America*, 89(May), 3869–3873. <http://doi.org/DOI 10.1073/pnas.89.9.3869>
- Das, A. B., Sadowska-Bartosz, I., Königstorfer, A., Kettle, A. J., & Winterbourn, C. C. (2018). Superoxide dismutase protects ribonucleotide reductase from inactivation in yeast. *Free Radical Biology and Medicine*, 116(December 2017), 114–122. <http://doi.org/10.1016/j.freeradbiomed.2018.01.001>

- Das, A., Varadarajan, S., Surenkhuu, B., Kweon, J., Abe, J., Ushio-fukai, M., & Fukai, T. (2018). Novel Role of Redox-Sensitive SUMOylation of Cu Transport Protein Atox1 in Inflammation and Atherosclerosis. In *Atherosclerosis, Vascular Biology and Development*.
- Desany, B. A., Alcasabas, A. A., Bachant, J. B., & Elledge, S. J. (1998). Recovery from DNA replicational stress is the essential function of the S-phase checkpoint pathway. *Genes and Development*, 3, 2956–2970.
- Dodani, S. C., Leary, S. C., Cobine, P. A., Winge, D. R., & Chang, C. J. (2011). A targetable fluorescent sensor reveals that copper-deficient SCO1 and SCO2 patient cells prioritize mitochondrial copper homeostasis. *Journal of the American Chemical Society*, 133(22), 8606–8616. <http://doi.org/10.1021/ja2004158>
- Dong, K., Addinall, S. G., Lydall, D., & Rutherford, J. C. (2013). The Yeast Copper Response Is Regulated by DNA Damage. *Molecular and Cellular Biology*, 33(20), 4041–4050. <http://doi.org/10.1128/MCB.00116-13>
- Dubinski, A. F., Camasta, R., Soule, T. G. B., Reed, B. H., & Glerum, D. M. (2018). Consequences of cytochrome c oxidase assembly defects for the yeast stationary phase. *Biochimica et Biophysica Acta - Bioenergetics*, 1859(6), 445–458. <http://doi.org/10.1016/j.bbabi.2018.03.011>
- Fei, E., Jia, N., Yan, M., Ying, Z., Sun, Q., Wang, H., ... Wang, G. (2006). SUMO-1 modification increases human SOD1 stability and aggregation. *Biochemical and Biophysical Research Communications*, 347(2), 406–412. <http://doi.org/10.1016/j.bbrc.2006.06.092>
- Fetherolf, M., Boyd, S. D., Winkler, D. D., & Winge, D. R. (2017). Oxygen-dependent activation of Cu,Zn-superoxide dismutase-1. *Metallomics*, 9(8), 1047–1059. <http://doi.org/10.1039/C6MT00298F>
- Furukawa, Y., Torres, A. S., & O'Halloran, T. V. (2004). Oxygen-induced maturation of SOD1: A key role for disulfide formation by the copper chaperone CCS. *EMBO Journal*, 23(14), 2872–2881. <http://doi.org/10.1038/sj.emboj.7600276>
- Georgatsou, E., Mavrogiannis, L. A., Fragiadakis, G. S., & Alexandraki, D. (1997). The yeast Fre1p/Fre2p cupric reductases facilitate copper uptake and are regulated by the copper-modulated Mac1p activator. *Journal of Biological Chemistry*, 272(21), 13786–13792. <http://doi.org/10.1074/jbc.272.21.13786>
- Georgouloupoulou, E., Fini, N., Vinceti, M., Monelli, M., Vacondio, P., Bianconi, G., ... Mandrioli, J. (2013). The impact of clinical factors, riluzole and therapeutic interventions on ALS survival: A population based study in Modena, Italy. *Amyotrophic Lateral Sclerosis and Frontotemporal Degeneration*, 14(5–6), 338–345. <http://doi.org/10.3109/21678421.2013.763281>
- Gerbeth, C., Schmidt, O., Rao, S., Harbauer, A. B., Mikropoulou, D., Opalinska, M., ... Meisinger, C. (2013). Glucose-induced regulation of protein import receptor tom22 by cytosolic and mitochondria-bound kinases. *Cell Metabolism*, 18(4), 578–587. <http://doi.org/10.1016/j.cmet.2013.09.006>

- Ghosh, A., Trivedi, P. P., Timbalia, S. A., Griffin, A. T., Rahn, J. J., Chan, S. S. L., & Gohil, V. M. (2014). Copper supplementation restores cytochrome c oxidase assembly defect in a mitochondrial disease model of COA6 deficiency. *Human Molecular Genetics*, 23(13), 3596–3606. <http://doi.org/10.1093/hmg/ddu069>
- Glerum, D. M., & Tzagoloff, A. (1998). Affinity purification of yeast cytochrome oxidase with biotinylated subunits 4, 5, or 6. *Anal Biochem*, 260(1), 38–43. Retrieved from http://www.ncbi.nlm.nih.gov/entrez/query.fcgi?cmd=Retrieve&db=PubMed&dopt=Citation&list_uids=9648650
- Glerum, D. M., Shtanko, A., & Tzagoloff, A. (1996). Characterization of COX17, a Yeast Gene Involved in Copper Metabolism and Assembly of Cytochrome Oxidase. *The Journal of Biological Chemistry*, 271(24), 14504–14509. <http://doi.org/10.1074/jbc.271.24.14504>
- Glerum, D. M., Shtanko, A., & Tzagoloff, A. (1996). SCO1 and SCO2 Act as High Copy Suppressors of a Mitochondrial Copper Recruitment Defect in *Saccharomyces cerevisiae*. *Journal of Biological Chemistry*, 271(34), 20531–20535.
- Gomes, I. M., Maia, C. J., & Santos, C. R. (2012). STEAP Proteins: From Structure to Applications in Cancer Therapy. *Molecular Cancer Research*, 10(5), 573–587. <http://doi.org/10.1158/1541-7786.MCR-11-0281>
- Graffmo, K. S., Forsberg, K., Bergh, J., Birve, A., Zetterström, P., Andersen, P. M., ... Brännström, T. (2013). Expression of wild-type human superoxide dismutase-1 in mice causes amyotrophic lateral sclerosis. *Human Molecular Genetics*, 22(1), 51–60. <http://doi.org/10.1093/hmg/ddc399>
- Gross, C., Kelleher, M., Iyer, V. R., Brown, P. O., & Winge, D. R. (2000). Identification of the copper regulon in *Saccharomyces cerevisiae* by DNA microarrays. *Journal of Biological Chemistry*, 275(41), 32310–32316. <http://doi.org/10.1074/jbc.M005946200>
- Gulec, S., & Collins, J. F. (2014). Molecular Mediators Governing Iron-Copper Interactions. *Annual Reviews Nutrition*, 95–116. <http://doi.org/10.1146/annurev-nutr-071812-161215>
- Haase, S. B., & Reed, S. I. (2002). Improved Flow Cytometric Analysis of the Budding Yeast Cell Cycle. *Cell Cycle*, 1(2), 132–136.
- Habich, M., Salscheider, S. L., Murschall, L. M., Hoehne, M. N., Fischer, M., Schorn, F., ... Riemer, J. (2019). Vectorial Import via a Metastable Disulfide-Linked Complex Allows for a Quality Control Step and Import by the Mitochondrial Disulfide Relay. *Cell Reports*, 26(3), 759–774.e5. <http://doi.org/10.1016/j.celrep.2018.12.092>
- Hamel, P., Saint-georges, Y., Pinto, B. De, Lachacinski, N., Altamura, N., & Dujardin, G. (2004). Redundancy in the function of mitochondrial phosphate transport in *Saccharomyces cerevisiae* and *Arabidopsis thaliana*. *Molecular Microbiology*, 51, 307–317. <http://doi.org/10.1046/j.1365-2958.2003.03810.x>
- Hangen, E., Féraud, O., Lachkar, S., Mou, H., Doti, N., Fimia, G. M., ... Modjtahedi, N. (2015). Interaction between AIF and CHCHD4 Regulates Respiratory Chain Biogenesis. *Molecular Cell*, 58(6), 1001–1014. <http://doi.org/10.1016/j.molcel.2015.04.020>

- Hassett, R., & Kosman, D. J. (1995). Evidence for Cu(II) Reduction as a Component of Cu Uptake by *Saccharomyces cerevisiae*. *Journal of Biological Chemistry*, 270(1), 128–134.
- Heaton, D. N., George, G. N., Garrison, G., & Winge, D. R. (2001). The mitochondrial copper metallochaperone Cox17 exists as an oligomeric, polycopper complex. *Biochemistry*, 40(3), 743–751. <http://doi.org/10.1021/bi002315x>
- Hiser, L., Valentin, M. Di, Hamer, A. G., & Hosler, J. P. (2000). Cox11p Is Required for Stable Formation of the Cu B and Magnesium Centers of Cytochrome c Oxidase. *Journal of Biological Chemistry*, 275(1), 619–623.
- Hlynialuk, C. J., Ling, B., Baker, Z. N., Cobine, P. A., Yu, L. D., Boulet, A., ... Leary, S. C. (2015). The Mitochondrial Metallochaperone SCO1 Is Required to Sustain Expression of the High-Affinity Copper Transporter CTR1 and Preserve Copper Homeostasis. *Cell Reports*, 10(6), 933–943. <http://doi.org/10.1016/j.celrep.2015.01.019>
- Horn, D., Al-Ali, H., & Barrientos, A. (2008). Cmc1p Is a Conserved Mitochondrial Twin CX9C Protein Involved in Cytochrome c Oxidase Biogenesis. *Molecular and Cellular Biology*, 28(13), 4354–4364. <http://doi.org/10.1128/MCB.01920-07>
- Horn, D., & Barrientos, A. (2008). Mitochondrial copper metabolism and delivery to cytochrome C oxidase. *IUBMB Life*, 60(7), 421–429. <http://doi.org/10.1002/iub.50>
- Hornig, Y. C., Cobine, P. A., Maxfield, A. B., Carr, H. S., & Winge, D. R. (2004). Specific copper transfer from the Cox17 metallochaperone to both Sco1 and Cox11 in the assembly of yeast cytochrome c oxidase. *Journal of Biological Chemistry*, 279(34), 35334–35340. <http://doi.org/10.1074/jbc.M404747200>
- Hung, I. H., Suzuki, M., Yamaguchi, Y., Yuan, D. S., Klausner, R. D., & Gitlin, J. D. (1997). Biochemical characterization of the Wilson disease protein and functional expression in the yeast *Saccharomyces cerevisiae*. *Journal of Biological Chemistry*, 272(34), 21461–21466. <http://doi.org/10.1074/jbc.272.34.21461>
- Huster, D., Purnat, T. D., Burkhead, J. L., Ralle, M., Fiehn, O., Stuckert, F., ... Lutsenko, S. (2007). High copper selectively alters lipid metabolism and cell cycle machinery in the mouse model of Wilson disease. *Journal of Biological Chemistry*, 282(11), 8343–8355. <http://doi.org/10.1074/jbc.M607496200>
- Illing, A. C., Shawki, A., Cunningham, C. L., & Mackenzie, B. (2012). Substrate Profile and Metal-ion Selectivity of Human Divalent, 287(36), 30485–30496. <http://doi.org/10.1074/jbc.M112.364208>
- Islinger, M., Li, K. W., Seitz, J., Völkl, A., & Lüers, G. H. (2009). Hitchhiking of Cu/Zn superoxide dismutase to peroxisomes - Evidence for a natural piggyback import mechanism in mammals. *Traffic*, 10(11), 1711–1721. <http://doi.org/10.1111/j.1600-0854.2009.00966.x>
- Itoh, S., Kim, H. W., Nakagawa, O., Ozumi, K., Lessner, S. M., Aoki, H., ... Fukai, T. (2008). Novel Role of Antioxidant-1 (Atox1) as a Copper-dependent Transcription Factor Involved in Cell

- Proliferation. *Journal of Biological Chemistry*, 283(14), 9157–9167.
<http://doi.org/10.1074/jbc.M709463200>
- Jaksch, M., Paret, C., Stucka, R., Horn, N., Müller-höcker, J., Horvath, R., ... Lochmüller, H. (2001). Cytochrome c oxidase deficiency due to mutations in SCO2, encoding a mitochondrial copper-binding protein, is rescued by copper in human myoblasts. *Human Molecular Genetics*, 10(26), 3025–3036.
- Jensen, L. T., & Culotta, V. C. (2005). Activation of CuZn superoxide dismutases from *Caenorhabditis elegans* does not require the copper chaperone CCS. *Journal of Biological Chemistry*, 280(50), 41373–41379. <http://doi.org/10.1074/jbc.M509142200>
- Jossen, R., & Bermejo, R. (2013). The DNA damage checkpoint response to replication stress: A Game of Forks. *Frontiers in Genetics*, 4(March), 1–14. <http://doi.org/10.3389/fgene.2013.00026>
- Kampfenkel, K., Kushnir, S., Babiyshuk, E., Inze, D., & Van Montagu, M. (1995). Molecular Characterization of A Putative Arabidopsis-Thaliana Copper Transporter and Its Yeast Homolog. *Journal of Biological Chemistry*, 270(47), 28479–28486.
<http://doi.org/10.1074/jbc.270.47.28479>
- Karch, C. M., Prudencio, M., Winkler, D. D., Hart, P. J., & Borchelt, D. R. (2009). Role of mutant SOD1 disulfide oxidation and aggregation in the pathogenesis of familial ALS. *Proceedings of the National Academy of Sciences*, 106(19), 7774–7779.
<http://doi.org/10.1073/pnas.0902505106>
- Kastan, M. I. B., Zhan, Q., El-deiry, W. S., Carrier, F., Jacks, T., Walsh, W. V., ... Fornace, A. J. (1992). A Mammalian Cell Cycle Checkpoint Pathway Utilizing p53 and GADD45 Is Defective in Ataxia-Telangiectasia. *Cell*, 71, 587–597.
- Kawamata, H., & Manfredi, G. (2008). Different regulation of wild-type and mutant Cu,Zn superoxide dismutase localization in mammalian mitochondria. *Human Molecular Genetics*, 17(21), 3303–3317. <http://doi.org/10.1093/hmg/ddn226>
- Kawamata, H., & Manfredi, G. (2010). Import, Maturation, and Function of SOD1 and Its Copper Chaperone CCS in the Mitochondrial Intermembrane Space. *Antioxidants & Redox Signaling*, 13(9), 1375–1384. <http://doi.org/10.1089/ars.2010.3212>
- Kayikci, O., & Nielsen, J. (2015). Glucose repression in *Saccharomyces cerevisiae*. *FEMS Yeast Research*, (March), 1–8. <http://doi.org/10.1093/femsyr/fov068>
- Keller, G., Bird, A., & Winge, D. R. (2005). Independent metalloregulation of Ace1 and Mac1 in *Saccharomyces cerevisiae*. *Eukaryotic Cell*, 4(11), 1863–1871.
<http://doi.org/10.1128/EC.4.11.1863-1871.2005>
- Khalimonchuk, O., Rigby, K., Bestwick, M., Pierrel, F., Cobine, P. A., & Winge, D. R. (2008). Pet191 is a cytochrome c oxidase assembly factor in *Saccharomyces cerevisiae*. *Eukaryotic Cell*, 7(8), 1427–1431. <http://doi.org/10.1128/EC.00132-08>

- Kocabay, A. E., Kost, L., Gehlhar, M., Rödel, G., & Gey, U. (2018). “Mitochondrial Sco proteins are involved in oxidative stress defense.” *Redox Biology*, 21(November 2018), 101079. <http://doi.org/10.1016/J.REDOX.2018.101079>
- Kojer, K., Bien, M., Gangel, H., Morgan, B., Dick, T. P., & Riemer, J. (2012). Glutathione redox potential in the mitochondrial intermembrane space is linked to the cytosol and impacts the Mia40 redox state. *EMBO Journal*, 31(14), 3169–3182. <http://doi.org/10.1038/emboj.2012.165>
- Kropat, J., Gallaher, S. D., Urzica, E. I., Nakamoto, S. S., Strenkert, D., Tottey, S., ... Merchant, S. S. (2015). Copper economy in Chlamydomonas: Prioritized allocation and reallocation of copper to respiration vs. photosynthesis. *Proceedings of the National Academy of Sciences*, 112(9), 2644–2651. <http://doi.org/10.1073/pnas.1422492112>
- Lang, M., Fan, Q., Wang, L., Zheng, Y., Xiao, G., Wang, X., ... Zhou, B. (2013). Inhibition of human high affinity copper importer Ctr1 orthologous in the nervous system of Drosophila ameliorates Aβ42-induced alzheimer’s disease-like symptoms. *Neurobiology Aging*, 34(11), 2604–2612. <http://doi.org/10.1016/j.neurobiolaging.2013.05.029>
- Leary, S. C., Cobine, P. A., Nishimura, T., Verdijk, R. M., de Krijger, R., de Coo, R., ... Shoubridge, E. A. (2013). COX19 mediates the transduction of a mitochondrial redox signal from SCO1 that regulates ATP7A-mediated cellular copper efflux. *Molecular Biology of the Cell*, 24(6), 683–691. <http://doi.org/10.1091/mbc.E12-09-0705>
- Leary, S. C., Cobine, P. A., Kaufman, B. A., Guercin, G. H., Mattman, A., Palaty, J., ... Shoubridge, E. A. (2007). The Human Cytochrome c Oxidase Assembly Factors SCO1 and SCO2 Have Regulatory Roles in the Maintenance of Cellular Copper Homeostasis. *Cell Metabolism*, 5(1), 9–20. <http://doi.org/10.1016/j.cmet.2006.12.001>
- Li, C. X., Gleason, J. E., Zhang, S. X., Bruno, V. M., Cormack, B. P., & Culotta, V. (2015). Candida albicans adapts to host copper during infection by swapping metal cofactors for superoxide dismutase. *Proceedings of the National Academy of Sciences*, 1–7. <http://doi.org/10.1073/pnas.1513447112>
- Liang, Y., Ewing, P. M., Laursen, W. J., Tripp, V. T., Singh, S., & Splan, K. E. (2014). Copper-binding properties of the BIR2 and BIR3 domains of the X-linked inhibitor of apoptosis protein. *Journal of Inorganic Biochemistry*, 140, 104–110. <http://doi.org/10.1016/j.jinorgbio.2014.07.010>
- Lin, S. J., Pufahl, R. A., Dancis, A., O’Halloran, T. V., & Culotta, V. C. (1997). A role for the Saccharomyces cerevisiae ATX1 gene in copper trafficking and iron transport. *Journal of Biological Chemistry*, 272(14), 9215–9220. <http://doi.org/10.1074/jbc.272.14.9215>
- Linz, R., & Lutsenko, S. (2007). Copper-transporting ATPases ATP7A and ATP7B: Cousins, not twins. *Journal of Bioenergetics and Biomembranes*, 39(5–6), 403–407. <http://doi.org/10.1007/s10863-007-9101-2>
- Liu, X. F., Elashvili, I., Gralla, E. B., Valentine, J. S., Lapinskas, P., & Culotta, V. C. (1992). Yeast Lacking Superoxide Dismutase. *Journal of Biological Chemistry*, 267(26), 18298–18302. Retrieved from <http://www.jbc.org/content/267/26/18298.full.pdf>

- Livak, K. J., & Schmittgen, T. D. (2001). Analysis of Relative Gene Expression Data Using Real-Time Quantitative PCR and the 2 CT Method. *Methods*, *408*, 402–408. <http://doi.org/10.1006/meth.2001.1262>
- Lode, A., Kuschel, M., Paret, C., & Rodel, G. (2000). Mitochondrial copper metabolism in yeast: interaction between Sco1p and Cox2p. *FEBS Letters*, *485*, 19–24.
- Lowry, O. H., Rosebrough, N. J., Farr, A. L., & Randall, R. J. (1951). Protein Measurement with the Folin Phenol Reagent. *Journal of Biological Chemistry*, (193), 265–275.
- Lumpkin, R. J., Gu, H., Zhu, Y., Leonard, M., Ahmad, A. S., Clauser, K. R., ... Komives, E. A. (2017). Site-specific identification and quantitation of endogenous SUMO modifications under native conditions. *Nature Communications*, *8*(1). <http://doi.org/10.1038/s41467-017-01271-3>
- Macreadie, I. G. (2008). Copper transport and Alzheimer's disease. *European Biophysics Journal*, *37*(3), 295–300. <http://doi.org/10.1007/s00249-007-0235-2>
- Madeo, F., Carmona-Gutierrez, D., Ring, J., Büttner, S., Eisenberg, T., & Kroemer, G. (2009). Caspase-dependent and caspase-independent cell death pathways in yeast. *Biochemical and Biophysical Research Communications*, *382*(2), 227–231. <http://doi.org/10.1016/j.bbrc.2009.02.117>
- Magri, A., Di Rosa, M. C., Tomasello, M. F., Guarino, F., Reina, S., Messina, A., & De Pinto, V. (2016). Overexpression of human SOD1 in VDAC1-less yeast restores mitochondrial functionality modulating beta-barrel outer membrane protein genes. *Biochimica et Biophysica Acta - Bioenergetics*, *1857*(6), 789–798. <http://doi.org/10.1016/j.bbabi.2016.03.003>
- Martins, D., & English, A. M. (2014). SOD1 oxidation and formation of soluble aggregates in yeast: Relevance to sporadic ALS development. *Redox Biology*, *2*(1), 632–639. <http://doi.org/10.1016/j.redox.2014.03.005>
- Maryon, E. B., Molloy, S. A., & Kaplan, J. H. (2013). Cellular glutathione plays a key role in copper uptake mediated by human copper transporter 1. *AJP: Cell Physiology*, *304*(8), C768–C779. <http://doi.org/10.1152/ajpcell.00417.2012>
- Matic, S., Muders, V., & Meisinger, C. (2018). ScienceDirect Tuning the mitochondrial protein import machinery by reversible phosphorylation : from metabolic switches to cell cycle regulation. *Current Opinion in Psychology*, *3*, 49–56. <http://doi.org/10.1016/j.cophys.2018.02.011>
- Maxfield, A. B., Heaton, D. N., & Winge, D. R. (2004). Cox17 Is Functional When Tethered to the Mitochondrial Inner Membrane. *Journal of Biological Chemistry*, *279*(7), 5072–5080. <http://doi.org/10.1074/jbc.M311772200>
- McEwen, J. E., Cameron, V. L., & Poyton, R. (1985). Rapid Method for Isolation and Screening of Cytochrome c Oxidase- Deficient Mutants of *Saccharomyces cerevisiae*. *Journal of Bacteriology*, *161*(3), 831–835.

- Merchant, S. S., Allen, M. D., Kropat, J., Moseley, J. L., Long, J. C., Tottey, S., & Terauchi, A. M. (2006). Between a rock and a hard place : Trace element nutrition in *Chlamydomonas*. *Biochimica et Biophysica Acta*, 1763, 578–594. <http://doi.org/10.1016/j.bbamcr.2006.04.007>
- Miller, M. A., Russo, J., Fischer, A. D., Leban, F. A. L., & Olivas, W. M. (2014). Carbon source-dependent alteration of Puf3p activity mediates rapid changes in the stabilities of mRNAs involved in mitochondrial function. *Nucleic Acids Research*, 42(6), 3954–3970. <http://doi.org/10.1093/nar/gkt1346>
- Monje-Casas, F., & Walker, J. M. (2017). *The Mitotic Exit Network*.
- Mufti, A. R., Burstein, E., & Duckett, C. S. (2007). XIAP: Cell death regulation meets copper homeostasis. *Archives of Biochemistry and Biophysics*, 463(2), 168–174. <http://doi.org/10.1016/j.abb.2007.01.033>
- Nedd, S., Redler, R. L., Proctor, E. A., Dokholyan, N. V., & Alexandrova, A. N. (2014). Cu,Zn-Superoxide Dismutase without Zn Is Folded but Catalytically Inactive. *Journal of Molecular Biology*, 426(24), 4112–4124. <http://doi.org/10.1016/j.jmb.2014.07.016>
- Nevitt, T., Öhrvik, H., & Thiele, D. J. (2012). Charting the travels of copper in eukaryotes from yeast to mammals. *Biochimica et Biophysica Acta - Molecular Cell Research*, 1823(9), 1580–1593. <http://doi.org/10.1016/j.bbamcr.2012.02.011>
- Nobrega, M. P., Bandeira, S. C. B., Beers, J., & Tzagoloff, A. (2002). Characterization of COX19, a widely distributed gene required for expression of mitochondrial cytochrome oxidase. *The Journal of Biological Chemistry*, 277(43), 40206–11. <http://doi.org/10.1074/jbc.M207348200>
- Ohgami, R. S., Campagna, D. R., McDonald, A., & Fleming, M. D. (2006). The Steap proteins are metalloreductases. *Blood*, 108(4), 1388–1394. <http://doi.org/10.1182/blood-2006-02-003681>
- Öhrvik, H., & Thiele, D. J. (2014). How copper traverses cellular membranes through the mammalian copper transporter 1, Ctr1. *Annals of the New York Academy of Sciences*, 1314(1), 32–41. <http://doi.org/10.1111/nyas.12371>
- Ojha, R., & Prasad, A. N. (2016). Menkes disease: what a multidisciplinary approach can do. *Journal of Multidisciplinary Healthcare*, 9, 371–385. <http://doi.org/10.2147/JMDH.S93454>
- Paasch, F., den Brave, F., Psakhye, I., Pfander, B., & Jentsch, S. (2018). Failed mitochondrial import and impaired proteostasis trigger SUMOylation of mitochondrial proteins. *Journal of Biological Chemistry*, 293, 599–609. <http://doi.org/10.1074/jbc.M117.817833>
- Page, M. D., Allen, M. D., Kropat, J., Urzica, E. I., Karpowicz, S. J., Hsieh, S. I., ... Merchant, S. S. (2012). Fe Sparing and Fe Recycling Contribute to Increased Superoxide Dismutase Capacity in Iron-Starved *Chlamydomonas reinhardtii*. *Plant Cell*, 24(June), 2649–2665. <http://doi.org/10.1105/tpc.112.098962>
- Pasinelli, P., Belford, M. E., Lennon, N., Bacskai, B. J., Hyman, B. T., Trotti, D., & Brown, R. H. (2004). Amyotrophic lateral sclerosis-associated SOD1 mutant proteins bind and aggregate with

- Bcl-2 in spinal cord mitochondria. *Neuron*, 43(1), 19–30.
<http://doi.org/10.1016/j.neuron.2004.06.021>
- Payne, A. S., & Gitlin, J. D. (1998). Functional Expression of the Menkes Disease Protein Reveals Common Biochemical Mechanisms Among the Copper-transporting P-type ATPases * of the conserved cysteine residues in the six amino-terminal M X C XX C metal binding domains confirmed the essential. *Journal of Biological Chemistry*, 273(6), 3765–3770.
- Punter, F. A., & Glerum, D. M. (2003). Mutagenesis reveals a specific role for Cox17p in copper transport to cytochrome oxidase. *Journal of Biological Chemistry*, 278(33), 30875–30880.
<http://doi.org/10.1074/jbc.M302358200>
- Radin, I., Gey, U., Kost, L., Steinebrunner, I., & Rödel, G. (2018). The mitochondrial copper chaperone COX11 plays an auxiliary role in the defence against oxidative stress.
- Rae, T. D., Schmidt, P. J., Pufahl, R. A., Culotta, V. C., & O'Halloran, T. V. (1999). Undetectable Intracellular Free Copper : The Requirement of a Copper Chaperone for Superoxide Dismutase. *Science*, 284(April), 805–809. <http://doi.org/10.1126/science.284.5415.805>
- Rak, M., Benit, P., Chretien, D., Bouchereau, J., Schiff, M., El-Khoury, R., ... Rustin, P. (2016). Mitochondrial cytochrome c oxidase deficiency. *Clinical Science*, 130(6), 393–407.
<http://doi.org/10.1042/CS20150707>
- Reaume, A. G., Elliott, J. L., Hoffman, E. K., Kowall, N. W., Ferrante, R. J., Siwek, D. F., ... Snider, W. D. (1996). Motor neurons in Cu/Zn superoxide dismutase-deficient mice develop normally but exhibit enhanced cell death after axonal injury. *Nature Genetics*, 13(1), 43–47.
<http://doi.org/10.1038/ng0596-43>
- Reddi, A. R., & Culotta, V. C. (2013). SOD1 integrates signals from oxygen and glucose to repress respiration. *Cell*, 152(1–2), 224–235. <http://doi.org/10.1016/j.cell.2012.11.046>
- Rodriguez-Castro, K. I., Hevia-Urrutia, F. J., & Sturniolo, G. C. (2015). Wilson's disease: A review of what we have learned. *World Journal of Hepatology*, 7(29), 2859–2870.
<http://doi.org/10.4254/wjh.v7.i29.2859>
- Rosen, D. R., Siddique, T., Patterson, D., Figlewicz, D. A., Sapp, P., Hentati, A., ... Deng, H. X. (1993). Mutations in Cu/Zn superoxide dismutase gene are associated with familial amyotrophic lateral sclerosis. *Nature*, 362(6415), 59–62. <http://doi.org/10.1038/362059a0>
- Ruy, F., Vercesi, A. E., & Kowaltowski, A. J. (2006). Inhibition of specific electron transport pathways leads to oxidative stress and decreased *Candida albicans* proliferation. *Journal of Bioenergetics and Biomembranes*, 129–135. <http://doi.org/10.1007/s10863-006-9012-7>
- Saydam, N., Steiner, F., Georgiev, O., & Schaffner, W. (2003). Heat and heavy metal stress synergize to mediate transcriptional hyperactivation by metal-responsive transcription factor MTF-1. *Journal of Biological Chemistry*, 278(34), 31879–31883.
<http://doi.org/10.1074/jbc.M302138200>

- Sea, K. W., Sheng, Y., Lelie, H. L., Barnese, L. K., Durazo, A., Valentine, J. S., & Gralla, E. B. (2013). Yeast copper-zinc superoxide dismutase can be activated in the absence of its copper chaperone. *Journal of Biological Inorganic Chemistry*, *18*(8), 985–992. <http://doi.org/10.1007/s00775-013-1047-8>
- Shapira, M., Segal, E., & Botstein, D. (2004). Disruption of Yeast Forkhead-associated Cell Cycle Transcription by Oxidative Stress. *Molecular Biology of the Cell*, *16*(1), 1–13.
- Sharp, P. (2004). The molecular basis of copper and iron interactions. *Proceedings of the Nutrition Society*, (63), 563–569. <http://doi.org/10.1079/PNS2004386>
- Shaw, S. L., Maddox, P., Skibbens, R. V., Yeh, E., Salmon, E. D., & Bloom, K. (1998). Nuclear and Spindle Dynamics in Budding Yeast. *Molecular Biology of Cell*, *9*(July), 1627–1631.
- Singh, A., & Xu, Y. J. (2017). Heme deficiency sensitizes yeast cells to oxidative stress induced by hydroxyurea. *Journal of Biological Chemistry*, *292*(22), 9088–9103. <http://doi.org/10.1074/jbc.M117.781211>
- Singh, I., Sagare, A. P., Coma, M., Perlmutter, D., Gelein, R., Bell, R. D., ... Deane, R. (2013). Low levels of copper disrupt brain amyloid- β homeostasis by altering its production and clearance. *Proceedings of the National Academy of Sciences*, *110*(36). <http://doi.org/10.1073/pnas.1302212110>
- Stathopoulos, P. B., Rumfeldt, J. A. O., Karbassi, F., Siddall, C. A., Lepock, J. R., & Meiering, E. M. (2006). Calorimetric analysis of thermodynamic stability and aggregation for Apo and Holo amyotrophic lateral sclerosis-associated Gly-93 mutants of superoxide dismutase. *Journal of Biological Chemistry*, *281*(10), 6184–6193. <http://doi.org/10.1074/jbc.M509496200>
- Tainer, J. A., Getzoff, E. D., Richardsont, J. S., & Richardson, D. C. (1983). Structure and mechanism of copper, zinc superoxide dismutase. *Nature*, *306*(November), 17–20.
- Timón-Gómez, A., Nývltová, E., Abriata, L. A., Vila, A. J., Hosler, J., & Barrientos, A. (2018). Mitochondrial cytochrome c oxidase biogenesis: Recent developments. *Seminars in Cell and Developmental Biology*, *76*, 163–178. <http://doi.org/10.1016/j.semcd.2017.08.055>
- Tokuda, E., Okawa, E., Watanabe, S., Ono, S. I., & Marklund, S. L. (2013). Dysregulation of intracellular copper homeostasis is common to transgenic mice expressing human mutant superoxide dismutase-1s regardless of their copper-binding abilities. *Neurobiology of Disease*, *54*, 308–319. <http://doi.org/10.1016/j.nbd.2013.01.001>
- Tsang, C. K. wa., Liu, Y., Thomas, J., Zhang, Y., & Zheng, X. F. S. (2014). Superoxide dismutase 1 acts as a nuclear transcription factor to regulate oxidative stress resistance. *Nature Communications*, *5*, 3446. <http://doi.org/10.1038/ncomms4446>
- Tsang, C. K., Chen, M., Cheng, X., Qi, Y., Chen, Y., Das, I., ... Zheng, X. F. S. (2018). SOD1 Phosphorylation by mTORC1 Couples Nutrient Sensing and Redox Regulation. *Molecular Cell*, *70*(3), 502–515.e8. <http://doi.org/10.1016/j.molcel.2018.03.029>

- Turski, M. L., & Thiele, D. J. (2009). New roles for copper metabolism in cell proliferation, signaling, and disease. *Journal of Biological Chemistry*, 284(2), 717–721. <http://doi.org/10.1074/jbc.R800055200>
- Tzagoloff, A., Akai, A., & Needleman, R. B. (1975). Assembly of the Mitochondrial Membrane System. *Journal of Biological Chemistry*, (20), 8228–8236.
- Valentine, J., Doucette, P. A., & Zittin Potter, S. (2005). Copper-Zinc Superoxide Dismutase and Amyotrophic Lateral Sclerosis. *Annu. Rev. Biochem*, 74, 563–93. <http://doi.org/10.1146/annurev.biochem.72.121801.161647>
- Varabyova, A., Topf, U., Kwiatkowska, P., Wrobel, L., Kaus-Drobek, M., & Chacinska, A. (2013). Mia40 and MINOS act in parallel with Ccs1 in the biogenesis of mitochondrial Sod1. *FEBS Journal*, 280(20), 4943–4959. <http://doi.org/10.1111/febs.12409>
- Veniamin, S., Sawatzky, L. G., Banting, G. S., & Glerum, D. M. (2011). Characterization of the peroxide sensitivity of COX-deficient yeast strains reveals unexpected relationships between COX assembly proteins. *Free Radical Biology and Medicine*, 51(8), 1589–1600. <http://doi.org/10.1016/j.freeradbiomed.2011.06.024>
- Vest, K. E., Leary, S. C., Winge, D. R., & Cobine, P. A. (2013). Copper import into the mitochondrial matrix in *Saccharomyces cerevisiae* is mediated by Pic2, a mitochondrial carrier family protein. *Journal of Biological Chemistry*, 288(33), 23884–23892. <http://doi.org/10.1074/jbc.M113.470674>
- Vest, K. E., Wang, J., Gammon, M. G., Maynard, M. K., White, O. L., Cobine, J. A., ... Cobine, P. A. (2016). Overlap of copper and iron uptake systems in mitochondria in *Saccharomyces cerevisiae*. *Open Biology*, 6(1). <http://doi.org/10.1098/rsob.150223>
- Werner-Washburne, M., Braun, E., Johnston, G. C., & Singer, R. A. (1993). Stationary phase in the yeast *Saccharomyces cerevisiae*. *Microbiological Reviews*, 57(2), 383–401. <http://doi.org/10.1093/nar/gkr782>
- Williams, J. C., Sue, C., Banting, G. S., Yang, H., Glerum, D. M., Hendrickson, W. A., & Schon, E. A. (2005). Crystal Structure of Human SCO1. *Journal of Biological Chemistry*, 280(15), 15202–15211. <http://doi.org/10.1074/jbc.M410705200>
- Wisnovsky, S. P., Wilson, J. J., Radford, R. J., Pereira, M. P., Chan, M. R., Laposa, R. R., ... Kelley, S. O. (2013). Targeting Mitochondrial DNA with a Platinum-Based Anticancer Agent. *Cell*, 20(11), 1323–1328. <http://doi.org/10.1016/j.chembiol.2013.08.010>
- Wood, L. K., & Thiele, D. J. (2009). Transcriptional activation in yeast in response to copper deficiency involves copper-zinc superoxide dismutase. *Journal of Biological Chemistry*, 284(1), 404–413. <http://doi.org/10.1074/jbc.M807027200>
- Yuan, D. S., Stearman, R., Dancis, A., Dunn, T., Beeler, T., & Klau. (1995). The Menkes/Wilson disease gene homologue in yeast provides copper to a ceruloplasmin-like oxidase required for iron uptake. *Proceedings of the National Academy of Sciences*, 92(March), 398–497.

- Zhang, C., Zhang, F., Zhou, P., & Zhang, C. (2016). Functional role of metalloproteins in genome stability. *Frontiers in Biology*, *11*(2), 119–131. <http://doi.org/10.1007/s11515-016-1392-4>
- Zhao, L., Wang, Z., Wu, H., Xi, Z., & Liu, Y. (2015). Glutathione selectively modulates the binding of platinum drugs to human copper chaperone Cox17. *Biochemical Journal*, *472*(2), 217–223. <http://doi.org/10.1042/BJ20150634>
- Zhao, L., Cheng, Q., Wang, Z., Xi, Z., Xu, D., & Liu, Y. (2014). Cisplatin binds to human copper chaperone Cox17: the mechanistic implication of drug delivery to mitochondria. *Chemical Communications (Cambridge, England)*, *50*(20), 2667–9. <http://doi.org/10.1039/c3cc48847k>
- Zhou, B., & Gitschier, J. (1997). hCTR1: A human gene for copper uptake identified by complementation in yeast. *Proceedings of the National Academy of Sciences of the United States of America*, *94*(14), 7481–7486. <http://doi.org/10.1073/pnas.94.14.7481>
- Zischka, H., & Lichtmanegger, J. (2014). Pathological mitochondrial copper overload in livers of Wilson's disease patients and related animal models. *Annals of the New York Academy of Sciences*, *1315*(1), 6–15. <http://doi.org/10.1111/nyas.12347>

Appendix A: qPCR Data with Galactose as a Carbon Source

This Appendix includes qPCR data for the *COX17*, *SCO1*, *COX11*, *COX4*, *CCS1*, *SOD1*, and *PIMI* genes with galactose as a primary carbon source, and *TDH2* qPCR data with both glucose and galactose as carbon sources.

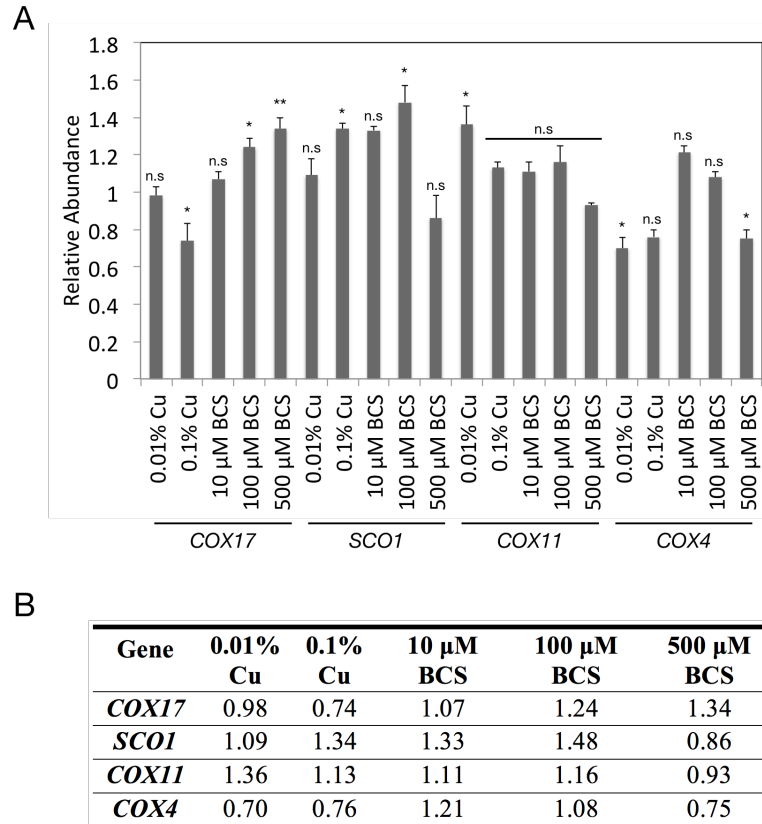


Figure A1.1 RT-qPCR of *COX17*, *SCO1*, *COX11*, and *COX4* with galactose

(A) Graphical representation of relative abundance of *COX17*, *SCO1*, *COX11* and *COX4*. RNA was isolated from yeast cells grown for 18 hours in YPGal + BCS. PCR was performed using cDNA on both the gene of interest and *ACT1* as a control. Values are representative of $\Delta\Delta Cq$ values. Three biological replicates were performed for each concentration. A one-way ANOVA was performed to determine statistical significance: not significant = n.s, $p < 0.05 = *$, $p < 0.01 = **$. Error bars represent \pm SEM. (B) Raw $\Delta\Delta Cq$ values.

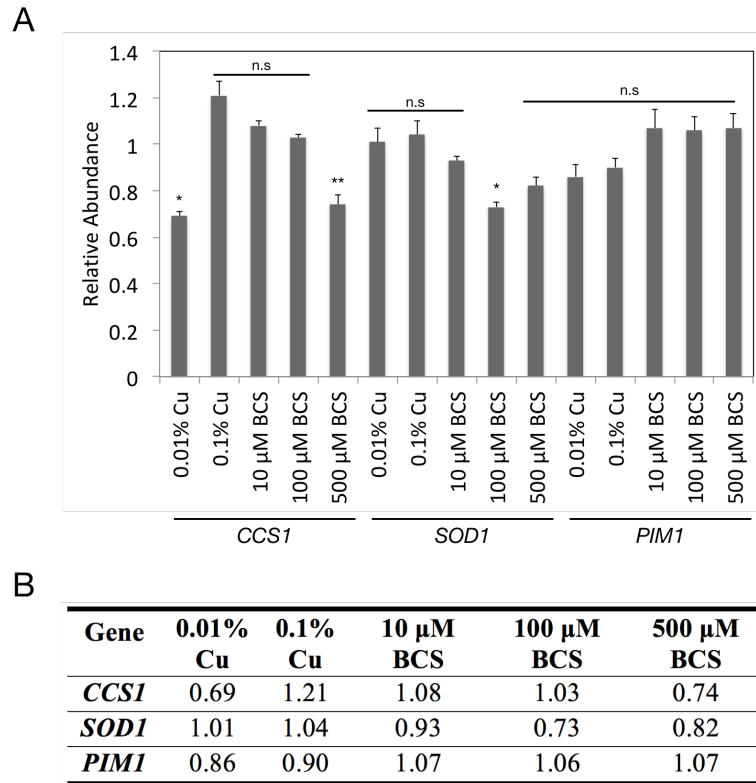


Figure A1.2 RT-qPCR of *CCSI*, *SOD1*, and *PIMI* with galactose

(A) Graphical representation of relative abundance of *CCSI*, *SOD1* and *PIMI*. RNA was isolated from yeast cells grown for 18 hours in YPGal + Cu or BCS. PCR was performed using cDNA on both the gene of interest and *ACT1* as a control. Values are representative of $\Delta\Delta Cq$ values. Three biological replicates were performed for each concentration. A one-way ANOVA was performed to determine statistical significance: not significant = n.s, $p < 0.05 = *$, $p < 0.01 = **$. Error bars represent \pm SEM. (B) Raw $\Delta\Delta Cq$ values.

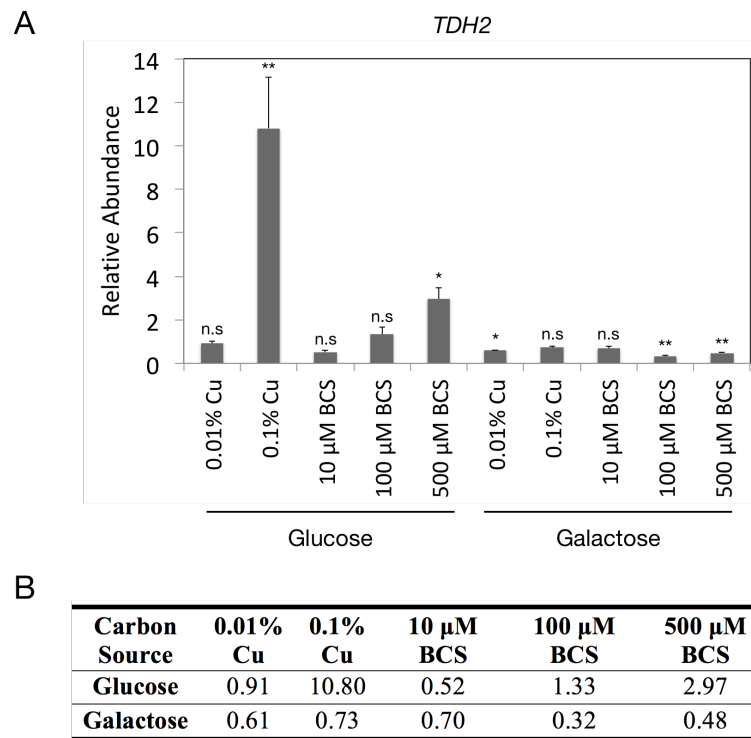


Figure A1.3 *TDH2* expression in glucose and galactose

(A) Graphical representation of relative abundance of *TDH2*. RNA was isolated from yeast cells grown for 18 hours in YPD or YPGal + Cu or BCS. PCR was performed using cDNA on both the gene of interest and *ACT1* as a control. Values are representative of $\Delta\Delta Cq$ values. Three biological replicates were performed for each concentration. A one-way ANOVA was performed to determine statistical significance: not significant = n.s., $p < 0.05 = *$, $p < 0.01 = **$. Error bars represent \pm SEM. (B) Raw $\Delta\Delta Cq$ values.

TDH2 was originally our second qPCR control (*ACT1* was the other) however expression was greatly varied with changing extracellular Cu concentrations, so using it as a control transcript would skew our results majorly. The differences in expression in glucose and galactose are not surprising, as *TDH2* is the ortholog of glyceraldehyde 3-phosphate dehydrogenase (GAPDH) in mammalian cells.